STUDIES OF ANTI-TRYPANOSOMAL *O*-METHYL AMIDOXIME PRODRUGS IN IDENTIFICATION OF NOVEL METABOLITES, APOPTOTIC EFFECTS, AND INHIBITION OF CYP1B1

Wujian Ju

A dissertation submitted to the faculty of the University of North Carolina at Chapel Hill in partial fulfillment of the requirements for the degree of Doctor of Philosophy in the Eshelman School of Pharmacy

Chapel Hill
2009

Approved by

Advisor: James Edwin Hall, Ph.D.

Chairman: Harold Kohn, Ph.D.

Reader: Alexander Tropsha, Ph.D.

Reader: Jian Liu, Ph.D.

Reader: Arlene Bridges, Ph.D.

ABSTRACT

Wujian Ju: Studies of Anti-Trypanosomal *O*-methyl Amidoxime Prodrugs in Identification of Novel Metabolites, Apoptotic Effects, and Inhibition of CYP1B1.
(under the direction of James E. Hall, Ph.D.)

Human African Trypanosomiasis (HAT), also known as sleeping sickness, afflicts hundreds of thousands of individuals in sub-Saharan Africa with another 60 million people at risk of infection. The agents that are currently available as anti-trypanosomals are generally unsatisfactory due to a combination of their low efficacy, dangerous side effects and difficulty in administration. Although drug development efforts have recently been focused on creating less toxic, more potent *O*-methyl amidoxime prodrugs with an orally bioavailable formulation, the overall mechanism of action of this series of compounds is unknown.

The focus of this research is to identify novel metabolites of the *O*-methyl amidoxime prodrugs, investigate the apoptotic effects by the prodrug and each metabolite, and the inhibitory effect to the metabolizing CYP1 enzymes. These results may help us to better understand the mechanism of actions and mechanism of toxicity of the anti-trypanosomal *O*-methyl amidoxime prodrugs, and therefore facilitate the further drug development in the future.

ACKNOWLEDGEMENTS

It is my great honor to acknowledge the people without whom this project would never have completed.

First, I would like to sincerely thank Dr. James Edwin Hall for his guidance, understanding, and patience during my graduate studies at UNC-Chapel Hill. His broad knowledge and experience in pharmaceutical sciences inspired me and encouraged me a lot in my research process. He always gave me opportunities to develop my own research interests and ability by allowing me to work independently. I benefited a lot from his mentoring and training.

I would also like to thank Dr. Harold Kohn, Dr. Alexander Tropsha, Dr. Jian Liu and Dr. Arlene Bridges, and Dr. Richard R. Tidwell, for providing insight and inspiration to my work.

I would like to thank all collaborators in my project, especially Dr. Arlene Bridges, Dr. Qi Jiang, Dr. Xinchun Shen, Dr. Xin Ming, Dr. Michael Z. Wang, Dr. David Boykin, Dr. John H. Ansede, Dr. Chad E. Stephens, Dr. Robert D. Voyksner, and Dr. Mohamed A. Ismail for their many suggestions and comments to help me overcome problems and enjoy research together. I am also very grateful to all my co-workers in our group for the friendship and in what could have otherwise been a difficult laboratory environment.

This dissertation work was financially supported by a grant from the Bill and Melinda Gates Foundation.

Finally, and the most importantly, I would like to thank my parents, sister, brother in law and my young nephew for their eternal love, support and encouragement, which built up my confidence to go through the most difficult time.

TABLE OF CONTENTS

LIST OF TABLES

LIST OF FIGURES

Figure

LIST OF SCHEMES

Scheme

LIST OF ABBREVIATIONS

ALT, alanine aminotransferase

AST, aspartate aminotransferase

BBB, blood brain barrier

CPT, camptothecin

CNS, central nervous system

CYP, cytochrome P450

DMSO, dimethyl sulfoxide

EMEM, Eagle's minimum essential medium

EROD, Ethoxyresorufin *O*-deethylation

FBS, sodium pyruvate and fetal bovine serum

FITC, fluorescein isothiocyanate

HAT, human African trypanosomiasis

HLM, human liver microsome

HPLC, high performance liquid chromatography

LCMS, liquid chromatography-mass spectrometry

NADPH, reduced form of nicotinamide adenine dinucleotide phosphate

NEAA, nonessential amino acids

PARP, poly ADP ribose polymerase

PI, propidium iodide

RF, resorufin

SDS-PAGE, sodium dodecyl sulfate polyacrylamide gel electrophoresis

TFA, trifluoroacetic acid

TMS, tetramethoxystilbene

WHO, World Health Organization

CHAPTER 1

INTRODUCTION

A. Trypanosomiasis

Human African trypanosomiasis (HAT), also known as African sleeping sickness, once the causative trypanosome parasites have established within the central nervous system (CNS) (Barrett et al., 2003; Barrett et al., 2007), afflicts nearly half a million people in sub-Saharan Africa at the end of the twentieth century, with another 60 million people at risk of infection (Denise et al. 1999; Cattand et al. 2001; Barrett et al. 2003).

There are two subspecies of human *Trypanosome brucei* were identified (Cox, 2002, Hide, 1999). *Trypanosoma brucei gambiense* (*T. b. gambiense*) was identified by Everett Dutton in 1902 as the causative agent of Gambian, or chronic human trypanosomiasis, which is prevalent in West and Central Africa (Figure 1.1). And *Trypanosoma brucei rhodesiense* (*T. b. rhodesiense*) was identified by J. W. W. Stephens and Harold Fantham in 1910 as the causative agent of the acute form of human trypanosomiasis, which is prevalent in Eastern and Southern Africa (Fevre et al., 2005).

Trypanosomiasis is a vector borne disease, with transmission occurring after the bite of an infected tsetse fly (Glossina sp.). It usually takes weeks or months for rhodesiense form or years for the gambiense form to develop to be fatal after infection. In the early stage of the infection, the parasites reside and proliferate in the subcutaneous tissues and hemolymphatic system, causing symptoms such as fever, headaches, joint pains and itching (WHO. 2006). In the late stage, the parasites cross the blood brain barrier (BBB) and invade the central nervous system (CNS) and the cerebrospinal fluid. More severe symptoms of the disease appear, including confusion, sensory disturbances and poor coordination (WHO. 2006). The

most important feature of the late stage is the disturbance of the sleep cycle, which gives the disease its name (Buguet et al., 1993). If untreated, sleeping sickness is fatal.

In recent years, vector control using extensive trapping and sterile insect technique was successfully employed to inhibit the transmission, and therefore the disease cases were significantly reduced (Allsopp et al., 2001; Vreysen et al., 2000). However, the coordination in the tsetse control was still very difficult in the African mainland. Vaccination is not a promising way neither, due to the rapid change of the surface antigen of the parasites (McCulloch et al., 2004).

The clinical diagnosis is primarily through detecting Winterbottom's sign and confirming using serological and parasitological techniques (Apted et al., 1980, Balasegaram et al., 2006, Jannin et al., 2004). However, the symptoms of the early stage trypanosomiasis are often vague and variable. Rapid, feasible and reliable diagnostic techniques are still in a great need for the detection of trypanosomiasis and determination of the infective stage in patients. Therefore, PCR-based tests (Deborggraeve et al., 2006) and a dot – ELISA test (Courtioux et al., 2005) have been developed and will be further investigated to verify the specificity and accuracy.

B. Treatment options

HAT is considered as a neglected disease, which affects people from among the world'spoorest populations and is not economically attractive for pharmaceutical industries (Barrett et al., 2007; Stich et al., 2003; Thuita et al., 2008). Currently only four drugs are available in clinic against HAT according to the causative subspecies and the infection stages (Pepin and Milord, 1994; Denise and Barrett, 2001; Keiser et al., 2001; Fairlamb, 2003; Burri et al., 2004; Brun and Balmer, 2006).

Pentamidine isethionate (Figure 1.2) is currently produced by Sanofi-Aventis as pentacarinat in 200mg ampoules for gambiense form of HAT by intramuscular injection with $4mgkg^{-1}d^{-1}$ for 7–10 days (Barrett et al., 2007; Sands et al., 1985; Burri et al., 2004). The extensive studies of pentamidine have shown that it can be enriched specifically by trypanosomes from low micromolar concentration to low millimolar range through the transporter P2 aminopurine permease, high-affinity pentamidine transporter 1 (HAPT1) and low-affinity pentamidine transporter 1 (LAPT1) (Damper and Patton, 1976; Berger et al., 1995; Carter et al., 1995; de Koning, 2001) The mode of action for pentamidine is not fully understood (Berger et al., 1993; Werbovetz, 2006). But pentamidine may bind DNA and destroy the mitochondrion (Hentzer and Kobayasi, 1977; Croft and Brazil, 1982; Simpson, 1986). Pentamidine has large volume of distribution and long terminal half-life in the pharmacological studies due to its extensive tissue retention and protein binding (Bronner et al., 1991). Pentamidine is metabolic unstable and it can be extensively metabolized by cytochrome P450 (Berger et al., 1992). Pentamidine causes multiple toxic effects, such as

hypotension, nephrotoxicity, leucopenia and liver enzyme abnormalities (Sands et al., 1985; Doua and Yapo, 1993).

Suramin (Figure 1.2) is produced by Bayer as Germanin for treatment of rhodesiense cases by intravenous injection (Voogd et al., 1993). Since this drug may bind many enzymes by electrostatic interaction, multiple pathways including glycolysis may be the targets (Wierenga et al., 1987). Endocytosis has been confirmed as the major route of entry (Fairlamb and Bowman, 1980). Suramin shows poor intestinal absorption and does not cross blood–brain barrier. The terminal half-life is quite long (Eisenberger and Reyno, 1994). The toxic effects include significant neurotoxicity, fatigue, anaemia, hyperglycaemia, hypocalcaemia, coagulopathies, neutropaenia, renal insufficiency and transaminitis (Kaur et al., 2002; Bitton et al., 1995)

Melarsoprol (Figure 1.2) is used against late stage rhodesiense disease and gambiense disease by intravenous injection. The drug uptake may be carried by the P2 aminopurine transporter and other routes (Carter and Fairlamb, 1993; Barrett and Fairlamb, 1999; Ma¨ser et al., 1999; Stewart et al., 2005; Matovu et al., 2003). The mode of action for melarsoprol is unclear. But it can cause the depletion of ATP (Vanschaftingen et al., 1987) and parasites lyse rapidly (Meshnick et al., 1978). Melarsoprol may be metabolized rapidly to form active metabolite melarsen oxide (Burri and Brun, 1992; Burri et al., 1993). Melasoprol and its metabolite melarsen oxide may cross blood-brain barrier and accumulate to the level enough to kill trypanosomes in the CNS. Melarsoprol has very severe toxic effects including pyrexia, headache, pruritis and thrombocytopaenia.

Eflornithine (Figure 1.2) or D,L-a-difluoromethylornithine produced by Marion Merrell Dow is used against *T. b. gambiense* in the late stage by by intravenous injection (Burri and Brun, 2003). It may inhibit the polyamine biosynthetic enzyme ornithine decarboxylase (ODC) in the parasites (Bacchi et al., 1980; Phillips et al., 1987; Bacchi and Yarlett, 1993) and cause them more susceptible to oxidative stress and other immunological insult (Barrett et al., 2007; Fairlamb et al., 1987). The uptake may be the transporter mediated in trypanosomes (Barrett and Gilbert, 2006).Side effects include fever, headache, hypertension, macular rash, peripheral neuropathy and tremor, gastrointestinal problems including diarrhoea (Chappuis et al., 2005).

As described above, the treatment options for trypanosomiasis are very limited. All the four clinical drugs have obvious disadvantages, such as poor oral bioavailability, requirement of parenteral administration and severe side effects. So the development of more effective, feasible and less toxic drugs is in a great need.

C. Development of Diadimine Compounds and Prodrugs

Diamidine furamidine (DB75) (Figure 1.3) is developed based on pentamidine by closing the central carbon chain to be furan ring to increase its metabolic stability. The diamidine furamidine was confirmed to have potent anti-parasitic activities against *Trypanosoma brucei*, *Plasmodium falciparum, Leishmania spp.,* and *Pneumocystis jirovecii in vitro and in vivo* (Das and Boykin, 1977; Bell et al., 1990; Brendle et al., 2002; Tidwell et al.,1990). The diamidine furamidine is a binder of DNA minor groove (Tidwell et al., 2003, Wilson et al., 2008). It shows selective and rapid uptake by the P2 aminopurine transporter, which enables this compound highly accumulated in the parasite (Mathis et al., 2006). However, as a dicationic molecule, DB75 carries two positive charges at the physiological condition and can not cross the cell membrane. Therefore, it showed poor oral bioavailability.

Pafuramidine maleate (DB289) (Figure 1.3) was then synthesized by introducing two *O*-methyl groups to the diamidine furamidine to mask the positive charges (Boykin et al., 1996). DB289 has shown enhanced permeability across intestinal epithelium (Zhou et al., 2002) and potent oral activities against trypanosomiasis and *Pneunocystis carinii* pneumonia in animal models (Boykin et al., 1996; Fitzpatrick et al., 2004). The phase I metabolic pathway of DB289 (scheme 3.1, adapted from Wang et al., 2006) has been determined *in vitro* using freshly isolated rat hepatocytes (Zhou, et al, 2004). DB289 was metabolized to form intermediate metabolites including M1, M2, M3 and M4, and the final active compound DB75 through sequential *O*-demethylation and *N*-dehydroxylation reactions, which are catalyzed by multiple enzymes, including CYP4F2, CYP4F3B, and CYP2J2 for the *O*-demethylations, and cytochrome b5/b5 reductase for the N-dehydroxylations (Wang et al,

2006; Saulter et al., 2005). DB289 is also confirmed to be metabolized to DB75 rapidly in humans in phase I clinical trial and a twice daily oral administration of DB289 maintains plasma DB75 at required antimicrobial concentration (Yeramian et al., 2001). As a prodrug, pafuramidine maleate became the first oral drug for HAT to enter clinical trials for the early stage. In August 2005, a pivotal phase III trial was started for 273 enrolled patients (Wenzler et al., 2009). In October 2008, an extended phase I study of healthy volunteers was started for the safety assessment for registration for HAT and Pneumocystis jiroveci (Wenzler et al., 2009). In the extended phase I trial, severe liver toxicity and delayed renal insufficiency were observed in a number of participants (Pholig et al., 2008). Therefore, the DB289 development program was stopped. The toxicity issue ended the development of this oral anti-trypanosomal prodrug and its analogues. Previous pharmacokenics studies of oral DB289 in rat and monkey showed multiple metabolites were formed and distributed in different organs and tissues with different half lifes. Especially DB75 had a very long half life and accumulate in liver (Midgley et al., 2007). It becomes an urgent need to understand the toxicity of this prodrug and its each metabolite.

Furamidine does not cross the blood–brain barrier. So it is not effective against late stage HAT. Many analogues of furamidine were synthesized and tested in order to find new clinical candidates effective to late stage HAT. An aza-analogue of furamidine, 6-[5-(4-amidinophenyl)-furan-2-yl]nicotinamidine (DB820) (Figure 1.3) was synthesized by adding a nitrogen into one of the phenyl rings (Ismail et al., 2003) and exhibited trypanocidal activity in rodent models of stage 2 disease. However, like furamidine it suffers from poor oral activity because of its positively charged amidine groups. The dimethoxyamidine

prodrug of DB820, *N*-methoxy-6-{5-[4-(*N*-methoxyamidino)phenyl]-furan-2-yl}-nicotinamidine (DB844), has potent oral activity in mouse models of both early stage and CNS African trypanosomiasis (Ismail *et al.* 2003) and thus was considered as a promising new prodrug for treating late stage human infection. However, severe dose limiting gastro intestinal toxicity in trypanosome infected vercet monkeys was recently reported (Thuita et al., 2008). Development of this compound has thus been dropped although new analoques continues to be pursued as CNS drug condidates. The metabolic pathway for the conversion of DB844 to DB820 in human liver microsomes (HLM) was reported (Ansede et al., 2005). *O*-demethylation and *N*-dehydroxylation reactions resulted in the production of eight major metabolites including the active DB820 metabolite providing evidence that DB844 may effectively be metabolized to its active metabolite *in vivo*.

D. Rationale for Proposed Studies

There is a great need for new treatments of human African trypanosomiasis and other parasitic diseases worldwide. Major pharmaceutical companies often neglect drug development for diseases of the developing world, such as sleeping sickness. Although the consortium's approach to the development of novel therapies has generated many dicationic compounds with anti-parasitic activity, there is little known about the exact mechanisms of action and mechanisms of toxicity.

Pharmacokenics studies of oral DB289 in rat and monkey showed multiple metabolites are formed and distributed in different organs and tissues with different half lifes. Especially DB75 has very long half life and accumulates in liver (Midgley et al., 2007). Since the toxicity issue is one of the major obstacles for the development of this oral anti-trypanosomal prodrug and its analogues, it becomes an urgent need to identify all the metabolites of this prodrug, understand the toxicity of this prodrug and its each metabolite, and investigate the potential interactions between these compounds and their metabolizing P450 enzymes.

The metabolic pathway for the conversion of DB844 to DB820 in human liver microsomes (HLM) was reported (Ansede et al., 2005). *O*-demethylation and *N*-dehydroxylation reactions resulted in the production of eight metabolites including the active DB820 metabolite providing evidence that DB844 may effectively be metabolized to its active metabolite in vivo. Multiple cytochrome P450s, including CYP4F2, CYP4F3B, CYP2J2, CYP1A2, CYP1A1 and CYP1B1, catalyze the first step *O*-demethylation in the pathway (Wang et al., 2006). Therefore, the in vivo efficacy of DB844 is dependent on the level of

expression, localization (hepatic vs. extrahepatic) and polymorphism of the CYP(s) involved in its metabolism. Recently, two novel and unexpected products (MX and MY) catalyzed by extrahepatic P450s CYP1A1 and CYP1B1 were discovered and indicated that the metabolic pathway of DB844 was very complex. Due to the instability of MX in the *in vitro* enzyme reaction conditions, it is very challenging to identify its structure, but on the other aspect, it might be very significant for the activity study and toxicity study.

Previous studies have confirmed that pentamidine and DB75 induce apoptotic-like death in *Leishmania donovani* and *Trypanosome cruzi* respectively (Singh and Dey 2007; De Souza et al., 2006). Although the mechanism is not fully elucidated, it might be because of their capacity of binding DNA and/or inhibiting topoisomerase II (Lausiaux et al., 2002 a and b; Singh and Dey et al., 2007). However, it has not been investigated yet if DB75 or the prodrug DB289 and its intermediate metabolites can induce apoptosis or necrosis in human cells. As we know, drug-induced liver injuries are by means of apoptosis and necrosis, for example amiodarone, benzarone (Kaufmann et al., 2005), and acetaminophen (Kon et al., 2004). Investigation into the apoptotic induction by DB289 and each metabolite may be helpful to elucidate their roles in the long term clinical toxicity.

In recent studies, we found that the conversion of DB289 to M1 catalyzed by the recombinant human CYP1B1 was incomplete and the sequential conversion of M1 to M2 was not observed. It might be explained by inhibition of the metabolizing CYP enzyme by the prodrug and/or its metabolites. Therefore, the investigation into the inhibitory abilities of

these compounds against CYP1B1 was carried out, which may enhance our knowledge of DB289 and perhaps lead to new applications for anti-cancer purpose.

The major hypothesis governing the experiments in this dissertation is that identification of novel metabolites, investigation of apoptotic effects, and study of inhibition against the metabolizing enzymes, can reinforce our understanding of the anti-trypanosomal *O*-methyl amidoxime prodrugs DB289, and therefore develop novel more active and less toxic drugs.

This hypothesis was evaluated through the following specific objectives:

1. Identify the structures of the novel metabolites MX and MY from DB844.
   a) Scale up generation and purification of MX and MY, since they are minor metabolites from the prodrug;
   b) Analyze the purified MX and MY with LC-MS to provide structural information;
   c) Propose candidate structures for MX and MY and determine the correct structures by comparing with synthetic compounds.

2. Investigate the apoptotic effects of the prodrug DB289 and its metabolites M1, M2, and M3 in the mammalian cell MCF-7.
   a) Determine the cytotoxicity of compounds using the Alamar Blue™ assay;
   b) Observe cell morphology and viability;
   c) Analyze the apoptotic effects using flow cytometry and western blotting;
   d) Determine the substrate depletion of these compounds during the apoptotic induction.

3. Determine the inhibition of DB289 and its metabolites M1 and M2

a) Analyze the substrate depletion and metabolite formation of DB289, M1 and M2;

b) Determine the *in vitro* inhibition potency using EROD assay and 4E2 and 2E2 formation assay.

Potential implications, future studies, and the conclusions drawn from this research are presented in Chapter 6.

Figure 1.1 A map of countries infected with HAT. The countries shown in colour have historically reported HAT. Those countries coloured in red are currently reporting in excess of 1000 cases per year. Those in brown currently report between 50 and 1000 cases per year. Those in blue report fewer than 50 cases per year, while those in green currently report no cases of HAT. Nearly 97% of all reported cases are caused by *T. b. gambiense*. *T. b. rhodesiense* is found in East and Southern Africa. (Figure courtesy of Dr Pere Simarro at the World Health Organization.) HAT, human African trypanosomiasis.

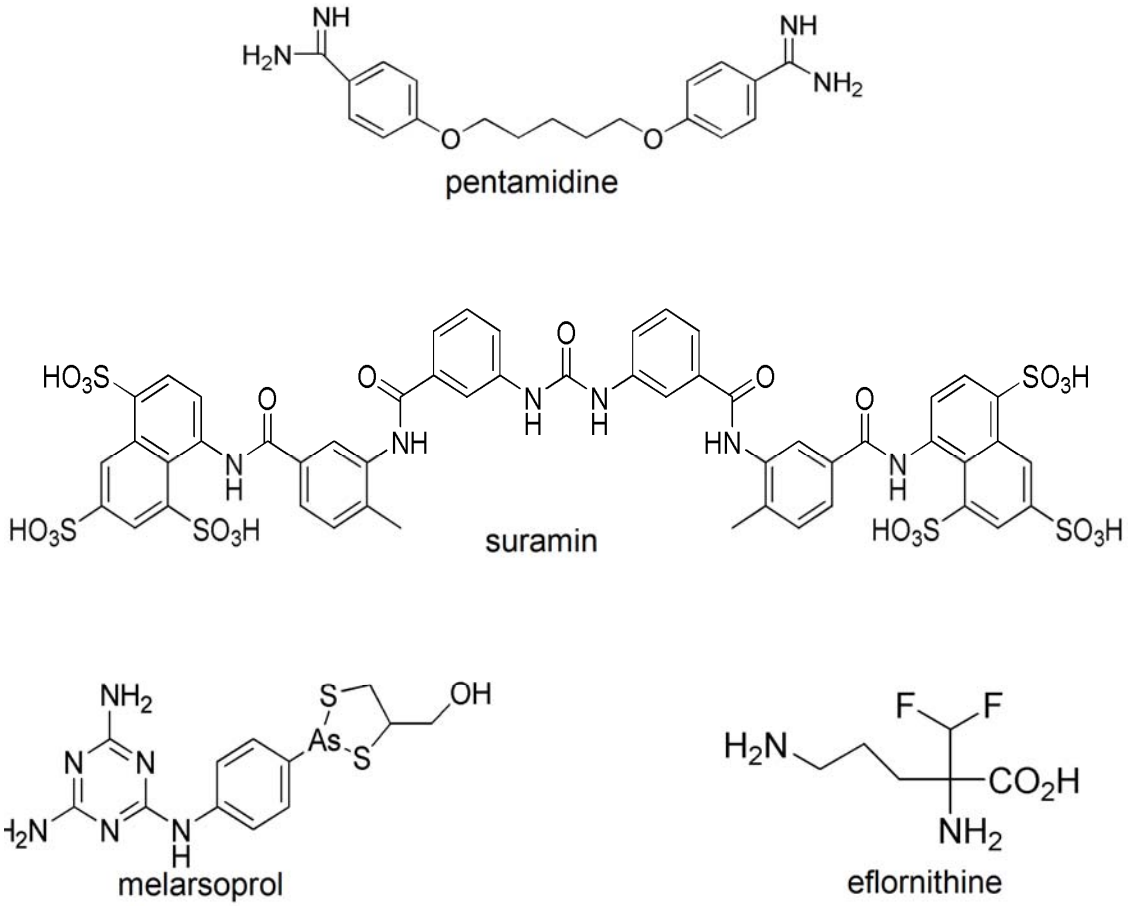

Figure 1.2 Clinical drugs for anti-trypanosomiasis.

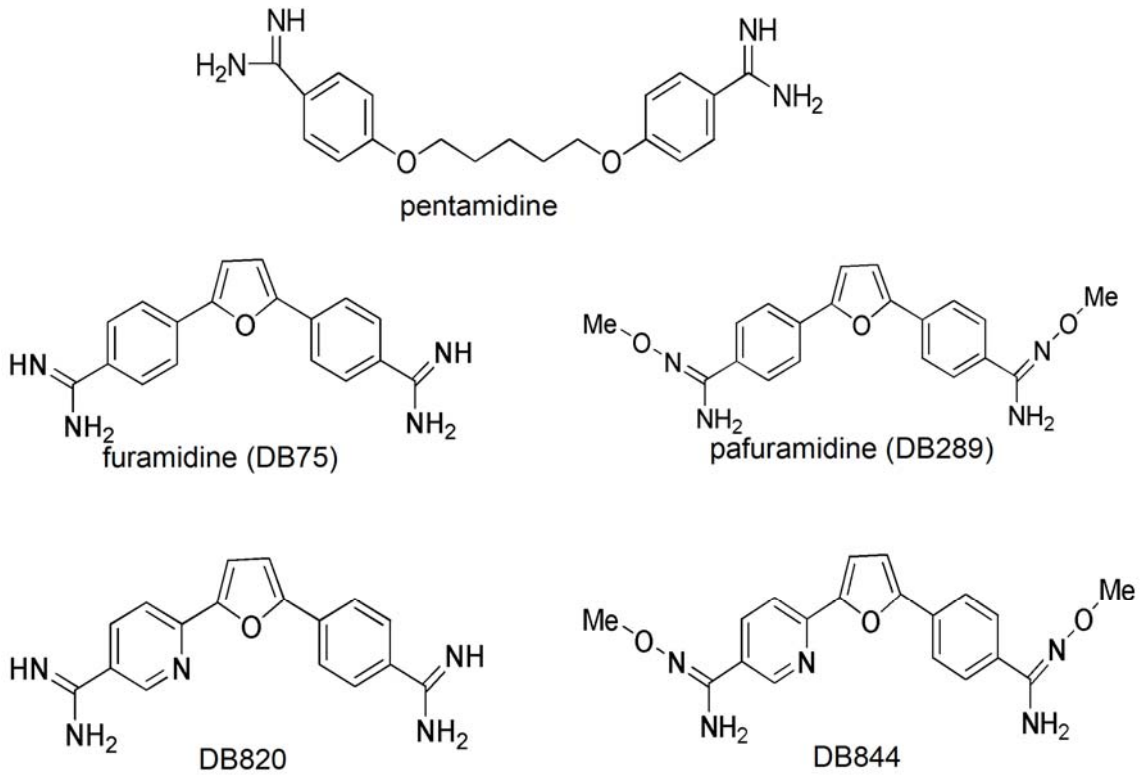

Figure 1.3 Structures of some important trypanocidal diamidines and prodrugs.

E. References

Allsopp R (2001). Options for vector control against trypanosomiasis in Africa. Trends Parasitol 17: 15–19. Anonymous (2006). Human African trypanosomiasis (sleeping sickness): epidemiological update. Wkly Epidemiol Rec 81: 71–80.

Ansede JH, Anbazhagan M, Brun R, Easterbrook JD, Hall JE, Boykin DW (2004). O-alkoxyamidine prodrugs of furamidine: in vitro transport and microsomal metabolism as indicators of in vivo efficacy in a mouse model of Trypanosoma brucei rhodesiense infection. J Med Chem 47: 4335–4338.

Ansede JH, Voyksner RD, Ismail MA, Boykin DW, Tidwell RR, Hall JE (2005). In vitro metabolism of an orally active O-methyl amidoxime prodrug for the treatment of CNS trypanosomiasis. Xenobiotica 35: 211–226.

Apted, F. I. (1980). Present status of chemotherapy and chemopropylaxis of human trypanosomiasis in the eastern hemisphere. Pharmacol Ther 11:391-413.

Bacchi CJ, Nathan HC, Hutner SH (1980). Polyamine metabolism – a potential therapeutic target in trypanosomes. Science 210: 332–334.

Bacchi CJ, Yarlett N (1993). Effects of antagonists of polyamine metabolism on African trypanosomes. Acta Trop 54: 225–236.

Balasegaram, M., S. Harris, F. Checchi, C. Hamel, and U. Karunakara. 2006. Treatment outcomes and risk factors for relapse in patients with early-stage human african trypanosomiasis (hat) in the republic of the congo. Bull World Health Organ 84:777-82.

Balasegaram M, Harris S, Checchi F, Ghorashian S, Hamel C, Karunakara U (2006). Melarsoprol versus eflornithine for treating late-stage Gambian trypanosomiasis in the Republic of the Congo. Bull World Health Organ 84: 783–791.

Barrett MP (1999). The fall and rise of sleeping sickness. Lancet 353: 1113–1114.

Barrett MP (2003). Drug resistance in sleeping sickness. WHO expert committee on African trypanosomiasis (sleeping sickness). pp 96–111.

Barrett MP, Burchmore RJS, Stich A, Lazzari JO, Frasch AC, Cazzulo JJ et al. (2003). The trypanosomiases. Lancet 362: 1469–1480.

Barrett MP, Boykin DW, Brun R and Tidwell RR (2007). Human African trypanosomiasis: pharmacological re-engagement with a neglected disease. Br. J. Pharmacol. 152:1155–1171.

Barrett MP, Gilbert IH (2006). Targeting of toxic compounds to the trypanosome's interior. Adv Parasitol 63: 126–183.

Bellofatto V, Fairlamb AH, Henderson GB, Cross GAM (1987). Biochemical-changes associated with alpha-difluoromethylornithine uptake and resistance in Trypanosoma brucei. Mol Biochem Parasitol 25: 227–238.

Berger BJ, Carter NS, Fairlamb AH (1993). Polyamine and pentamidine metabolism in African trypanosomes. Acta Trop 54: 215–224.

Berger BJ, Carter NS, Fairlamb AH (1995). Characterization of pentamidine-resistant Trypanosoma brucei brucei. Mol Biochem Parasitol 69: 289–298.

Berger BJ, Naiman NA, Hall JE, Peggins J, Brewer TG, Tidwell RR (1992). Primary and secondary metabolism of pentamidine by rats. Antimicrob Agents Chemother 36: 1825–1831.

Bitton RJ, Figg WD, Venzon DJ, Dalakas MC, Bowden C, Headlee D et al. (1995). Pharmacologic variables associated with the development of neurologic toxicity in patients treated with suramin. J Clin Oncol 13: 2223–2229.

Bronner U, Doua F, Ericsson O, Gustafsson LL, Miezan TW, Rais M et al. (1991). Pentamidine concentrations in plasma, whole blood and cerebrospinal fluid during treatment of Trypanosoma gambiense infection in Cote d'Ivoire. Trans R Soc Trop Med Hyg 85: 608–611.

Brun R, Balmer O (2006). New developments in human African trypanosomiasis. Curr Opin Infect Dis 19: 415–420. Brun R, Schumacher R, Schmid C, Kunz C, Burri C (2001). The phenomenon of treatment failures in human African trypanosomiasis. Trop Med Intl Health 6: 906–914.

Buguet A, Bert J, Tapie P, Tabaraud F, Doua F, Lonsdorfer J et al. (1993). Sleep-wake cycle in human African trypanosomiasis. J Clin Neurophysiol 10: 190–196.

Burri C, Baltz T, Giroud C, Doua F, Welker HA, Brun R (1993). Pharmacokinetic properties of the trypanocidal drug melarsoprol. Chemotherapy 39: 225–234.

Burri C, Brun R (1992). An in vitro bioassay for quantification of melarsoprol in serum and cerebrospinal fluid. Trop Med Parasitol 43: 223–225.

Burri C, Brun R (2003). Eflornithine for the treatment of human African trypanosomiasis. Parasitology Res 90: S49–S52.

Burri C, Stich A, Brun R (2004). Current chemotherpay of human African trypanosomiasis. In: Maudlin I, Holmes PH, Miles MA (eds). The Trypanosomiases. CABI: Oxford, pp 403–420.

Carter NS, Berger BJ, Fairlamb AH (1995). Uptake of diamidine drugs by the P2 nucleoside transporter in melarsen-sensitive and -resistant Trypanosoma brucei brucei. J Biol Chem 270: 28153–28157.

Carter NS, Fairlamb AH (1993). Arsenical-resistant trypanosomes lack an unusual adenosine transporter. Nature 361: 173–176.

Chappuis F, Loutan L, Simarro P, Lejon V, Buscher P (2005). Options for field diagnosis of human African trypanosomiasis. Clin Microbiol Rev 18: 133–146.

Courtioux, B., S. Bisser, P. M'Belesso, E. Ngoungou, M. Girard, A. Nangouma, T. Josenando, M. O. Jauberteau-Marchan, and B. Bouteille. 2005. Dot enzyme-linked immunosorbent assay for more reliable staging of patients with human african trypanosomiasis. J Clin Microbiol 43:4789-95.

Cox, F. E. (2002). History of human parasitology. Clin Microbiol Rev 15:595-612.

Croft SL, Brazil RP (1982). Effect of pentamidine isethionate on the ultrastructure and morphology of Leishmania mexicana amazonensis in vitro. Ann Trop Med Parasitol 76: 37–43.

Damper D, Patton CL (1976). Pentamidine transport and sensitivity in brucei-group trypanosomes. J Protozool 23: 349–356.

Das BP, Boykin DW (1977). Synthesis and antiprotozoal activity of 2,5-bis(4-guanylphenyl)furans. J Med Chem 20: 531–536.

de Koning HP (2001). Uptake of pentamidine in Trypanosoma brucei brucei is mediated by three distinct transporters: implications for cross-resistance with arsenicals. Mol Pharmacol 59: 586–592.

Deborggraeve, S., F. Claes, T. Laurent, P. Mertens, T. Leclipteux, J. C. Dujardin, P. Herdewijn, and P. Buscher. 2006. Molecular dipstick test for diagnosis of sleeping sickness. J Clin Microbiol 44:2884-9.

Denise H, Barrett MP (2001). Uptake and mode of action of drugs used against sleeping sickness. Biochem Pharmacol 61: 1–5.

Doua F, Yapo FB (1993). Human trypanosomiasis in the Ivory Coast – therapy and problems. Acta Tropica 54: 163–168.

Eisenberger MA, Reyno L (1994). Suramin. Cancer Treat Rev 20: 259–273.

Fairlamb AH (2003). Chemotherapy of human African trypanosomiasis: current and future prospects. Trends Parasitol 19: 488–494.

Fairlamb AH, Bowman IBR (1980). Uptake of the trypanocidal drug suramin by bloodstream forms of Trypanosoma brucei and its effect on respiration and growth-rate in vivo. Mol Biochem Parasitol 1: 315–333.

Fairlamb AH, Henderson GB, Bacchi CJ, Cerami A (1987). In vivo effects of difluoromethylornithine on trypanothione and polyamine levels in blood-stream forms of Trypanosoma brucei. Mol Biochem Parasitol 24: 185–191.

Fevre EM, Picozzi K, Fyfe J, Waiswa C, Odiit M, Coleman PG et al. (2005). A burgeoning epidemic of sleeping sickness in Uganda. Lancet 366: 745–747.

Hentzer B, Kobayasi T (1977). The ultrastructural changes of Leishmania tropica after treatment with pentamidine. Ann Trop Med Parasitol 71: 157–166.

Hide, G. (1999). History of sleeping sickness in east africa. Clin Microbiol Rev 12:112-25.

Ismail MA, Brun R, Easterbrook JD, Tanious FA, Wilson WD, Boykin DW (2003). Synthesis and antiprotozoal activity of aza-analogues of furamidine. J Med Chem 46: 4761–4769.

Jannin, J., and P. Cattand. 2004. Treatment and control of human African trypanosomiasis. Curr Opin Infect Dis 17:565-71.

Kaur M, Reed E, Sartor O, Dahut W, Figg WD (2002). Suramin's development: what did we learn? Invest New Drugs 20: 209–219.

Keiser J, Stich A, Burri C (2001). New drugs for the treatment of human African trypanosomiasis: research and development. Trends Parasitol 17: 42–49.

Ma¨ser P, Sutterlin C, Kralli A, Kaminsky R (1999). A nucleoside transporter from Trypanosoma brucei involved in drug resistance. Science 285: 242–244.

Mathis AM, Holman JL, Sturk LM, Ismail MA, Boykin DW, Tidwell RR et al. (2006). Accumulation and intracellular distribution of antitrypanosomal diamidine compounds DB75 and DB820 in African trypanosomes. Antimicrob Agents Chemother 50: 2185–2191.

Matovu E, Stewart ML, Geiser F, Brun R, Maser P, Wallace LJM et al. (2003). Mechanisms of arsenical and diamidine uptake and resistance in Trypanosoma brucei. Eukaryot Cell 2: 1003–1008.

Pholig, G., S. Bernhard, J. Blum, C. Burri, A. Mpanya Kabeya, J.-P. Fina Lubaki, A. Mpoo Mpoto, B. Fungula Mununguu, G. Kambau Manesa Deo, P. Nsele Mutantu, F. Mbo Kuikumbi, A. Fukinsia Mintwo, A. Kayeye Mununguu, A. Dala, S. Macharia, C. Miaka Mia Bilenge, V. Kande Betu Ku Mesu, J. Ramon Franco, N. Dieyi Dituvanga, and C. Olson. 2008. Phase 3

trial of pafuramidine maleate (DB289), a novel, oral drug, for treatment of first stage sleeping sickness: safety and efficacy, abstr. 542. 57th Meet. Am. Soc. Trop. Med. Hyg., New Orleans.

McCulloch R (2004). Antigenic variation in African trypanosomes: monitoring progress. Trends Parasitol 20: 117–121.

Pepin J, Milord F (1994). The treatment of human African trypanosomiasis. Adv Parasitol 33: 1–47.

Phillips MA, Wang CC (1987). A Trypanosoma brucei mutant resistant to alpha-difluoromethylornithine. Mol Biochem Parasitol 22: 9–17.

Sands M, Kron MA, Brown RB (1985). Pentamidine – a review. Rev Infect Dis 7: 625–634.

Saulter JY, Kurian JR, Trepanier LA, Tidwell RR, Bridges AS, Boykin DW et al. (2005). Unusual dehydroxylation of antimicrobial amidoxime prodrugs by cytochrome b5 and NADH cytochrome b5 reductase. Drug Metab Dispos 33: 1886–1893.

Simpson L (1986). Kinetoplast DNA in trypanosomatid flagellates. Int Rev Cytol 99: 119–179.

Stewart ML, Krishna S, Burchmore RJS, Brun R, de Koning HP, Boykin DW et al. (2005). Detection of arsenical drug resistance in Trypanosoma brucei with a simple fluorescence test. Lancet 366: 486–487.

Stich, A., M. P. Barrett, and S. Krishna. 2003. Waking up to sleeping sickness. Trends Parasitol 19:195-7.

Sturk LM, Brock JL, Bagnell CR, Hall JE, Tidwell RR (2004). Distribution and quantitation of the anti-trypanosomal diamidine 2,5-bis(4-amidinophenyl)furan (DB75) and its N-methoxy prodrug DB289 in murine brain tissue. Acta Trop 91: 131–143.

Thuita, J. K., S. M. Karanja, T. Wenzler, R. E. Mdachi, J. M. Ngotho, J. M. Kagira, R. R. Tidwell, and R. Brun. 2008. Efficacy of the diamidine DB75 and its prodrug DB289, against murine models of human African trypanosomiasis. Acta Trop. 108:6–10.

Vanschaftingen E, Opperdoes FR, Hers HG (1987). Effects of various metabolic conditions and of the trivalent arsenical melarsen oxide on the intracellular levels of fructose 2,6-bisphosphate and of glycolytic-intermediates in Trypanosoma brucei. Eur J Biochem 166: 653–661.

Voogd TE, Vansterkenburg ELM, Wilting J, Janssen LHM (1993). Recent research on the biological activity of suramin. Pharmacol Rev 45: 177–203.

Vreysen MJ, Saleh KM, Ali MY, Abdulla AM, Zhu ZR, Juma KG et al. (2000). Glossina austeni (Diptera: Glossinidae) eradicated on the island of Unguja, Zanzibar, using the sterile insect technique. J Econ Entomol 93: 123–135.

Wang MZ, Saulter JY, Usuki E, Cheung YL, Hall M, Bridges AS et al. (2006). CYP4F enzymes are the major enzymes in human liver microsomes that catalyze the O-demethylation of the antiparasitic prodrug DB289 [2,5-bis(4-amidinophenyl)furan-bis-O-methylamidoxime]. Drug Metab Dispos 34: 1985–1994.

Werbovetz K (2006). Diamidines as antitrypanosomal, antileishmanial and antimalarial agents. Curr Opin Investig Drugs 7: 147–157.

WHO http://www.who.Int/mediacentre/factsheets/fs259/en/.

Wierenga RK, Swinkels B, Michels PA, Osinga K, Misset O, Van Beeumen J et al. (1987). Common elements on the surface of glycolytic enzymes from Trypanosoma brucei may serve as topogenic signals for import into glycosomes. EMBO J 6: 215–221.

CHAPTER 2

IDENTIFICATION OF NOVEL METABOLITES CATALYZED BY CYP1A1 AND CYP1B1 FROM AN ORALLY ACTIVE *O*-METHYL AMIDOXIME PRODRUG DB844 FOR THE TREATMENT OF CNS TRYPANOSOMIASIS

A. ABSTRACT

N-methoxy-6-{5-[4-(*N*-methoxyamidino)phenyl]-furan-2-yl}-nicotinamidine (DB844) is an orally active prodrug against CNS African trypanosomiasis in mouse and monkey models. *In vivo*, it is biotransformed to form the active diamidine 6-[5-(4-amidinophenyl)-furan-2-yl]nicotinamidine (DB820) through a very complex metabolic pathway. Multiple cytochrome P450s, including CYP4F2, CYP4F3B, CYP2J2, CYP1A2, CYP1A1 and CYP1B1, catalyze DB844 *O*-demethylation, the first step in this pathway. Recently we discovered that extra-hepatic CYP1A1 and CYP1B1, but not CYP4F2, CYP4F3B, CYP2J2 and CYP1A2, catalyze DB844 conversion to a novel unstable metabolite (MX), which subsequently degrades to another unknown metabolite (MY). MX molecular ion was determined by LC-MS as *m/z* 351.1, which corresponds to a loss of "NH" from the prodrug. LC-MS^3 spectra of MX formed from unlabeled and deuterium labeled DB844 verified that the methyl group on the pyridine side remained in these compounds. Neither the pyridine ring nor the phenyl ring is altered. MX degraded to MY when stored in aqueous solution at room temperature overnight. LC-MS analysis of MY indicated that it lost "NH" and gained "O" from MX. With this information, the structures of MX and MY were proposed. MY (methyl 4-(5-(5-(N'-methoxycarbamimidoyl)pyridin-2-yl)furan-2-yl)benzoate) was synthesized and has been confirmed to be identical to the degraded stable metabolite MY using LC-MS^3. The potential anti-CNS trypanosomal activity and toxicity of MX and MY need further investigation.

B. INTRODUCTION

African trypanosomiasis, also known as African sleeping sickness, is a parasitic infection that has a 100% fatality rate if left untreated. Drugs currently available for the treatment of trypanosomiasis suffer from poor oral bioavailability and therefore must be administered through intravenous or intramuscular injections, which makes it difficult to properly treat patients in rural Africa where this disease is endemic. Furthermore, many of these drugs are highly toxic. Melarsoprol causes fatal encephalopathy in 2 to 12% of patients (Pepin and Milord 1991); although pentamidine itself is not so highly toxic, it can be converted by cytochrome P450 (CYP) to more toxic metabolites. 2,5-Bis(4-amidinophenyl)furan (furamidine; DB75), a dicationic structural analog of pentamidine, was developed as an alternative treatment for African trypanosomiasis (Das and Boykin 1977, Steck *et al.* 1982, Steck *et al.* 1981). Like many other trypanocides, furamidine has potent in vitro activity but suffers from poor oral bioavailability. The lipophilic methoxyamidine prodrug of furamidine, pafuramidine (DB289), was developed to improve the oral bioavailability of this drug and has recently completed Phase II trials for the treatment of primary stage trypanosomiasis. However, pafuramidine was not curative in mouse or monkey models of late stage infection (Brun, R. and Ndung'u, S.G., 2004, Personal communication) and thus several furamidmethoxime/furamidine analogs have since been synthesized and tested as alternative treatments for late stage infection (Ansede *et al.* 2004; Ismail *et al.* 2003; Ismail *et al.* 2004).

6-[5-(4-amidinophenyl)-furan-2-yl]nicotinamidine (DB820) is an aza-analogue of furamidine with potent in vitro antitrypanosomal activity (Scheme 2.1). However, like furamidine it suffers from poor oral activity because of its positively charged amidine groups.

The dimethoxyamidine prodrug of DB820, *N*-methoxy-6-{5-[4-(*N*-methoxyamidino)phenyl]-furan-2-yl}-nicotinamidine (DB844), has potent oral activity in mouse models of both early stage and CNS African trypanosomiasis (Ismail *et al.* 2003) and thus was considered as a promising new prodrug for treating late stage human infection. However, severe dose limiting gastro intestinal toxicity in trypanosome infected vercet monkeys was recently reported (Thuita et al., personal communication). Development of this compound has thus been dropped although new analoques continues to be pursued as CNS drug condidates. The metabolic pathway for the conversion of DB844 to DB820 in human liver microsomes (HLM) was reported (Ansede et al., 2005). *O*-demethylation and *N*-dehydroxylation reactions resulted in the production of eight metabolites including the active DB820 metabolite providing evidence that DB844 may effectively be metabolized to its active metabolite *in vivo*. Multiple cytochrome P450s, including CYP4F2, CYP4F3B, CYP2J2, CYP1A2, CYP1A1 and CYP1B1, catalyze the first *O*-demethylation step in the pathway (Wang et al., 2006). Therefore, the in vivo efficacy of DB844 is dependent on the level of expression, localization (hepatic vs. extrahepatic) and polymorphism of the CYP(s) involved in its metabolism. Recently, two novel and unexpected products (MX and MY) catalyzed by extrahepatic P450s CYP1A1 and CYP1B1 were discovered and indicated that the metabolic pathway of DB844 was more complex (Scheme 2.2). CYP1A1 and CYP1B1 expressions have been reported in several tissues including brain, kidney and lung. Over expression of CYP1B1 has been demonstrated in a number of primary human tumors (Maecker *et al*, 2003). In this report, LC-MS analysis of MX and MY provided clues to their structures and the mechanism of formation. These results will help us to elucidate the whole

biotransformation of the prodrug DB844 and better understand the efficacy and toxicity *in vivo* for the treatment of CNS trypanosomiasis in the future.

C. METHODS AND MATERIALS

Materials: DB844, M1A, M1B, M2, DB820 and deuterium labeled DB844 analogues were synthesized as reported (Boykin et al., 1996, Stephens et al., 2001; Anbazhagan et al., 2003). Human recombinant CYP1A1, CYP1B1, and CYP1A2 + P450 reductase Supersomes were purchased from BD Gentest (Bedford, MA, USA). Ammonium formate, formic acid, trifluoroacetic acid (TFA), β-NADPH, and other inorganic chemicals were from Sigma (St. Louis, MO, USA). *E. coli* expressing human CYP1A1 was made by Cypex Ltd., Scotland, UK.

DB844 depletion by human recombinant CYP1A1, CYP1B1, and CYP1A2.

Prior to each experiment, DB844 was prepared as 10 mM stock solution in DMSO. In the reaction mixtures, DB844 was added at a final concentration of 3 μM to 100 mM potassium phosphate buffer (pH 7.4) supplemented with 3.3 mM $MgCl_2$. Human recombinant CYPs were added at a final concentration of 50 pmol /ml for CYP1A1, CYP1B1 or CYP1A2. The reaction mixtures were incubated at 37^{o}C for five min prior to the addition of 1 mM NADPH to initiate the reaction. Aliquots (250 μL) were taken and the reactions were terminated by the addition of 125 μL of acetonitrile and samples were placed on ice. Precipitated protein was removed by centrifugation (21,000 x g for 10 min) and the supernatant was removed and placed in amber HPLC vials and sealed with Teflon lined caps. Samples were analyzed immediately by LC-UV with mobile phase gradient S as described below and DB844 was quantitated using DB844 standards at different concentrations for calibration. Experiments were performed in triplicate and data of average ± standard deviations are presented.

DB844 metabolite formations by human recombinant CYP1A1, CYP1B1, and CYP1A2.

Reaction mixtures were similar as described above, except that human recombinant CYPs were added at optimized final concentrations of 10 pmol /ml for CYP1A1, and 50 pmol/ ml for CYP1B1 or CYP1A2 to achieve comparable metabolism profiles with suitable amount of metabolites. The reactions were carried out, and the samples were processed the same way as described in the DB844 depletion studies. Samples were analyzed immediately by LC-UV and LC-MS with mobile phase gradient S as described below.

Scale up generation and purification of MX and MY.

Scale up generation of MX, MY by *E. coli* expressing human CYP1A1 was done by Cypex Ltd., Scotland, UK. Briefly, DB844 at a final concentration of 10 μM was incubated with *E. coli* expressing human CYP1A1 suspended in culture medium. Pillot experiments were conducted to optimize the incubation conditions and harvest time for the maximal production of MX and MY. Then, 2 liters of scale up incubation was performed under the optimized conditions and the reaction was quenched by addition of equal volume of ice cold acetonitrile. Then *E. coli* was span down and supernatant solution was transferred to another receptacle. The pallet was extracted by ice cold acetonitrile and was spun down again. The supernatant was combined with the previous solution and aliquoted into small 50 ml centrifuge tubes and stored on dry ice prior to usage. The MX and MY identities were confirmed by retention times and masses of LC-MS compared to metabolic samples from the human recombinant CYP1A1 reaction.

This scale up sample was concentrated 200 fold with solid phase extraction followed by elution with acetonitrile. Then, MX and MY were purified by LC-UV with a semi-prep Bonus-RP column and gradient S as described in LC-UV conditions. In order to get better separation of MX from the adjacent peak M1B, the slow gradient S was applied and the

retention times of metabolites were longer than ones under gradient A. MX and MY were collected within a narrow range of time at their retention times. These purified samples were immediately passed through solid phase extraction cartridge to remove buffer and reconstituted in 1:1 acetonitrile / water.

Conversion of MX to MY.

One ml samples from the quenched scale up reaction of MX and MY, and 100 µl purified MX were kept at room temperature. Forty µl samples were taken at time 0 and time 6 h and analyzed by LC-UV immediately. The chromatography curves were overlaid with same ratio of retention time and UV signal intensity. The peaks of MX and MY were expanded to show the peak height changes of MX and MY.

Metabolic studies of deuterium labeled DB844.

Deuterium labeled DB844 analogues, including DB844-D_4, DB844-CD_3(py), and DB844-CD_3(phe), were incubated with human recombinant CYP1A1 under the same conditions as described for DB844 metabolite formation. The quenched reaction samples were concentrated 10 fold by solid phase extraction and elution with acetonitrile. Then, MX and MY formed from deuterium labeled DB844 in these concentrated samples were analyzed by LC-UV and LC-MS^3.

HPLC-UV conditions.

Analysis of DB844 and its metabolites or purification of MX and MY were performed on an Agilent 1100 series HPLC with a UV detector. Samples were separated on an Agilent ZORBAX bonus-RP column (2.1 x 150 mm, 5 µm) for analytical purpose or an Agilent semi-prep ZORBAX bonus-RP column (9.4 x 250 mm, 5 µm) for purification purpose. The system was operated at 0.35 mL/min with a gradient mixing mobile phase buffer A (0.025%

TFA in deionized water) and mobile phase buffer B (0.025% TFA in acetonitrile: deionized water/ 80:20). Mobile phase gradient F was used for initial analysis of DB844 depletion and metabolites formation by human recombinant CYP1s: 90% buffer A plus 10 % buffer B at time 0 min, to 100% buffer B at time 22 min, followed by post washing with 90% buffer A plus 10 % buffer B for 6 min. Mobile phase gradient S was used for later purification of MX and MY, confirmation of purified products, analysis of conversion from MX to MY and LC-MS^3 for fragmentation profiles: 90% buffer A plus 10 % buffer B at time 0 min, to 40 % buffer A plus 60 % buffer B at time 25 min, to 100 % buffer B at time 28 min and keep 100% buffer B until 33 min, followed by post washing with 90% buffer A plus 10 % buffer B for 6 min. The wave length of the UV detector was set to 359 nm. The columns were maintained at room temperature. For analytical purposes, 10 µl samples were injected. For purification purposes, up to 400 µl samples were injected without saturation of the semi-prep column.

LC-MS conditions:

Qualitative assessments of DB844 and its metabolites were performed on an Agilent 1100 series HPLC coupled to a LC-MS ion trap mass spectrometer. HPLC conditions were described as above. The HPLC was directly linked to the ion trap MS equipped with a pneumatically assisted electrospray (ESI) interface operated in the positive mode. Nitrogen was used as the nebulizer gas at 45 psi and as the drying gas heated to 350°C at a flow rate of 9 L/min to evaporate solvents in the spray chamber. The instrument was tuned with the Agilent Tuning mix. The voltage settings for the API electrospray interface were: 0 V (grounded); sampling capillary, -3000 V; end plate offset, -500 V; capillary exit offset, 35 V. The other lenses (skimmer, octopole, and lens voltages) were set to the optimal values for the

transmission of the Agilent tuning compound ions at *m/z* 322 and 622. The trap drive radiofrequency amplitude was set at 43 *m/z* (minimum value for stable mass in the ion trap) in the ion trap while ions were being accumulated from the API source. The ion charge control (ICC) was set to allow a maximum of 20,000 charges or 50 ms. Full-scan mass spectra were acquired with a scan rate of 13,000 *m/z* per second over a range of *m/z* 100-650. Auto MS/MS and MS/MS/MS was used to acquire MS2 and MS3 spectra for ions between *m/z* 200 and 650 that were above a threshold of 40,000 counts. The MS2 and MS3 spectra were acquired using a fragmentation amplitude ramp (end cap voltage) of 0.3 to 2 V in 40 ms. The CID spectra were generated at a q_z of 0.35 with helium collision gas. Data was processed on Bruker version 4.1 data analysis software.

Synthesis of proposed MY.

A mixture of 2-bromo-5-(4-methoxyamidino-2-pyridyl)furan (296 mg, 1.0 mmol) (prepared according to Ismail et al., 2004), (4-methoxycarbonylphenyl)boronic acid (200 mg, 1.1 mmol, purchased from Combi-Blocks, Inc.), palladium acetate (10 mg, 4.5 mol%), and powdered potassium phosphate (420 mg, 2.0 mmol) in MeOH (12 mL) was stirred under nitrogen at room-temperature for 3 hr. The mixture was then diluted with water to give a green solid, which was filtered off and washed with water. Recrystallization from MeOH (~200 mL, with concentration to ~50 mL) gave, after standing overnight at room temperature, orange/tan crystals (114 mg, 32%), mp 231-234 ^{o}C.

D. RESULTS

DB844 depletion catalyzed by human recombinant CYP1A1, CYP1B1, and CYP1A2.

DB844 depletion by human recombinant CYP1A1, CYP1B1, and CYP1A2 was analyzed (figure 2.1). The human recombinant CYP1 family enzymes all showed the capacity to catalyze the metabolism of the prodrug DB844, which were confirmed by the loss of parent compound in the reactions. CYP1A1, CYP1B1 and CYP1A2 resulted in a 92.2 (± 3.6), 66.7 (± 7.4) and 75.3 (± 6.1) percent loss of prodrug after 30 min of incubation, respectively.

DB844 metabolite formation catalyzed by human recombinant CYP1A1, CYP1B1, and CYP1A2.

DB844 first underwent an *O*-demethylation to form either M1A or M1B mono-amidoxime/mono-methoxyamidine metabolites (figure 2.2), as previously reported (Ansede et al., 2005). The subsequent reduction of the amidoxime functionality required cytochrome b_5/b_5 reductase activity. Recombinant CYPs express no measurable levels of cytochrome b_5 activity to catalyze the amidoxime reduction, thus, the only metabolites that were formed from DB844 in recombinant CYPs were the products of an *O*-demethylation including M1A, M1B and M2 (DB821) (Scheme 2.1 for chemical structures and Scheme 2.2 for the metabolic pathway). The *O*-demethylation products M1A, M1B and M2 were observed in recombinant CYP1A1 and 1A2 catalyzed reactions, and M1A and M1B but no M2 were observed in recombinant CYP1B1catalyzed reaction. These known metabolites were identified by LC retention time and mass measured by full-scan ion trap MS compared with authentic standards. However, LC-UV analysis of the CYP1A1 and CYP1B1 reactions indicated the production of two additional metabolites with retention times MX (8.5 min) and MY (12.4 min) distinct from that of the three known demethylation metabolites M1A (9.1

min), M1B (8.3 min), and M2 (6.6 min) (figure 2.2). LC-MS also determined that the prodrug DB844 had a molecular ion of 366.2 *m/z*. M1A or M1B had a molecular ion of 352.2 *m/z*, which was consistent with a 14 *m/z* net loss of "CH_2" from the prodrug. M2 had a molecular ion of 338.2 *m/z*, which was consistent with a 28 *m/z* net loss of two "CH_2"s from the prodrug. However, MX had a molecular ion of 351.2 *m/z*, which indicated that it had an even number of nitrogen atoms, therefore most likely was a 15 *m/z* net loss of "NH" from the prodrug. So MX is not the same as the *O*-demethylation metabolites. LC-MS didn't solve the mass of MY under the same conditions due to its low abundance and high background noise when MY was eluted.

Scale up generation and purification of MX and MY.

To get stronger $LCMS^3$ signals for more structural information, 2 liter of scale up reaction was carried out to generate MX and MY. This sample was concentrated with solid phase extraction. MX and MY were purified by a semi-prep LC. Later Both LC-UV and LC-MS confirmed that MX and MY formed by *E.coli* expressing CYP1A1 were the same as those formed by human recombinant CYP1A1 and CYP1B1 (data not shown).

Conversion of MX to MY.

Although the reaction was quenched by acetonitrile and CYP1A1 was removed by precipitation, the amount of MX in the supernatant mixture decreased and the amount of MY increased after 6 h storage at room temperature, which were determined by LC-UV (figure 2.3A and 2.3 B.). However at the same conditions, prodrug DB844 and other metabolites M1, M2 remained the same in the mixture after 6 h storage. When MX was purified from the scale up sample by collecting MX at a narrow range of retention time (14.0 min) using semi-prep HPLC, MY was also found at the same time, as determined by LC-UV, although MY

had a retention time (28.2 min) much longer than MX under the same separation conditions. However, no prodrug or other metabolites M1A, M1B, or M2 was found in this purified MX sample by careful LC-UV full length scan and LC-MS full-ion scan, which excluded the possibility of MY contamination by overloading the reaction mixture sample to semi-prep column. Another possibility is that MX was converted to MY during purification. We also found after this purified MX was stored at room temperature for 10 h, it converted to MY (figure 2.3C).

This conversion was tested under different conditions and was found not to be dependent on light; it was slowed down by storage at lower temperatures of 4 ^{o}C, -20 ^{o}C, or -80 ^{o}C (data not shown). When the purified MX was dried down and reconstituted in organic solvent DMSO, it was stable for more than several months. Later in order to reduce loss of MX, purified MX was reconstituted in DMSO immediately after purification and stored it at -80 ^{o}C until just prior to usage.

These results indicated that MX could slowly convert to MY in quenched reaction mixtures, during purification, and during storage after purification. Much higher stability of MX in DMSO without water indicated that conversion from MX to MY required water. So it showed that a sequential pathway exits from prodrug DB844 to MX, which was catalyzed by CYP1A1 and CYP1B1, and from MX to MY, which required water instead of any enzyme.

LC-MS^3 fragmentation spectra of M1B, MX, MY formed from DB844 and deuterium labeled DB844.

Samples prepared from CYP1A1reaction with DB844 and purified as described in the methods and subjected to ion trap mass spectrometry for metabolite identification. LC-MS^3 fragmentation spectra of M1B, MX, MY formed from DB844 were shown in fig 4 . M1B had a molecular ion $[M1B+H]^+$ of 352.2 *m/z* (figure 2.4A). This M1B parent ion underwent collision induced dissociation (CID) to form a daughter molecular ion of 305.1 *m/z*, which was 47 *m/z* loss corresponding to "OCH_3NH_2"on the pyridine ring side. This molecular ion (305.1 m/z) was selected to undergo another CID to form several daughter ions including a major one of 288.0 *m/z*, which was 17 *m/z* loss corresponding to "OH" on the phenyl ring side. MX had a molecular ion $[MX+H]^+$ of 351.3 *m/z* (figure 2.4B). Very interestingly, this MX parent ion formed a daughter ion of 304.1 *m/z*, which was also 47 *m/z* loss corresponding to "OCH_3NH_2". Then, this molecular ion (304.1 *m/z*) gave 2 major daughter molecular ions after another CID, which were 289.0 *m/z* (15 *m/z* loss corresponding to "CH_3") and 272.0 *m/z*. MY had a molecular ion $[MX+H]^+$ of 352.3 *m/z* (figure 2.4C). Due to the even value 352 *m/z*, MY should have an odd number of nitrogen. Since MY formed from MX in water without CYPs enzymes and MY had 1 *m/z* more than MX, it is very likely that MY was formed by net loss of "NH" and gain of "O" from MX.

Very interestingly, this MY parent ion also formed a daughter ion of 305.1 *m/z*, which was also 47 *m/z* loss corresponding to "OCH_3NH_2". Then, this molecular ion (305.1 *m/z*) gave one major daughter molecular ion after another CID, which was 273.0 *m/z*, and several minor daughter ions. These results showed that M1B, MX, and MY all had intact "OCH_3NH_2" on the pyridine ring side.

To further dissect the reaction site in the DB844 molecule to form MX and MY, deuterium labeled DB844s was incubated with CYP1A1 to generate metabolites. The reaction samples

were concentrated as described in the methods and applied to LC-MS^3 analysis (figure 2.5) MX formed from DB844-CD_3(py) showed a molecular ion of 354.1 *m/z*, which has 3 *m/z* more than MX from DB844, indicating that D_3 labeling was remained in MX. MS^2 generated a daughter ion 303.9 *m/z*, corresponding to 50 *m/z* loss of "OCD_3NH_2", indicating OCD_3NH_2 on the pyridine ring side was intact. MS^3 generated several daughter ions including 288.8 *m/z*, which was 15 *m/z* loss corresponding to "CH_3". Similar results were also found in LC-MS^3 analysis of MY formed from DB844-CD_3(py), that OCD_3NH_2 on the pyridine ring side was intact. When we repeated these experiments using DB844 with CD_3 labeled on the phenyl ring side (figure 2.6), we found consistently that "OCH_3NH_2" remained in MX, and MY. Very interestingly, MS^3 of MX gave two major daughter ions including one at 288.9 *m/z*, which was 18 *m/z* loss corresponding to "CD_3". So it also indicated that CD_3 was remained on the phenyl ring side after reaction to form MX from DB844-CD_3(phe).

LC-MS^2 analysis of MX formed from DB844 with D_4 labeled in the pheyl ring was also performed This MX had a molecular ion of 355.2 *m/z*, which was 4 *m/z* more than MX from DB844 without labeling (figure. 2.7). It indicated that the D_4 labeling in phenyl ring remained.

These LC-MS^3 results showed that metabolic reactions from DB844 by CYP1A1 and CYP1B1 to form MX and MY occurred on the phenyl ring side, while the pyridine side was intact. The methyl group on the phenyl ring side remained in MX and MY. MX had net loss of "NH" from DB844 and MY had net loss of "NH" and gain of "O" from MX.

Proposed metabolic reaction and MX and MY structures.

According to the structural information obtained from the above experiments, we proposed the reaction of MX and MY formation and their structures (figure. 2.8). First, CYP1A1 or

CYP1B1 inserted a molecular oxgen into the C=N double bond on the phenyl ring side to form a triangle structure, which was followed by an O-methyl bond shift to the carbon of the triangle structure, subsequently causing the NO bond to be broken with a NO leaving from the molecule and another double bond formed between the carbon and the other nitrogen. This product MX has calculated molecular weight of 350.0, the same as the experimental molecular weight. Then this MX underwent hydrolysis by being attacked by OH^- in water and replaced NH to finally form MY, which has net loss of "NH" and gain of "O" and matches the molecular weight 351.0.

Confirmation of MY structure by HPLC and LC-MS^3

The proposed MY structure (methyl 4-(5-(5-(N'-methoxycarbamimidoyl)pyridin-2-yl)furan-2-yl)benzoate) was synthesized as described in Methods (figure. 2.9).

Synthetic MY (CES-IX-32) had an LC retention time of 27.8 -28.3 min and molecular ion *m/z* of 352.2. This parent ion underwent CID to form one major fragment with *m/z* of 305.1, which underwent further CID to form four major fragments with *m/z* of 273.0, 245.0, 218.0, and 162.9. Under the same analytical conditions, metabolite MY showed the same LC retention time, *m/z* of the molecular ion, and the fragmentation pattern as the synthetic MY. Therefore, this novel metabolite MY was assigned the structure as proposed in figure. 2.10.

E. Discussion

MX, a novel metabolite, was formed from the antitrypanosomial prodrug DB844 by extra-hepatic CYP1A1 and CYP1B1, and had a molecular weight 350, representing a net loss of "NH". MX was different from the known *O*-demethylation metabolites M1A/B and M2. The amounts of MX and MY were very low. It became a challenge for us to solve their structure. We scaled up the generation of MX and MY using *E.coli* expressing CYP1A1 and purified MX and MY. We found that MX degraded to MY in water independent of enzyme activity. LCMS analysis indicated that MY had molecular weight 350 from a net loss of "NH" and gain of "O" from MX. Structural analysis of MX and MY formed from DB844 and deuterium labeled DB844 analogues by LC-MS^3 verified that the reaction happened on the phenyl ring side and the methyl group remained. The formation reaction of MX and MY was proposed and MY was synthesize and confirmed by LC retention time and MS^3 fragmentation pattern. So MY structure was assigned as methyl 4-(5-(5-(N'-methoxycarbamimidoyl)pyridin-2-yl)furan-2-yl)benzoate. Further study is needed to synthesize and confirm the MX structure.

MX and MY formation were not observed in *in vitro* metabolism studies with liver microsomes, which maybe because CYP1A1 and CYP1B1 are not expressed in liver. In the future, we need to investigate if MX and MY can form in other tissues and organs especially brain, lung, ovaries, testes, and prostate, where CYP1A1 and CYP1B1 are expressed. Since MX was an unstable metabolite, it may have the chance to react with biomolecules when it forms in cells, although the amounts of MX and MY were very low in our *in vitro* studies using human recombinant CYP1A1 and CYP1B1. So, the efficacy and toxicity of MX and MY need be investigated in the future.

A)

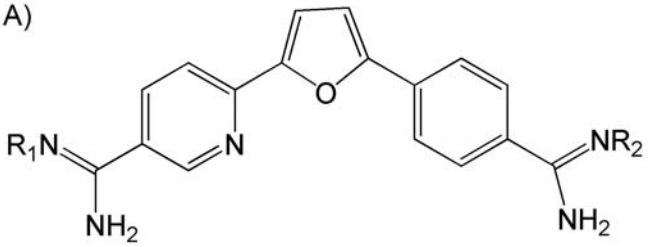

DB844	$R_1=R_2=OCH_3$
M1A	$R_1=OH$, $R_2=OCH_3$
M1B (DB1058)	$R_1=OCH_3$, $R_2=OH$
M2 (DB821)	$R_1=R_2=OH$
M3A	$R_1=H$, $R_2=OCH_3$
M3B	$R_1=OCH_3$, $R_2=H$
M4A	$R_1=H$, $R_2=OH$
M4B	$R_1=OH$, $R_2=H$
DB820	$R_1=R_2=H$
DB844-phenyl-D3	$R_1=OCH_3$, $R_2=OCD_3$
DB844-pyridine-D3	$R_1=OCD_3$, $R_2=OCH_3$
DB844-D6	$R_1= R_2=OCD_3$

B)

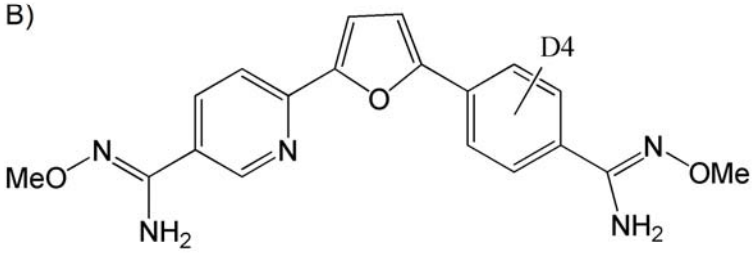

Scheme 2.1. Chemical structures of DB844 and its metabolites. (A)DB844, its known metabolites and DB844 with deuterium labeled on methoxy group. (B) DB844 deuterium labeled in the phenyl ring.

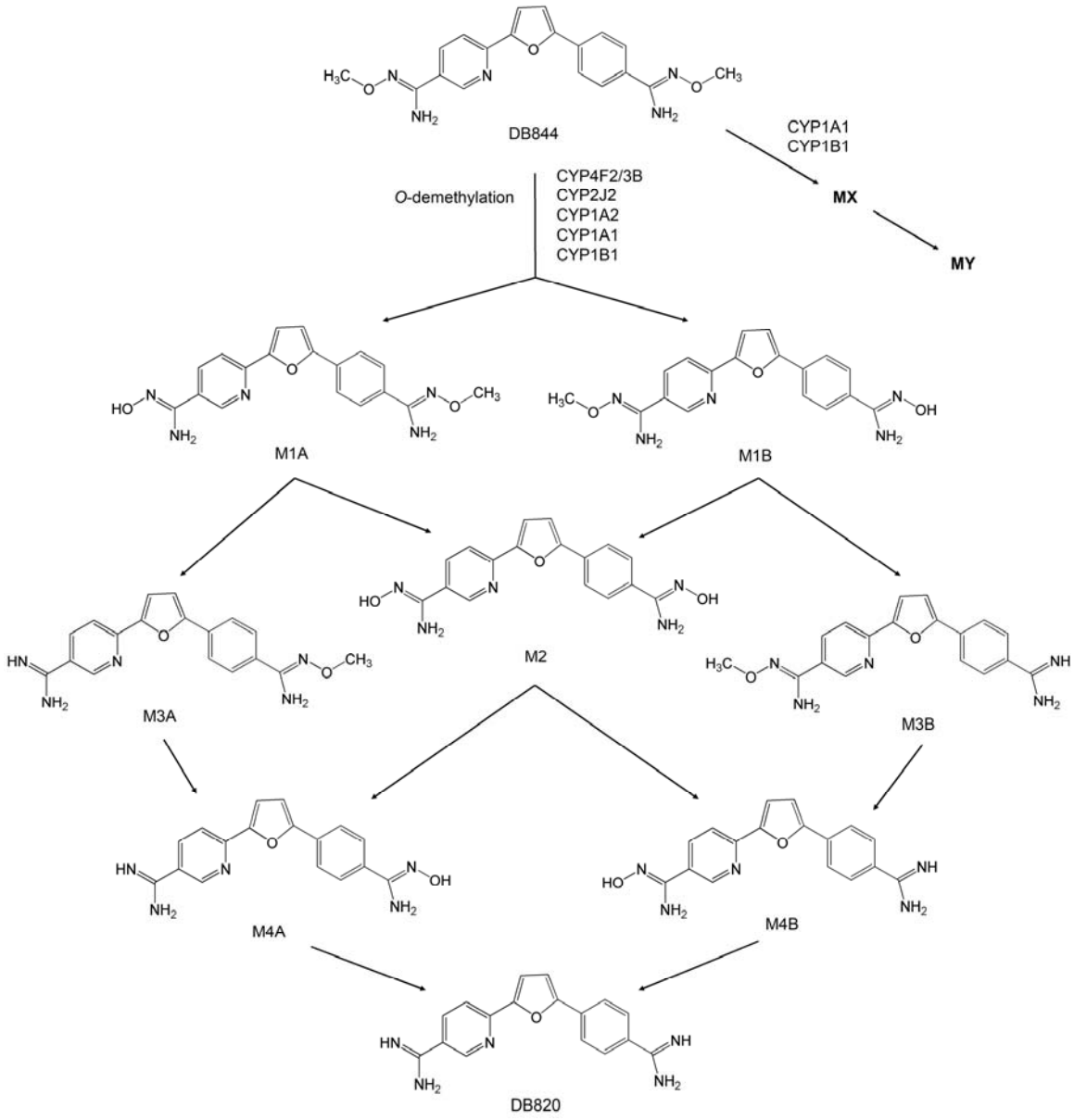

Scheme 2.2. Metabolic pathway of DB844. Sequential *O*-demethylations and *N*-dehydroxylations formed 8 known metabolites including M1A, M1B, M2, M3A, M3B, M4A, M4B, and the active diamidine DB820. The first *O*-demethylation can be catalyzed by CYP4F2/3B, CYP2J2, CYP1A2, CYP1A1, and CYP1B1. Two novel metabolites MX and its degradated MY were discovered. This reaction can be catalyzed by CYP1A1 or CYP1B1.

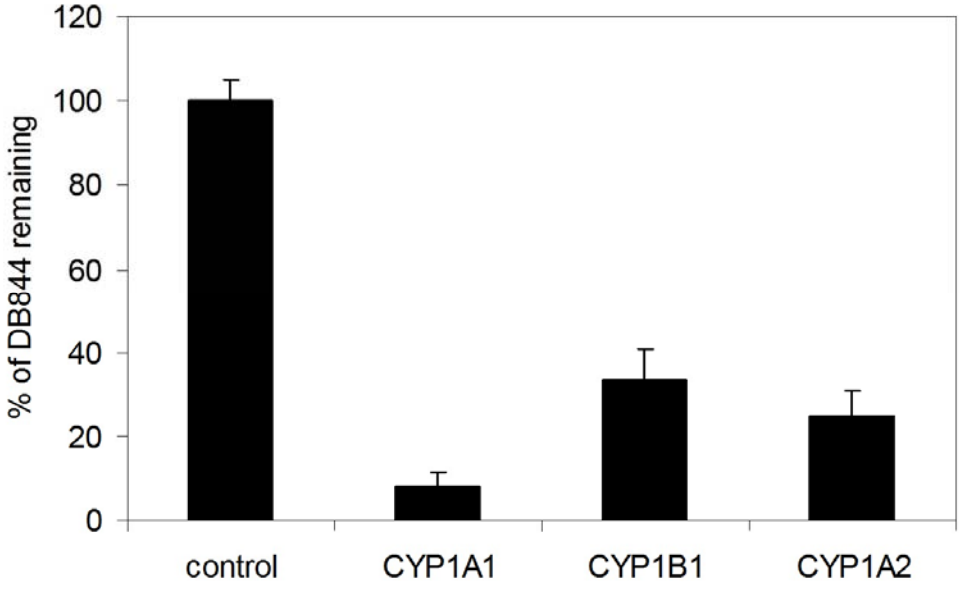

Figure 2.1. DB844 depletion catalyzed by human recombinant CYP1A1, CYP1B1, and CYP1A2. DB844 was incubated at a final concentration of 3 μM with 50 pmol/ml human recombinant CYP. Data represents the percent of DB844 remaining after 30 min incubation at 37^{o}C with individual human recombinant CYP. Experiments were performed in triplicate and the average ± standard deviations are presented.

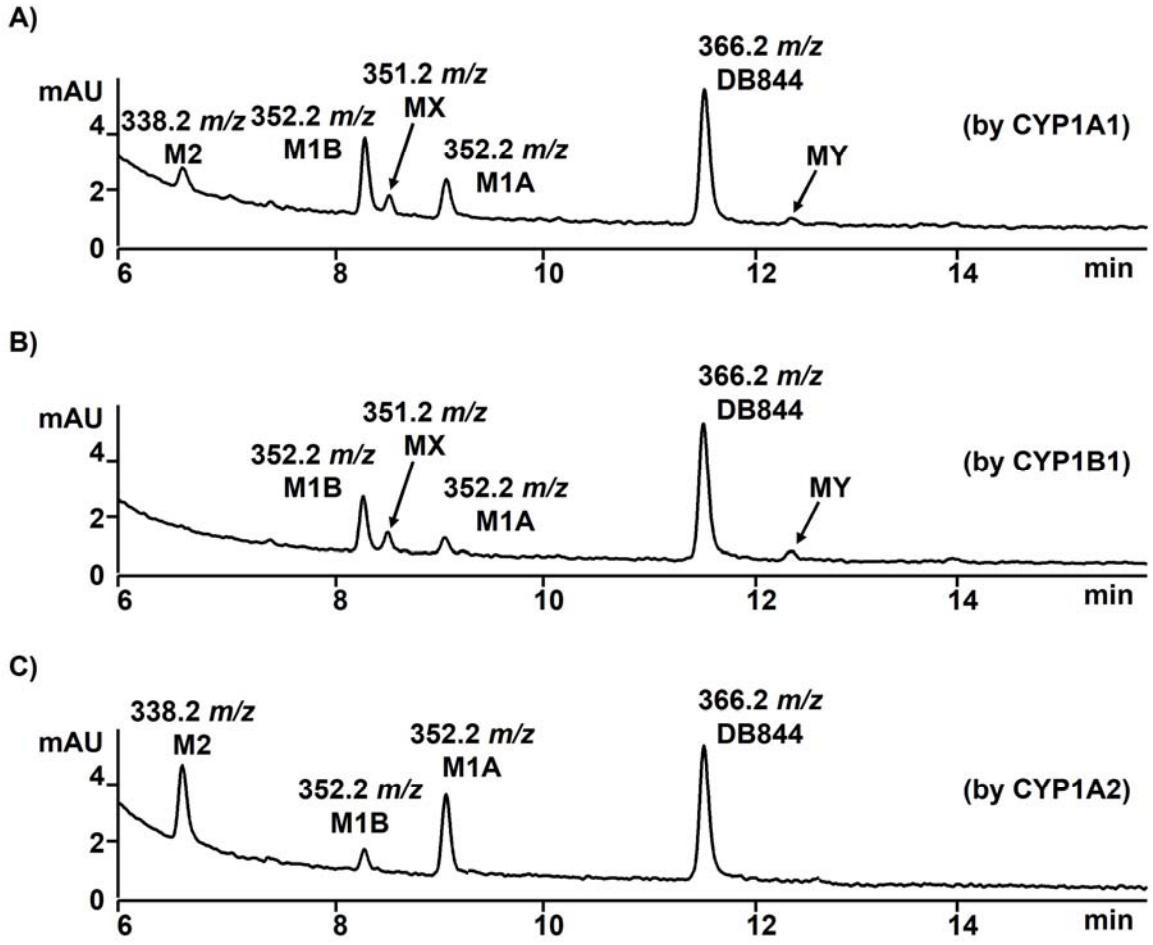

Figure 2.2. DB844 metabolite formation catalyzed by human recombinant CYP1A1, CYP1B1, and CYP1A2. DB844 was incubated at a final concentration of 10 μM with 10 pmol/ml CYP1A1, 50 pmol/ml CYP1B1 or CYP1A2 at 37 ^{o}C for 30 min. Metabolites were analyzed by LC-UV (359 nm) and identified by LC-MS.

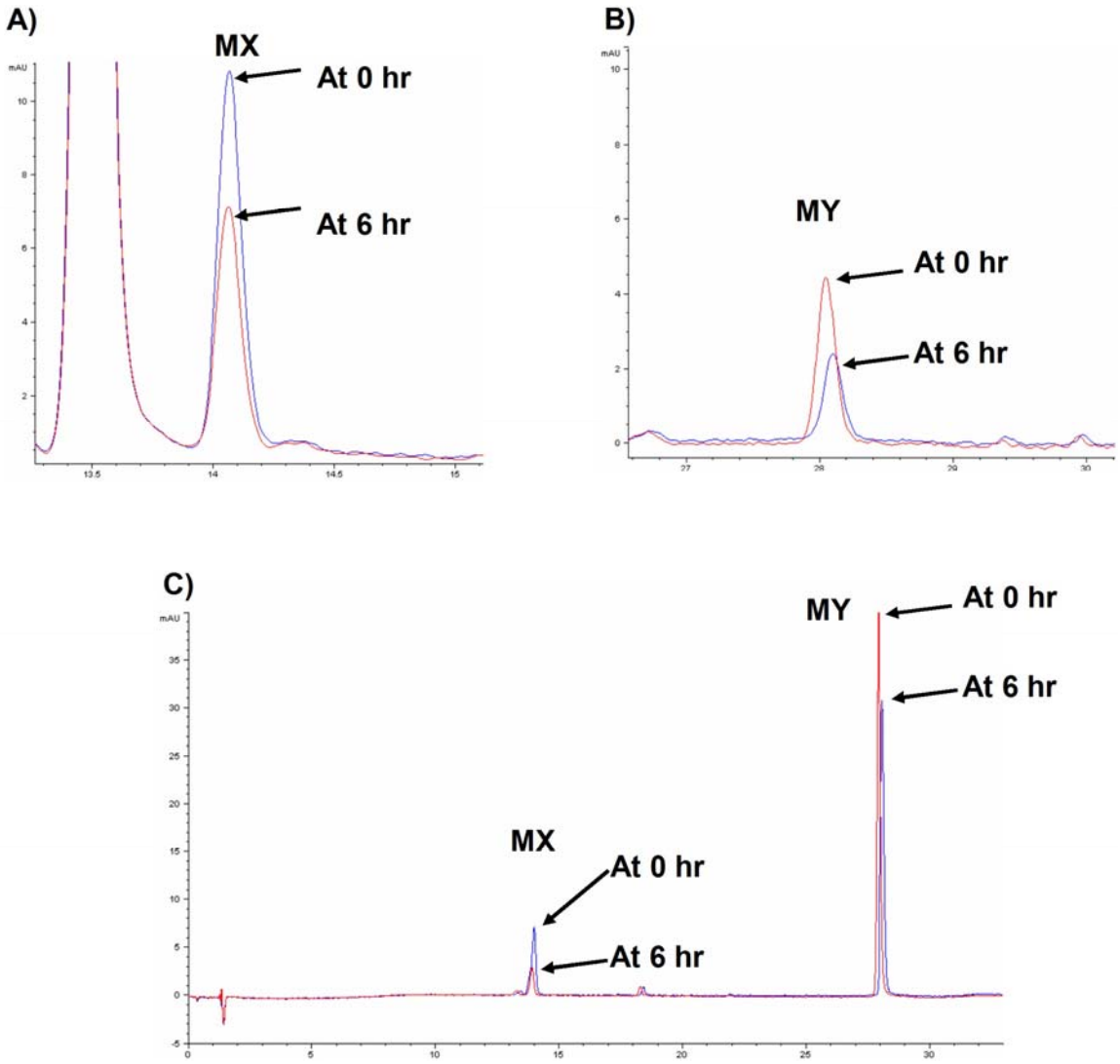

Figure 2.3. Conversion of MX to MY. The sample from the quenched scale up reaction, and purified MX were kept at room temperature for 0 hr and 6 hr and analyzed by LC-UV immediately. A) MX in the scale up reaction, and B) MY in the scale up reaction at different times. C) MX and MY in the purified MX sample at different time.

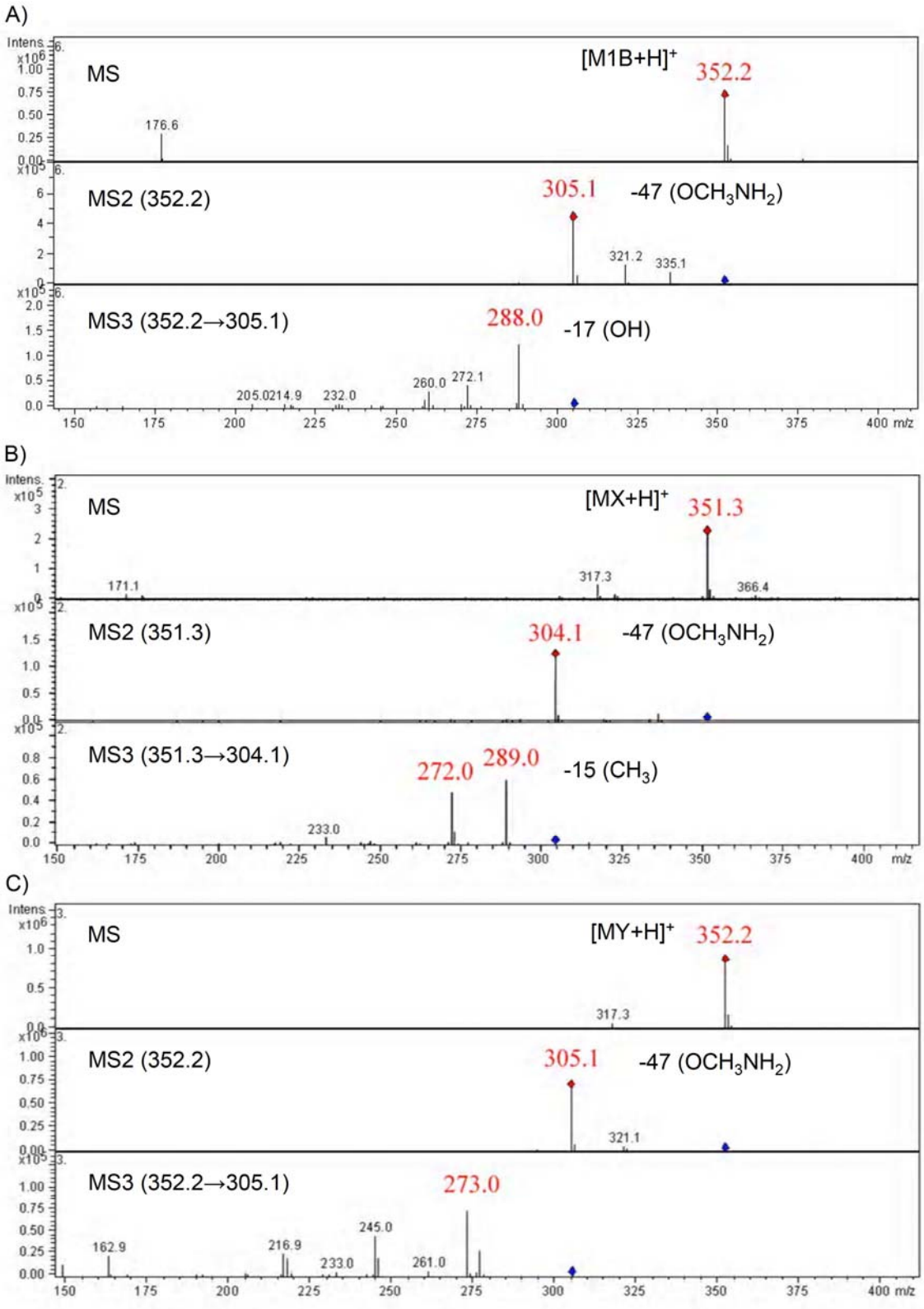

Figure 2.4. LC-MS^3 spectra of M1B, MX, and MY.

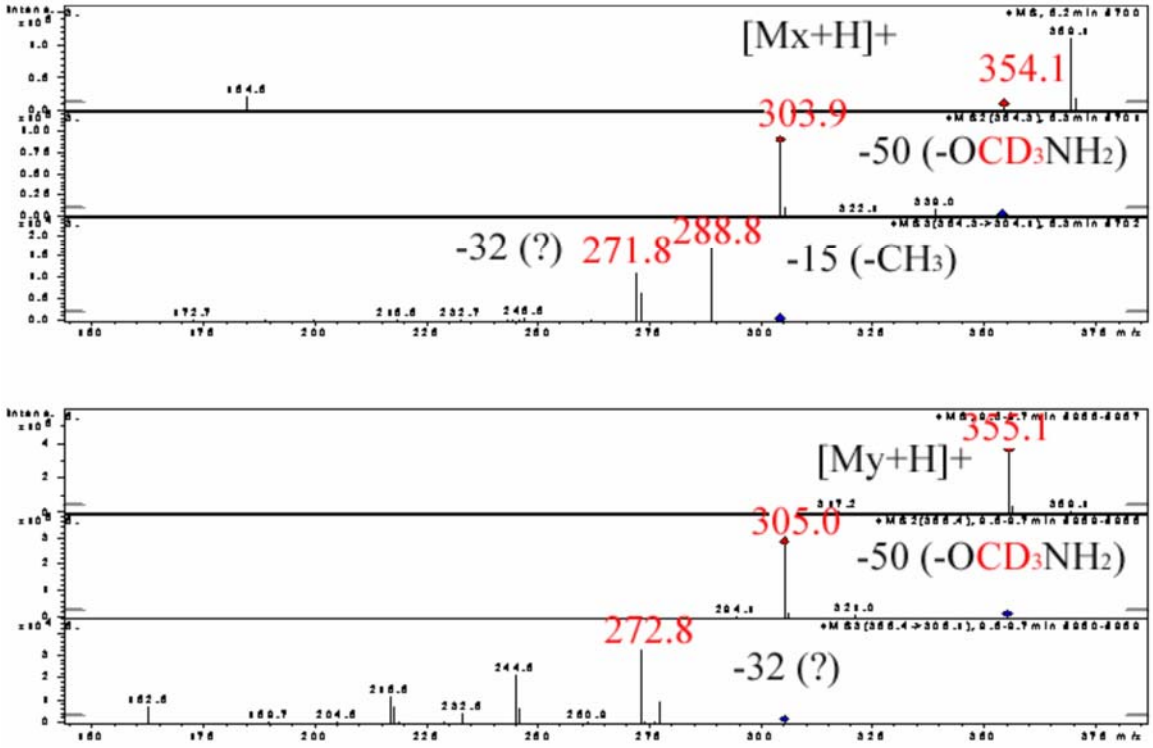

Figure 2.5. LC-MS^3 spectra of MX, MY, and M1B formed from DB844-CD_3(py).

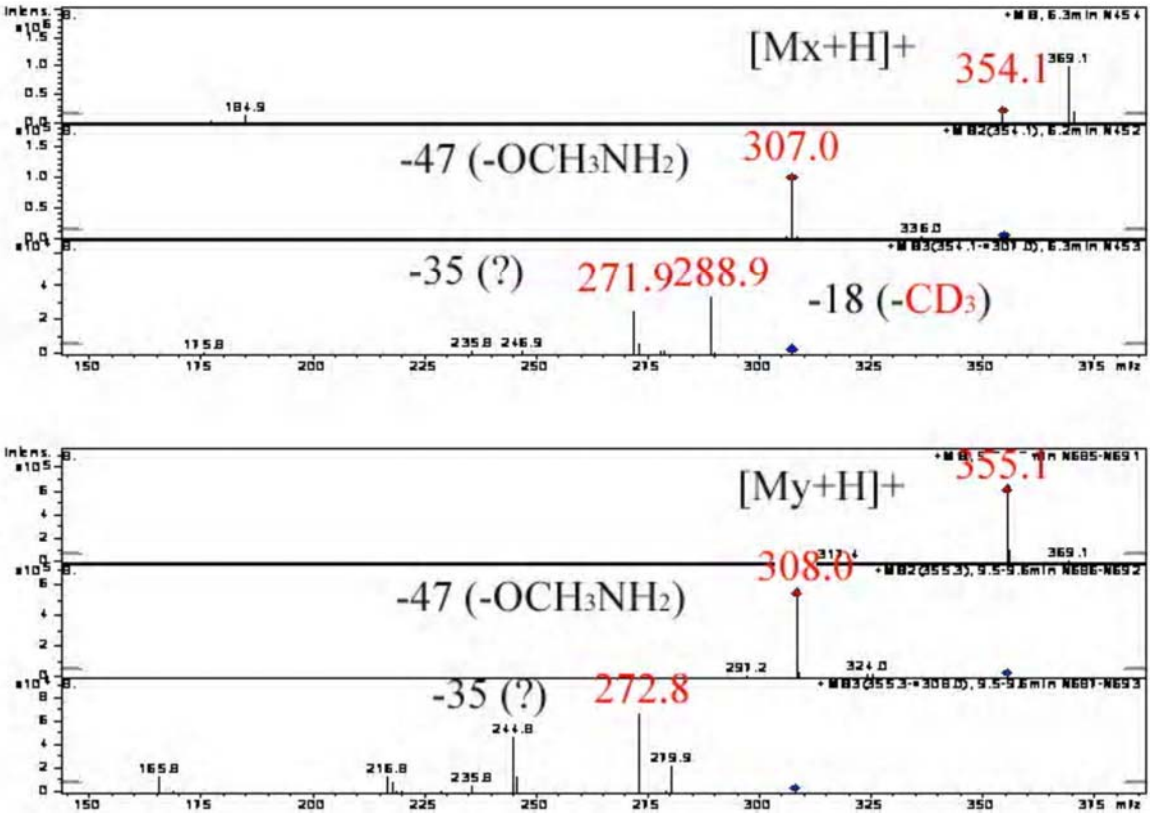

Figure 2.6. LC-MS^3 spectra of MX, MY, and M1B formed from DB844-CD_3(phe).

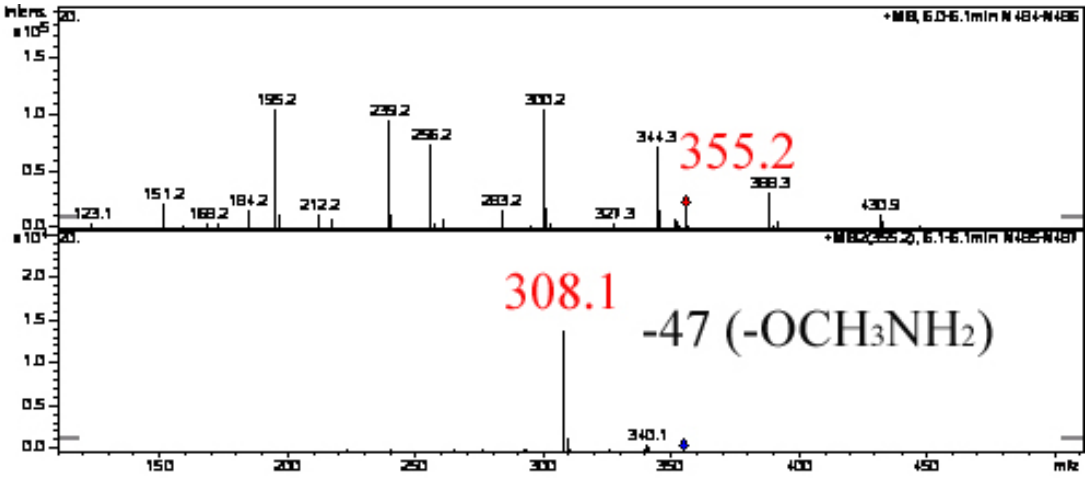

Figure 2.7. LC-MS^2 spectra of MX formed from DB844-D_4.

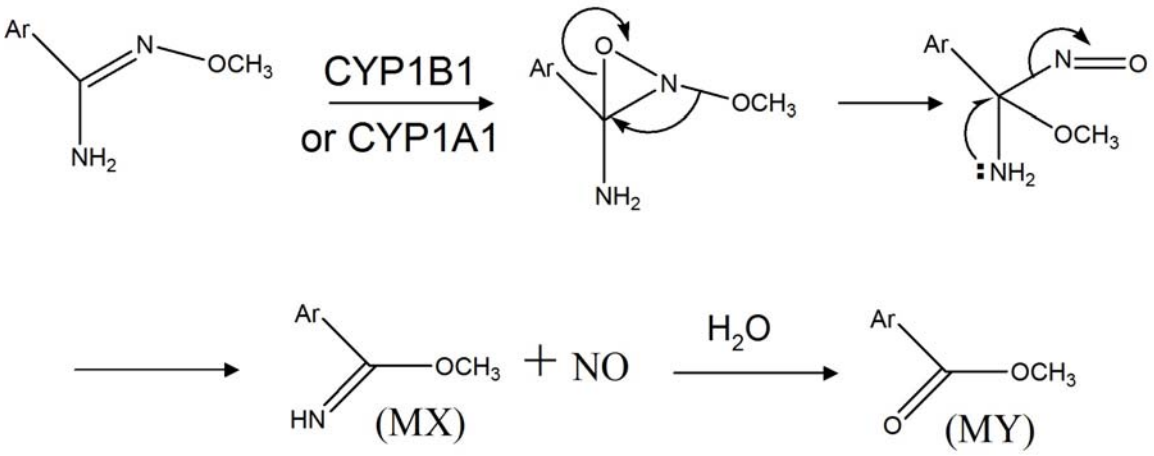

Figure 2.8. Proposed metabolic reaction to form MX and MY.

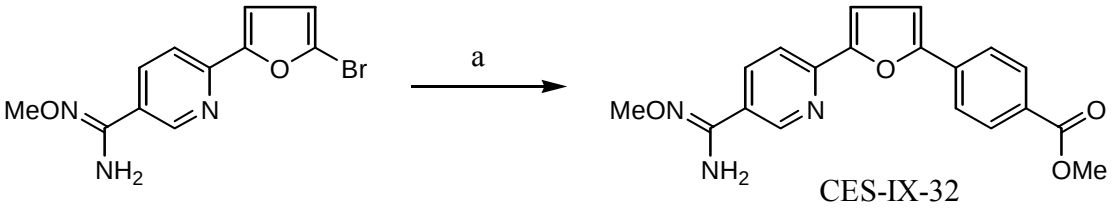

CES-IX-32

[a]Reagents and conditions: (4-carbomethoxyphenyl)boronic acid, $Pd(OAc)_2$, K_3PO_4, MeOH, 3hr

Figure 2.9. Reaction scheme of MY synthesis.

A)

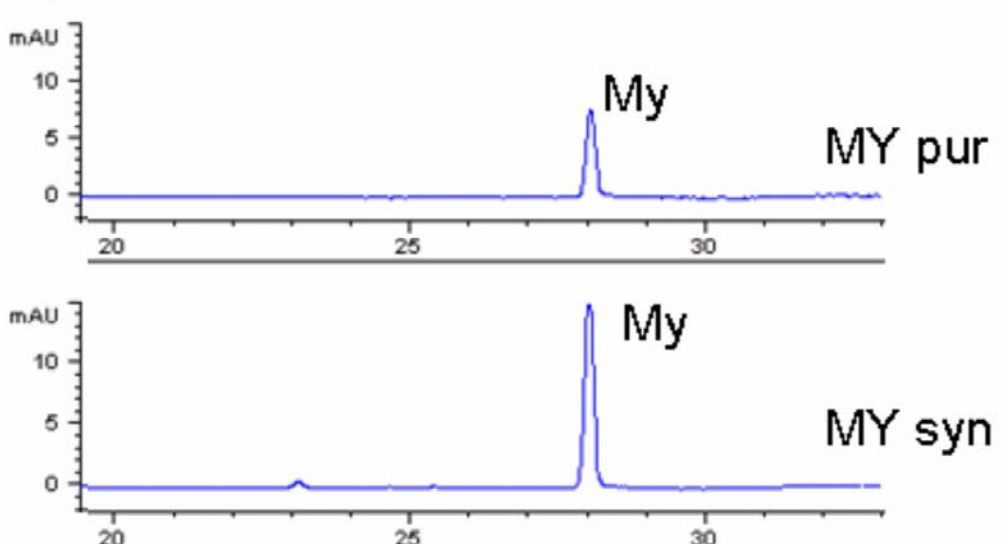
mAU
10
5
0
My
MY pur
20
25
30
mAU
10
5
0
My
MY syn
20
25
30

B)

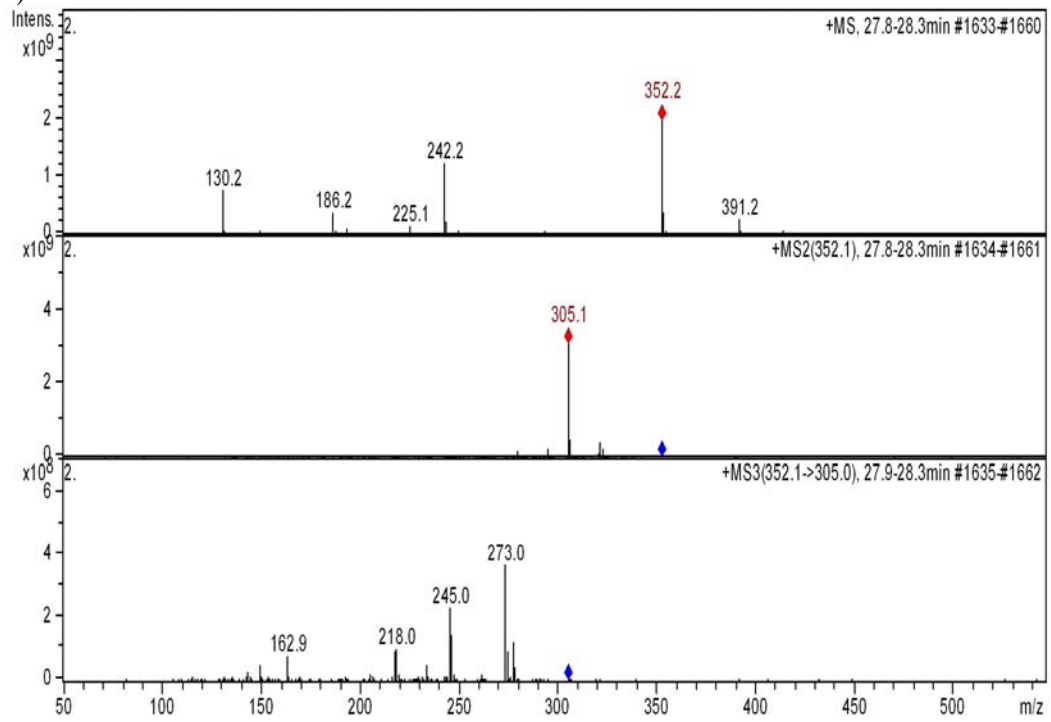
Intens.
x10^9
+MS, 27.8-28.3min #1633-#1660
352.2
242.2
130.2
186.2
225.1
391.2
x10^9
+MS2(352.1), 27.8-28.3min #1634-#1661
305.1
x10^8
+MS3(352.1->305.0), 27.9-28.3min #1635-#1662
273.0
245.0
162.9
218.0
50
100
150
200
250
300
350
400
450
500
m/z

C)

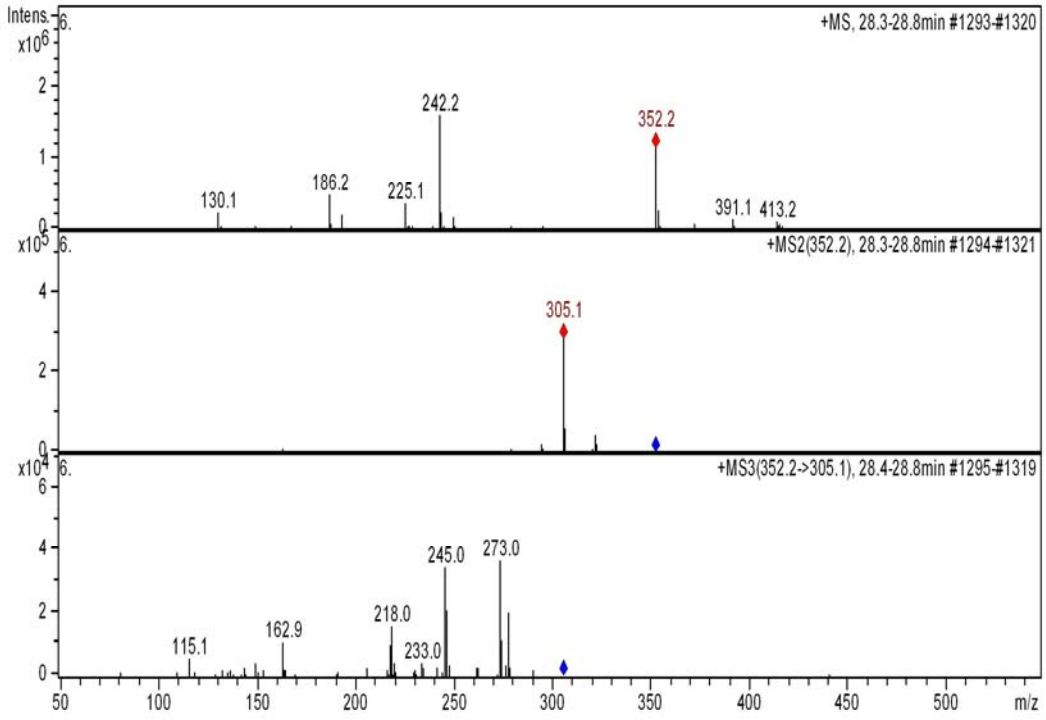

Figure 2.10. Confirmation of MY structure by HPLC and LC-MS^3.

F. Acknowledgments

This work was supported by the Bill and Melinda Gates Foundation and the Medicines for Malaria Venture.

G. References

Ansede JH, Voyksner RD, Ismail MA, Boykin DW, Tidwell RR, Hall JE. In vitro metabolism of an orally active O-methyl amidoxime prodrug for the treatment of CNS trypanosomiasis. Xenobiotica. 2005 Mar;35(3):211-26.

Boykin DW, Kumar A, Hall JE, Bender BC, Tidwell RR (1996). Anti- Pneumocystis activity of bis-amidoximes and bis-O-alkylamidoxime prodrugs. Bioorg Med Chem Lett 6: 3017–3020.

Das BP, Boykin DW (1977). Synthesis and antiprotozoal activity of 2,5-bis(4-guanylphenyl)furans. J Med Chem 20: 531–536. Davis RH, Lieu P, Ristow JL (1994). Neurospora mutants affecting polyamine-dependent processes and basic-amino-acid transport mutants resistant to the polyamine inhibitor, alpha-difluoromethylornithine. Genetics 138: 649–655.

Ismail, Mohamed A.; Boykin, David W.. Synthesis of deuterium-labelled 6-[5-(4-amidinophenyl)furan-2-yl]nicotinamidine and N-alkoxy-6-{5-[4-(N-alkoxyamidino)phenyl]furan-2-yl}nicotinamidines. Journal of Labelled Compounds & Radiopharmaceuticals 2004, 47(4), 233-242.

Ismail, Mohamed A.; Brun, Reto; Easterbrook, Judy D.; Tanious, Farial A.; Wilson, W. David; Boykin, David W.. Synthesis and antiprotozoal activity of aza-analogues of furamidine. Journal of Medicinal Chemistry (2003), 46(22), 4761-4769.

Legros D, Ollivier G, Gastellu-Etchegorry M, Paquet C, Burri C, Jannin J,and Buscher P. Treatment of human African trypanosomiasis-present situation and needs for research and development. The Lancet Infectious Diseases 2002 July, (2) : 437-40.

Maecker B, Sherr DH, Vonderheide RH, von Bergwelt-Baildon MS, Hirano N, Anderson KS, Xia Z, Butler MO, Wucherpfennig KW, O'Hara C, Cole G, Kwak SS, Ramstedt U, Tomlinson AJ, Chicz RM, Nadler LM, Schultze JL. The shared tumor-associated antigen cytochrome P450 1B1 is recognized by specific cytotoxic T cells. Blood. 2003 Nov 1;102(9):3287-94. Epub 2003 Jul 17

Pepin J, Milord F. African trypanosomiasis and drug-induced encephalopathy: risk factors and pathogenesis.Trans R Soc Trop Med Hyg. (1991) Mar-Apr;85(2):222-4.

Steck EA, Kinnamon KE, Davidson Jr DE, Duxbury RE, Johnson AJ, Masters RE (1982). Trypanosoma rhodesiense: evaluation of the antitrypanosomal action of 2,5-bis(4-guanylphenyl)furan dihydrochloride. Exp Parasitol 53: 133–144.

Stephens CE, Patrick DA, Chen H, Tidwell RR and Boykin DW (2001) Synthesis of Deuterium Labelled 2,5-Bis(4-amidinophenyl)furan, 2,5-Bis(4-ethoxyamidinophenyl)furan, and 2,7-Diamidinocarbazole. J. Labelled Cpd. Radiopharm. 44:197-208.

Wang MZ, Saulter JY, Usuki E, Cheung YL, Hall M, Bridges AS et al. (2006). CYP4F enzymes are the major enzymes in human liver microsomes that catalyze the O-demethylation of the antiparasitic prodrug DB289 [2,5-bis(4-amidinophenyl)furan-bis-O-methylamidoxime]. Drug Metab Dispos 34: 1985–1994.

CHAPTER 3

APOPTOSIS INDUCED BY THE ANTI-TRYPANOSOMAL DRUG PAFURAMIDINE DB289 AND ITS METABOLITES M1, M2, M3 AND FURAMIDINE DB75 IN HUMAN MCF-7 CELLS

A. ABSTRACT

Pafuramidine DB289 (2,5-bis-(4-amidinophenyl)furan-bis-*O*-methylamidoxime), an oral prodrug of furamidine DB75 (2,5-bis-(4-amidinophenyl)furan), exhibits enhanced bioavailability and potent activities against trypanosomiasis and *Pneunocystis carinii* pneumonia in animal models. DB289 is biotransformed to intermediate metabolites M1, M2, M3 and M4, and the final active compound DB75 in humans. DB289 has passed phase I and phase II clinical trials for African trypanosomiasis, malaria, and *Pneunocystis carinii* pneumonia. However, recently DB289 failed in an extended phase I clinical trial for African trypanosomiasis due to its severe liver toxicity and delayed kidney toxicity. The mechanism of this toxicity is not known now. Since many drug-induced liver injuries are by means of apoptosis and necrosis, and DB75 has been confirmed to be capable of inducing apoptotic-like death in *Trypanosome cruzi*, we hypothesized that DB75 or the prodrug DB289 and its intermediate metabolites can induce apoptosis or necrosis in human cells. In this study, Alamar blue™ assay and microscopy determined that DB289, M1, M2, M3 and DB75 induce cytotoxicity to MCF-7 cells with different potencies, highest with M3, followed by M1 and DB75, and the lowest with DB289 and M2. Both flow cytometry analysis and western blotting demonstrated that M1, M3, and DB75 induce apoptosis instead of necrosis in MCF-7 cells, while DB289 and M2 don't. The metabolic study showed that most of 10 μM M1, M3 and DB75 remained after 72 hr incubation in the presence of MCF-7 cells, which demonstrated M1, M3 and DB75 mainly contribute to the apoptotic effects. In conclusion, M1, M3, and DB75 instead of DB289 and M2 induce apoptosis in human MCF-7 cells.

B. INTRODUCTION

Furamidine DB75 (2,5-bis-(4-amidinophenyl)furan), a pentamidine analogue, has potent anti-parasitic activities against *Trypanosoma brucei, Plasmodium falciparum, Leishmania spp.*, and *Pneumocystis jirovecii in vitro and in vivo* (Das and Boykin, 1977; Bell et al., 1990; Brendle et al., 2002; Tidwell et al.,1990). However, it was ineffective when orally administrated in animal models, because of its poor bioavailablity. To improve the oral absorption, pafuramidine (DB289, 2,5-bis-(4-amidinophenyl)furan-bis-*O*-methylamidoxime), a prodrug of DB75, has been developed to introduce two methoxy groups to mask the dicatonic diamidines. DB289 has shown enhanced permeability across intestinal epithelium (Zhou et al., 2002) and potent oral activities against trypanosomiasis and *Pneunocystis carinii* pneumonia in animal models (Boykin et al., 1996; Fitzpatrick et al., 2004). The phase I metabolic pathway of DB289 (scheme 3.1, adapted from Wang et al., 2006) has been determined *in vitro* using freshly isolated rat hepatocytes (Zhou, et al, 2004). DB289 was metabolized to form intermediate metabolites including M1, M2, M3 and M4, and the final active compound DB75 through sequential *O*-demethylation and *N*-dehydroxylation reactions, which are catalyzed by multiple enzymes, including CYP4F2, CYP4F3B, and CYP2J2 for the *O*-demethylations, and cytochrome b5/b5 reductase for the N-dehydroxylations (Wang et al, 2006; Saulter et al., 2005). DB289 is also confirmed to be metabolized to DB75 rapidly in humans in phase I clinical trial and a twice daily oral administration of DB289 maintains plasma DB75 at required antimicrobial concentration (Yeramian et al., 2001). Then, DB289 passed phase II clinical trials for African trypanosomiasis in the Democratic Republic of Congo and Angola, for malaria in Thailand, and for *Pneumocystis carinii* pneumonia in Peru.

In October 2008, an extended phase I study of healthy volunteers was started for the safety assessment for registration for HAT and Pneumocystis jiroveci (Wenzler et al., 2009). In the extended phase I trial, severe liver toxicity and delayed renal insufficiency were observed in a number of participants (Pholig et al., 2008). The toxicity issue ended the development of this oral anti-trypanosomal prodrug and its analogues. Previous pharmacokenics studies of oral DB289 in rat and monkey showed multiple metabolites were formed and distributed in different organs and tissues with different half lifes. Especially DB75 had a very long half life and accumulate in liver (Midgley et al., 2007). It becomes an urgent need to understand the toxicity of this prodrug and its each metabolite. Drug-induced liver injuries are by means of apoptosis and necrosis; for example amiodarone, benzarone (Kaufmann et al., 2005), and acetaminophen (Kon et al., 2004). Previous studies have confirmed that pentamidine and DB75 induce apoptotic-like death in *Leishmania donovani* and *Trypanosome cruzi* respectively (Singh and Dey 2007; De Souza et al., 2006). Although the mechanism is not fully elucidated, it might be because of their capacity to bind DNA and/or inhibiting topoisomerase II (Lausiaux et al., 2002, Singh and Dey et al., 2007). However, it has not been investigated yet if DB75 or the prodrug DB289 and its intermediate metabolites can induce apoptosis or necrosis in human cells. In this study, we used the human MCF-7 cell line, which is a well established cell line for study of drug-induced apoptosis and necrosis (Gao et al., 2003). It also has low P450s level (Yu et al., 2001), which may exhibit slow metabolism or no metabolism to DB289 and each metabolite, so that it allows us to test their direct cytotoxicity after a long treatment times (up to 72 h). Tetramethoxystilbene (TMS) and camptothecin (CPT) served as positive controls to induce apoptosis and necrosis as reported previously (Chun et al., 2005; Gao et al., 2003). This study of apoptotic or necrotic effects by

DB289 and its metabolites is a part of studies to help elucidate which metabolites may potentially contribute to long term clinical toxicity. The studies may enhance our knowledge of the structure and toxicity relationship and enable us to choose safe structures as scaffolds to design safer prodrugs.

C. Materials and Methods

Chemicals and reagents.

DB289 (2,5-bis-(4-amidinophenyl)furan-bis-*O*-methylamidoxime), M1 (2-(4-hydroxyamidinophenyl)-5-(4-methoxyamidinophenyl)furan), M2 (2,5-bis(4-amidinophenyl)furan-bis-*O*-amidoxime), M3 (2-(4-amidinophenyl)-5-(4-ethoxyamidino-phenyl)-furan), DB75 (2,5-bis-(4-amidinophenyl)furan), and stable isotopically labeled internal standards d8-DB289 (d8-2,5-bis(4-amidinophenyl)furan-bis-*O*-methylamidoxime) and d8-DB75 (d8-2,5-bis-(4-amidinophenyl)furan) were synthesized as previously described (Boykin et al., 1996, Stephens et al., 2001; Anbazhagan et al., 2003). Tetramethoxystilbene (TMS) was obtained from Cayman Chemical (Ann Arbor, MI). Camptothecin (CPT), ammonium formate, formic acid, and other inorganic chemicals were obtained from Sigma Chemical Co. (St. Louis, MO). Cell culture medium and components including Eagle's minimum essential medium (EMEM), nonessential amino acids (NEAA, 100x), sodium pyruvate and fetal bovine serum (FBS) of GIBCO were obtained from Invitrogen (Carlsbad, CA). Trypsin-EDTA solution (1x) was obtained from Sigma Chemical Co. (St. Louis, MO). Alamar Blue™ was obtained from Bioscouce (Camarillo, CA). Annexin V-FITC apoptosis detection kit was obtained from BD Pharmingen (San Jose, CA, USA). Antibody against PARP was from obtained from Cell Signaling Technology (Danvers, MA).

Cell culture.

Human breast carcinoma cell line MCF-7 was maintained in EMEM medium supplemented with NEAA, sodium pyruvate, and 10 % FBS under standard cell culture conditions at 37°C and 5% CO_2 in a humid environment. Cells were passed once very 3 days with standard trypsinization procedure.

Cytotoxicity Assay.

The cytotoxicity of compounds was determined using the Alamar Blue™ assay. The protocol was modified and optimized from the one recommended by the manufacturer (Ahmed et al., 1994). MCF-7 cells were seeded in 96-well plates at a density of 3,000 cells / well in 90 µl culture medium. After one day, cells were treated with different concentrations of compounds including DB289, M1, M2, M3, DB75, TMS and DMSO (0.5% v/v) with triplicates for 72 hr. At 66 hr, Alamar Blue™ dye 10 µl / well was added to wells , which were then continuously incubated for 6 hr. Then, the samples were measured in a plate reader with excitation wave length at 560 nm and emission wave length at 590 nm. IC_{50} values were determined using GraphPad Prism 4.0 (San Diego, CA). The values of drug concentrations were transformed to log scale. The cell viability of each sample was expressed as a percentage of the Alamar Blue™ fluorescence intensity verse the control (DMSO treated). Sigmoidal dose response curves were created to fit the data and to determine the IC_{50} values.

Cell morphology and viability.

3×10^5 MCF-7 cells were treated with DB289 (at 2, 5, 10 µM), M1 (at 2, 5, 10, 25 µM), M2 (at 2, 5, 10, 25 µM), M3 (at 2, 5, 10, 25, 50 µM), DB75 (at 2, 5, 10, 25, 50, 100 µM), DMSO 0.5% v/v (negative control), or TMS (positive control) (at 2, 5, 10, 25 µM) at 37°C for 72 hr, and then observed under a microscope (Olympus IX70) with the 10 x objective len. The images were taken using Qcapture 2.56.

Flow cytometry analysis of apoptosis.

3×10^5 MCF-7 cells were treated with specific concentrations of DB289, M1, M2, M3, DB75, DMSO (negative control), or TMS (positive control) for a specific time, and then

harvested by trypsinization followed by centrifugation at 1,000 g at 4 ^{o}C for 5 min. The cell pellets were washed twice with potassium phosphate buffer PBS (pH 7.4). Cell staining was performed according to the protocol of the Annexin V-FITC apoptosis detection kit. Briefly, 1 x 10^5 cells were suspended in 100 µl binding buffer and mixed with 5 µl of Annexin V-FITC and 5 µl of propidium iodide (PI), and incubated for 15 min at 25^{o}C in the dark. Flow cytometry analysis was performed with a Becton Dickinson FACS Caliber as described previously (Coffield et al., 2004). Data was analyzed using software CellQuest gating on cells with normal size. Dots in the region R4 as Annexin V (-) and PI (-) represented viable cells. Dots in the region R5 as Annexin V (+) and PI (-) represent early-stage apoptotic cells. Dots in the region R3 as Annexin V (+) and PI (+) represent late-stage apoptotic cells. So, dots in R3 plus R5 represent all the apoptotic cells. Dots in the region R2 Annexin V (-) and PI (+) represent necrotic cells.

Western blotting analysis of apoptotic marker protein PARP.

1 x 10^6 MCF-7 cells were seeded in 10 cm cell culture dishes and grown at 37 ^{o}C in the cell incubator for 24 hr. Then, cells were treated with 10 µM DB289, M1, M2, M3, DB75, DMSO 0.5% v/v (negative control), or 10 µM TMS (positive control) (Park, 2007) for 72 hr or treated with 6 µM CPT (positive control) (Rastogi et al., 2006) from 66 hr for 6 hr before harvest. After the treatments, cells were scraped gently from the dish surface and spun down by centrifugation at 1,000 g at 4 ^{o}C for 5 min to remove the medium. The harvested cells were washed twice with cold 100 mM potassium phosphate buffer PBS (pH 7.4). The cells were lysed by 200 µl lysing buffer for each cell sample and sonicated for an appropriate period of time. After keeping on ice for 30 min, the cell extracts were prepared by centrifugation at 10,000 g at 4 ^{o}C for 30 min and aspirating the supernatant. The total protein

concentration of each cell lysate was determined using Pierce BCA Protein Assay Kit. About 20 µg of each sample or one rainbow pre-stained protein marker was loaded into the wells of 8% SDS-PAGE gel and the proteins were separated with BioRad SDS-PAGE gel cassette and transferred onto nitrocellulose membranes with BioRad semi-dry protein transferring cassette under the conditions recommended by BioRad. Membranes were blocked in Tris-buffered saline containing 5% non-fat milk and 0.05% Tween 20 at 4 ^{o}C overnight. Western blotting was performed by hybridizing the membranes with 1:1000 diluted primary anti-PARP antibody for 2 hr at room temperature followed by four times of 10 min washing with washing buffer. Then samples were hybridized with 1:5000 diluted secondary goat anti-rabbit IgG antibody conjugated with horseradish peroxidase for 1 hr at room temperature. After being washed four times with washing buffer for 10 min, the membranes were added to SuperSignal West Pico Chemiluminescent substrate and exposed to film and the bands were identified after development of the film. The molecular weight was determined by comparing with the protein markers.

Metabolism of DB289, M1, M2, M3 and DB75 in MCF-7 cells.

100 µl MCF-7 cells were seeded in the 96-well plate at the concentration 3,000 cells/well and incubated them at 37 ^{o}C for 24 hr. Then, cells or medium without cells (negative control) were treated with 1 µM or 10 µM DB289 and its metabolites M1, M2, M3 and the active drug DB75, in triplicate. Samples at 0, and 72h were taken and the medium was removed. One hundred µl organic extraction solution (7:1 methanol/water + 0.1% trifluoroacetic acid) was added to the cells, which was mixed well and kept for 30 min. Then, the extraction solution was combined with the medium. The samples were mixed well and kept on ice for 20 min to precipitate proteins. Samples were spun at 4000 rpm 15 min at 4^{o}C. Two hundred

µl supernatant was heated,then dried under nitrogen flow. Samples were reconstituted in 200 µl solution containing 50% methanol plus 50% water, then vortexed and spun at 4000 rpm 15 min at 4^{o}C. Ninety eight µl supernatant was then taken and 2 µl internal standards d8-DB289 and d8-DB75 was added to a final concentration at 0.5 µM. Standards of DB289, M1, M2, M3 and DB75 were prepared under the same conditions at various concentrations ranging from 1 nM to 15 µM. Blanks were from the DMSO 0.5% treated cell samples with the same methods.

LC/MS/MS analysis.

The LC/MS/MS analytic methods for DB289, M1, M2, M3 and DB75 were modified based on the previously described methods (Sturk et al., 2004; Mathis et al., 2007). Briefly, the LC/MS/MS system consisted of two solvent delivery pumps (Shimadzu Scientific, Columbia, MD), a thermostated (6°C) LEAP HTC autosampler (Carrboro, NC), and an Applied Biosystems API4000 triple-quadrupole mass spectrometer. The sample injection volume was 4 µl. A Zorbax Bonus RP column (2.1 mm x 150 mm; 5 µm) from Agilent (New Castle, DE, USA) was used to separate compounds with flow rate 350 µl per min. The mobile phase A consisted of 15 mM ammonium formate and 0.1% TFA in HPLC-grade water. Mobile phase B consisted of 15 mM ammonium formate and 0.1% TFA in 4:1 (v/v) HPLC-grade acetonitrile/ water. The elution gradient started from 95% mobile phase A plus 5% mobile phase B, which shifted linearly to 20% mobile phase A plus 80% mobile phase B at 20 min, then shifted linearly to 100% mobile phase B at 25 min, returning to starting condition for 6 min to equilibrate. User-controlled voltages, gas pressures, and source temperature were optimized for the detection of the parent and product ions of the compounds. All compounds were analyzed in positive-ion mode, using multiple reaction monitoring.

Statistical Analysis

Data are presented as the mean ± SD from independent triplicate experiments unless otherwise noted. $P > 0.05$ was considered as significant. T tests (unpaired, two-tailed) were performed if only two groups were analyzed. ANOVA followed by Tukey's test was used for comparison of more than 2 groups.

D. RESULTS

Cytotoxicity Assay.

To determine the cytotoxic effects by DB289 and its metabolites, MCF-7 cells were treated with different concentrations of DB289, M1, M2, M3, DB75, TMS and DMSO (0.5% v/v) for 72 hrs. Then, the cell viability was determined by Alamar Blue^{TM} assay. DB289 and its four metabolites showed cytotoxicity with different potenies in MCF-7 cells (figure 3.1). With progressive higher concentration of treated compounds the cytotoxicity was increased. The most potent compound was M3 (IC_{50} = 4.6 µM), which was followed by M1 (IC_{50} = 15.1 µM) and DB75 (IC_{50} = 21.1 µM). Due to the solubility limits, the maximum concentration tested was 10 µM for DB289 and 25 µM for M2, at which only about 20% and 30% cell inhibitions were achieved, respectively.

Cell morphology and viability.

To determine the cytotoxic effects, cell morphological changes and viability were observed for MCF-7 cells after treatment of DB289 (at 2, 10 µM), M1, M2, M3, DB75 (at 2, 10, 25 µM), or DMSO 0.5% v/v (negative control), or TMS (positive control) (at 2, 10, 25 µM) in 6-well plates (figure 3.2). TMS, M1, M3, and DB75 showed cytotoxicity in a concentration-dependent manner. Treated with a high concentration (25 µM) of M1, M3, or DB75, most of the cells detached from the culture surface and suspended in the medium. Their shape became round and their size varied. A similar phenomenon was observed from the cells treated with positive control 25 µM TMS. In contrast, the vehicle DMSO treated cells showed normal growth, attached to the culture surface and maintained normal fibroblast-like morphology and grew to around 90% confluency after 72hr. However, (due to the solubility) the high concentration 10 µM of the prodrug DB289 and 25 µM M2 treated cells showed very little cytotoxic effect. Most of the cells still attached to the culture surface and

maintained normal fibroblast like morphology. Only small numbers of the cells suspended and their shape became round with various size.

Flow cytometry analysis of apoptosis.

To determine if the cytotoxic effect by DB289, M1, M2, M3, and DB75 is through apoptosis or necrosis, the cells were exposed to 10 μM each compound for 72 hr, then were stained with Annexin V and PI followed by flow cytometry analysis. We found that comparing with the apoptotic cells in the untreated cells, chemical treated cells had increased apoptotic cells to different degrees (figure 3.3): untreated (4.41 ± 0.25 %), negative control DMSO (4.61 ± 0.94 %), positive control TMS (13.17 ± 0.43 %), DB289 (6.5 ± 1.34 %), M1 (20.99 ± 2.95 %), M2 (5.20 ± 0.44 %), M3 (32.72 ± 3.03 %), and DB75 (13.52 ± 1.19 %). So, M1, M3, DB75 and TMS treated cells had significantly increased apoptotic cells. However, DB289, M2 and DMSO treated cells had no such increase. The necrotic cells in the all these chemically treated cells were close to the spontaneous necrotic cells in the untreated cells: untreated (1.98 ± 0.13 %), DMSO (2.31 ± 0.48 %), TMS (3. 66 ± 0.71 %), DB289 (1.79 ± 0.26 %), M1 (2.40 ± 0.62 %), M2 (2.34 ± 0.60 %), M3 (1.95 ± 1.19 %), and DB75 (1.25 ± 0.25 %). These results showed that M1, M3 and DB75 induced cytotoxicity mainly through apoptosis instead of necrosis in MCF-7 cells, while DB289 and M2 didn't induce apoptosis or necrosis. The positive control TMS also induced apoptosis instead of necrosis in our experiments, which is the same as reported previously (Chun et al., 2005).

We also measured the apoptotic cells and necrotic cells induced by 10 μM TMS, M1, M3, DB75, and the vehicle DMSO (0.5 % v/v) at different time points after treatments. The results (figure 3.4a) show that the apoptotic cells in the DMSO treated cells remained the same at 24 hr, 48 hr, and 72 hr. However, the apoptotic cells continuously increased in 10

μM TMS, M1, M3, and DB75 treated cells at 24hr, 48 hr, and 72 hr. However, the necrotic cells (figure 3.4b) in all these chemically treated cells didn't change significantly at 24hr, 48 hr, and 72 hr. These results further confirmed the ongoing apoptosis instead of necrosis in M1, M3, DB75 and TMS treated MCF-7 cells.

Western blotting analysis of the apoptotic marker protein PARP.

To further confirm these compounds induced apoptosis, we used western blotting to detect the cleavage of the marker protein PARP in MCF-7 cells during apoptosis. 10 μM M1, M3 or DB75 treated cells showed cleavage of PARP from full length 116 kD to form 89kD (figure 3.5). Such cleavage of PARP was also observed from the cell lysate treated with positive control drugs CPT and TMS, which are consistent with previous publications. There was no cleavage found from the cells treated with 10 μM DB289, M2 and the negative control DMSO under the same conditions. These cleavage results of the apoptotic marker PARP confirmed that M1, M3, and DB75 but not DB289 and M2, induced apoptosis in MCF-7 cells, consistent with results from our flow cytometry experiments.

Metabolism of DB289, M1, M2, M3 and DB75 in MCF-7 cells.

To test if the metabolic stability of the treated compounds and the formation of their downstream metabolites, metabolism studies of 1 μM or 10 μM DB289, M1, M2, M3 and DB75 in MCF-7 cells or medium without cells were carried out.

After incubation in the medium without the cells for 72 hr, 1 μM substrate remained (figure 3.6a.): DB289 (99.78 ± 2.47 %), M1 (96.83 ± 0.62 %), M2 (85.07 ± 1.77 %), M3 (84.17 ± 5.16 %), DB75 (81.44 ± 9.28 %). When incubated in MCF-7 cells for 72 hr, the 1 μM substrate remained: DB289 (33.72 ± 1.45 %), M1 (72.84 ± 1.83 %), M2 (70.92 ± 10.17 %), M3 (53.98 ± 1.3 %), DB75 (79.98 ± 3.66 %). So, the further substrate depletion in the

presence of MCF-7 cells showed that cell required metabolism of DB289, M1, M2, and M3 occurred. However, there was no cell required metabolism to DB75.

After incubation in the cell culture medium without the cells for 72 hr, the 10 μM substrate remained (figure 3.6b.) : DB289 (91.1 ± 2.93 %), M1 (93.21 ± 7.17 %), M2 (87.98 ± 5.64 %), M3 (84.18 ± 5.3 %), DB75 (84.29 ± 2.4 %). When incubated in MCF-7 cells for 72 hr, the 10 μM substrate remained: DB289 (48.84 ± 12.15 %), M1 (88.6 ± 0.97 %), M2 (73.02 ± 1.34 %), M3 (82.34 ± 1.55 %), DB75 (89.66 ± 9.83 %) after incubated with the MCF-7 cells for 72 hr. Cell required metabolism still happened to DB289 and M2. So, there was no cell required metabolism to DB75. However, in the case of M1 or M3, the substrate depletions were very similar when incubated with MCF-7 cells or without cells. So, the cell metabolic enzymes were relatively saturated by 10 μM M1 or M3.

Formation of metabolites M1 was also determined in a time course study of DB289 incubation in MCF-7 cells (figure 3.7). M1 was formed in a time-dependent manner.

So, 10 μM M1, M3, and DB75 remained most of them after 72 hr incubation in MCF-7 cells, during which they induced apoptosis as we observed above.

E. DISCUSSION

Pafuramidine DB289 (2,5-bis-(4-amidinophenyl)furan-bis-*O*-methylamidoxime), an oral prodrug of furamidine DB75 (2,5-bis-(4-amidinophenyl)furan), exhibits enhanced bioavailability and potent activities against trypanosomiasis and *Pneunocystis carinii* pneumonia in animal models. DB289 is biotransformed to intermediate metabolites M1, M2, M3 and M4, and the final active DB75 in human. DB289 has successfully passed phase I and phase II clinical trials trials for African trypanosomiasis, malaria, and Pneumocystis pneumonia. However, recently DB289 failed in the extended phase I clinical trial for African trypanosomiasis due to severe liver toxicity and delayed kidney toxicity. The mechanism of this toxicity is not yet clear. Since many drug-induced liver injuries are by means of apoptosis and necrosis and DB75 has been confirmed to be capable of inducing apoptotic-like death in *Trypanosome cruzi*, it is interesting to investigate if DB75 or the prodrug DB289 and its intermediate metabolites can induce apoptosis or necrosis in human cells.

In this study, we found that DB289, M1, M2, M3 and DB75 showed cytotoxicity to MCF-7 cells with different potencies, with M3 the most potent compound, followed by M1 and DB75. DB289 and M2 achieved less than 30% inhibition of cell growth at the highest concentrations tested. The cell morphology and viability observed by microscopy showed concentration-dependent inhibition of cell growth by these compounds, which were consistent with the cytotoxicity results. Annexin IV and PI double staining followed by flow cytometry analysis confirmed that M1, M3 and DB75, but not DB289 and M2, induced apoptosis instead of necrosis in MCF-7 cells. These apoptotic effects by M1, M3 and DB75 occurred in a time-dependent manner. Western blotting also confirmed ongoing apoptosis by

showing that the apoptotic marker PARP was cleaved to form the 89kD fragment in the M1, M3 and DB75 treated cells but at DB289 and M2 treated cells. Finally, the metabolic study showed that most of 10 μM M1, M3 and DB75 remained after 72 hr incubation in the presence of MCF-7 cells, which demonstrated M1, M3 and DB75 mainly contribute directly to the apoptotic effects.

In this study, we used synthetic compounds of the highest purity that we can obtain. DB289, M2 and DB75 are more than 95% pure. DB289 and M2 didn't show ability to induce apoptosis. DB75 has low potency to induce apoptosis. M3 appeared to be most potent. M3 has impurity DB75 about 10%, which maybe contributes to a small part of the apparent potency. M1 has impurity M2, M3, and DB75, which maybe also contribute to small part of the potency.

In the previous pharmacokinetics study of single orally dosed DB289, metabolism formed M1 has a relatively short half life, M3 has a relatively long half life and high level in blood and urine, DB75 has much longer half life and accumulated in liver. They all can induce apoptosis in our results. In future studies, we need examine at their cytotoxic effects to hepatic cells, especially DB75. Another important consideration is that the clinical toxicity occurred after repeated dosage for a long time, so the intermediated metabolites M1 and M3 may also have a chance to accumulate and generate the toxicity if the P450 are inhibited after long time dosing. M1 and M3 are more potent in inducing apoptosis than DB75 but less abundant in liver and blood. Further studies are needed to determine how much they may contribute to the toxicity. The interesting thing is that M2 shows a short half life and low

levels in the pharmacokinetics study and doesn't induce apoptosis or necrosis in our results. So in the future we will be eager to know if M2 is a safe scaffold to design other less toxic prodrugs.

There are also some questions in our experiments that are not clear yet. First, although DB75 has been confirmed as a DNA binder and can distribute in nucleus in human cell lines (Lansiaux et al., 2002), it is not known how it crosses mammalian cell membrane. M1 and M3 may pass the cell membrane by passive diffusion. But the targets of M1 and M3 to induce apoptosis are not known, which could be different from the targets of DB75. Elucidation of the whole process of apoptosis by these compounds may be also important.

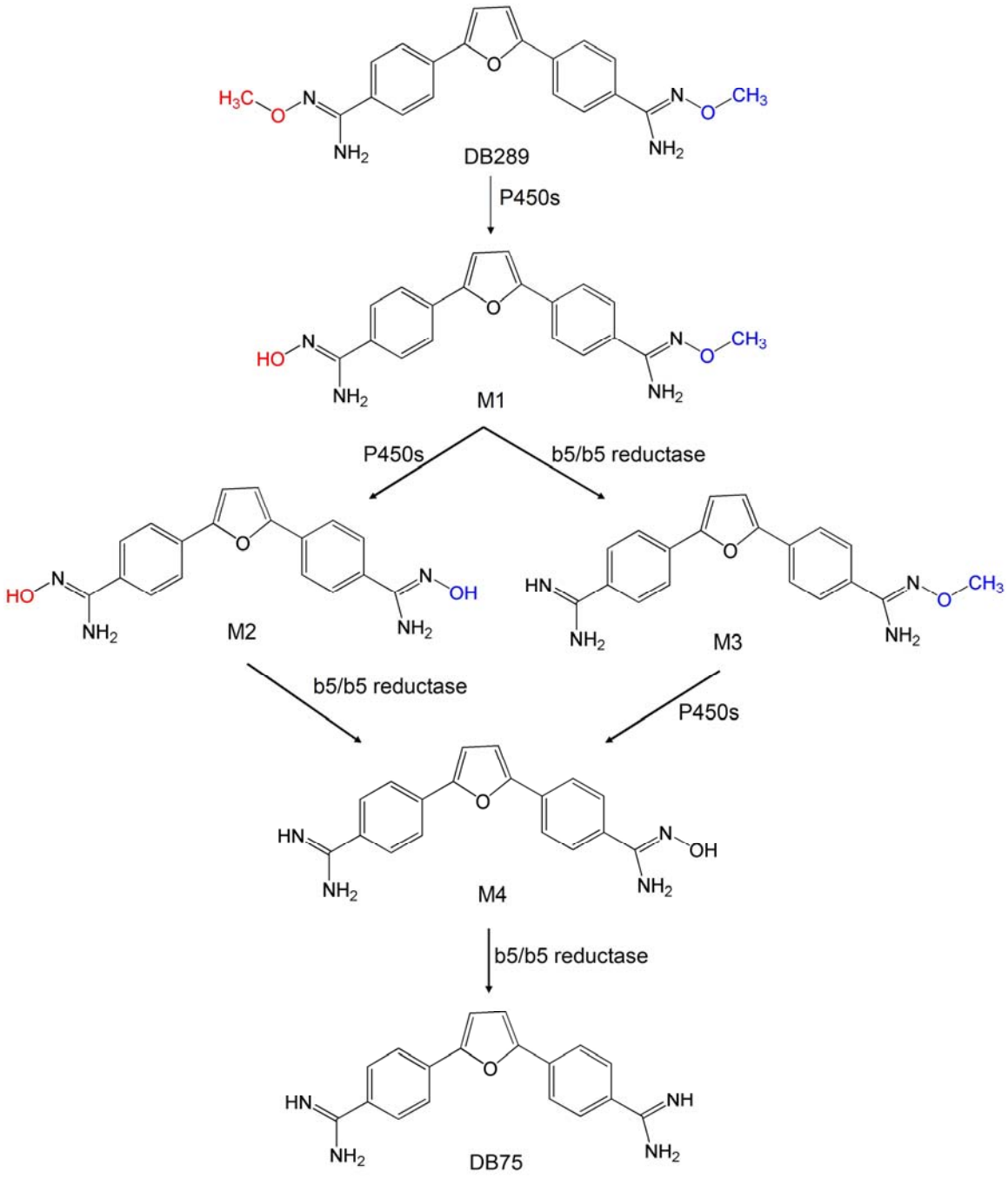

Scheme 3.1. Metabolic pathway of prodrug DB289. (Adapted from Wang et al., 2006).

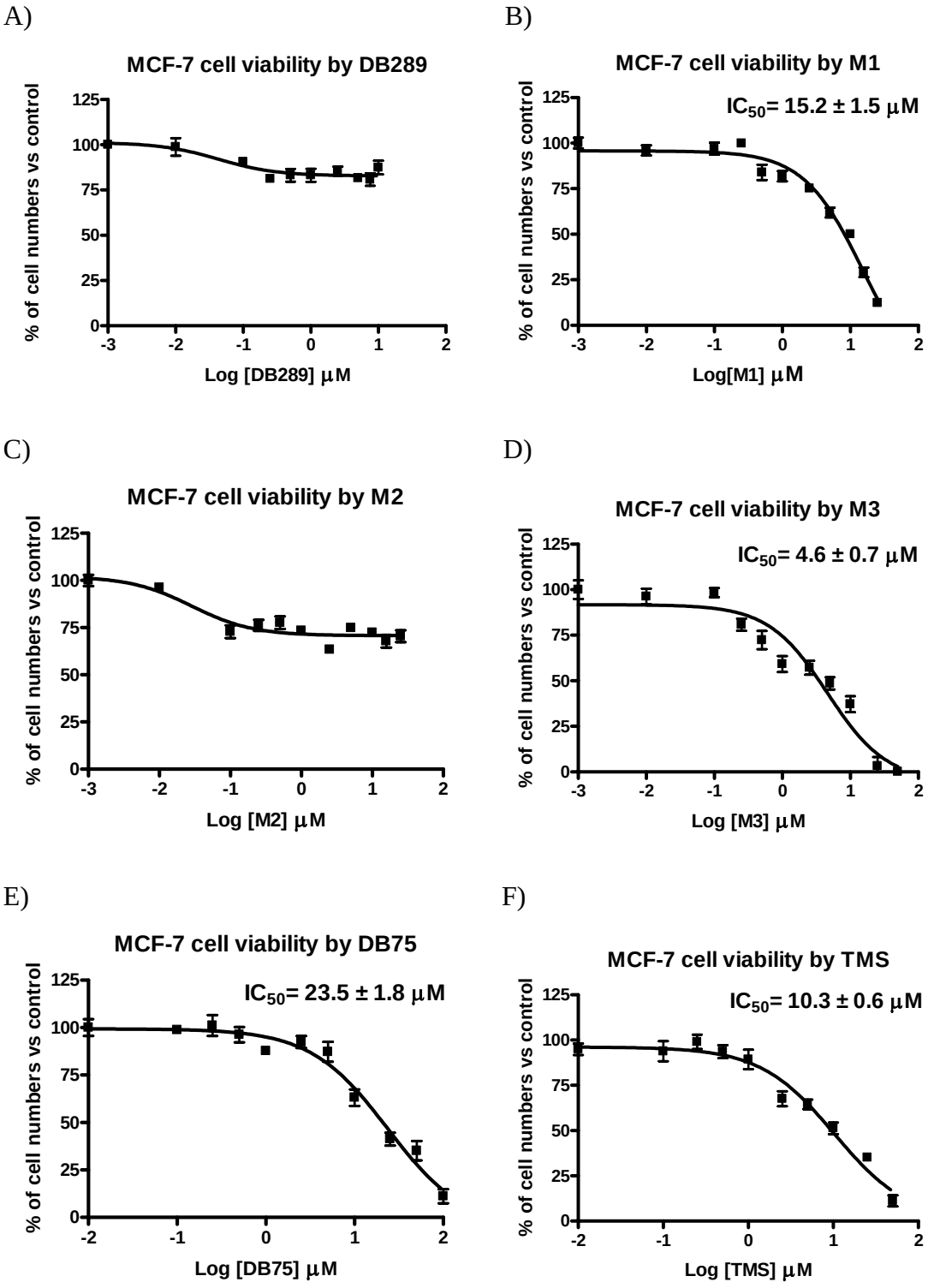

Figure. 3.1. Cytotoxicity of compounds. MCF-7 cells were seeded in 96-well plates at a density of 3,000 cells/well and treated with different concentrations of compounds A) DB289, B) M1, C) M2, D) M3 and E) DB75 for 72 hr. The cell viability was measure by Alamar

Blue™ assay and IC_{50} values were determined by GraphPad Prism. Data represent the mean ± S.D. of triplicate experiments.

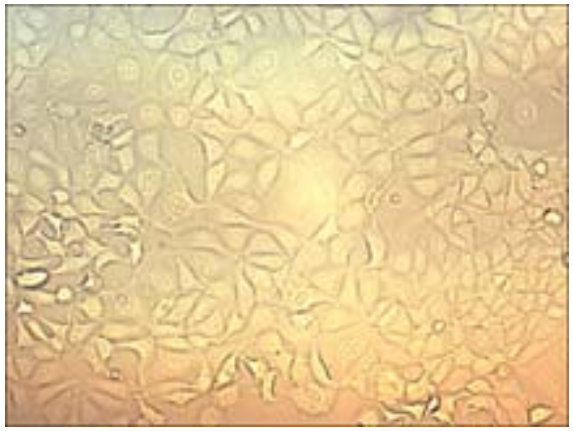

DMSO 0.5% v/v

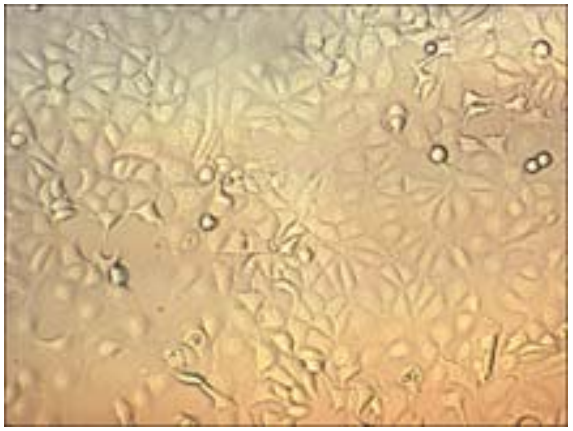

DB289 2 µM

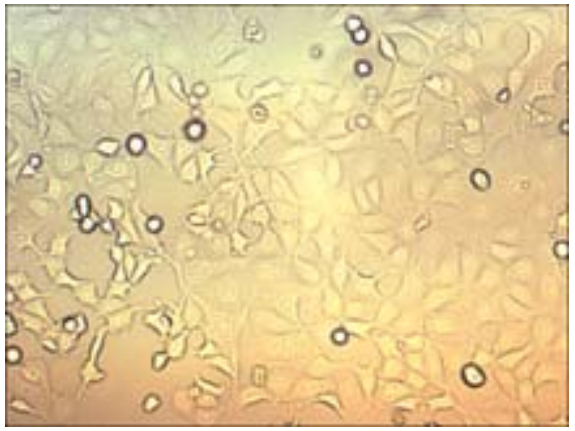

DB289 10 µM

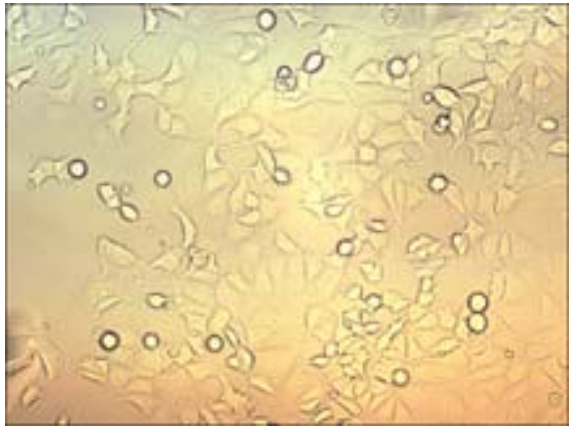

M1 2 µM

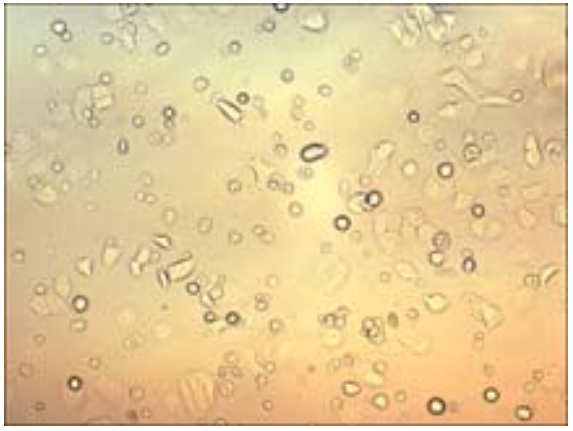

M1 10 µM

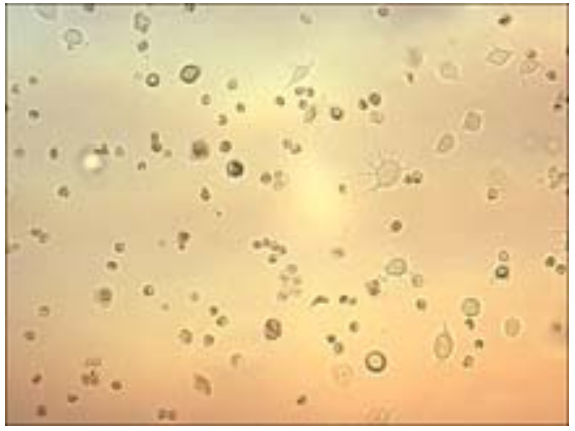

M1 25 µM

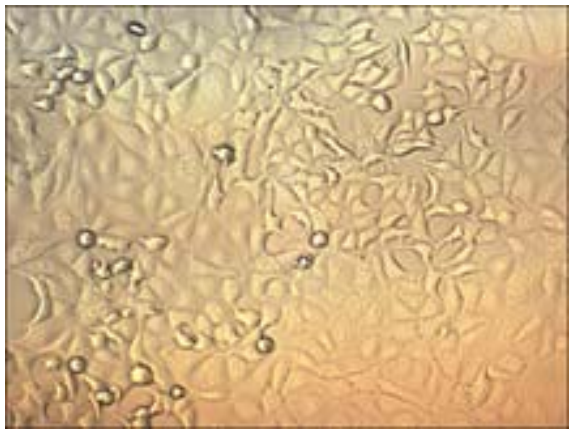

M2 2 µM

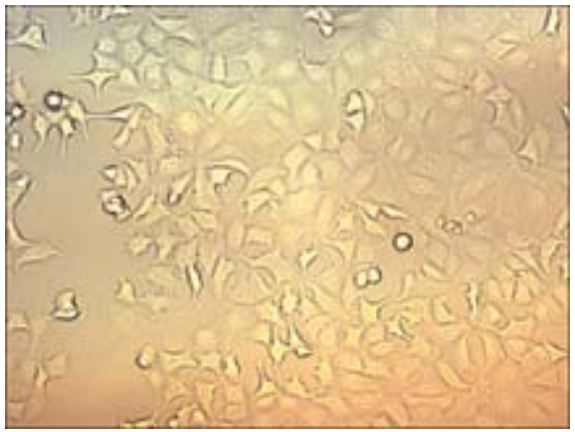

M2 10 µM

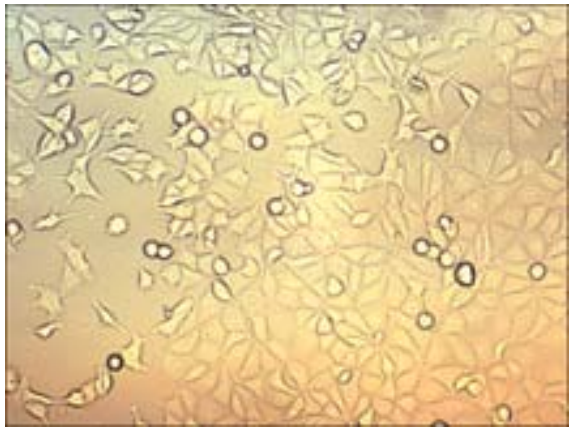

M2 25 µM

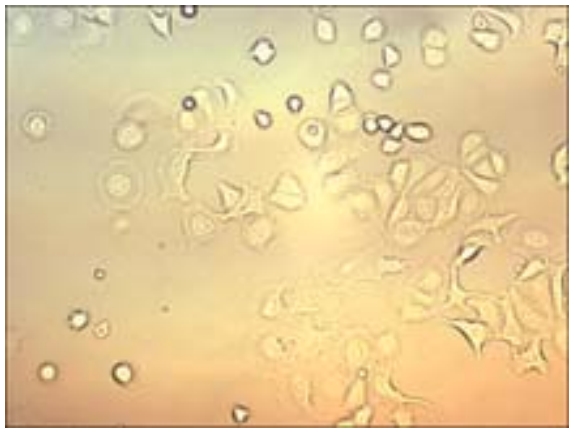

M3 2 µM

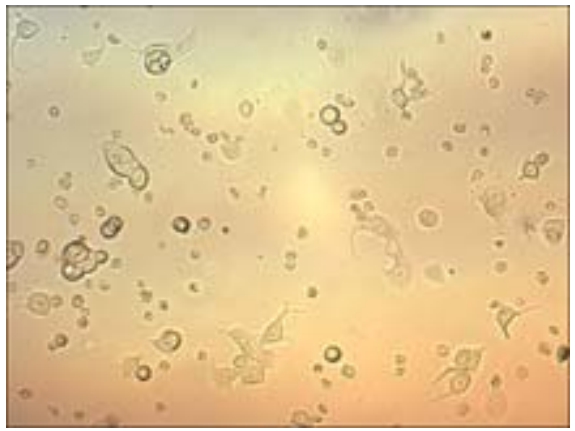

M3 10 µM

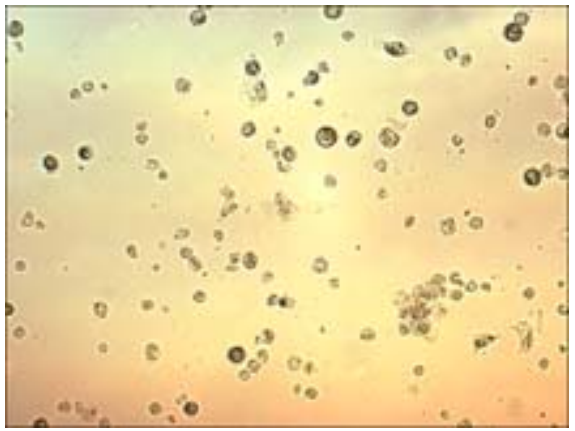

M3 25 µM

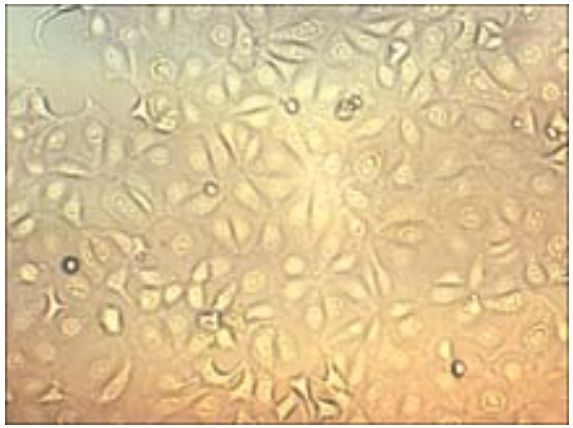

DB75 2 µM

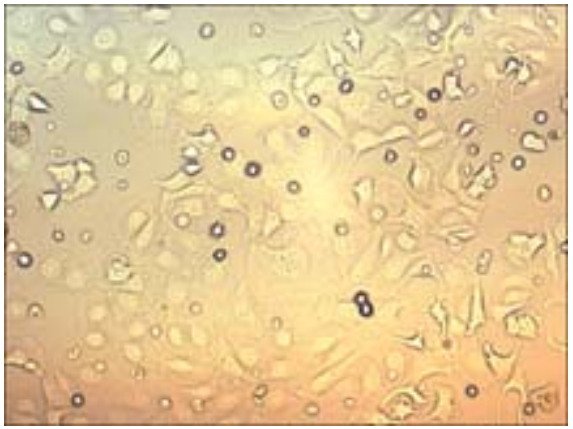

DB75 10 µM

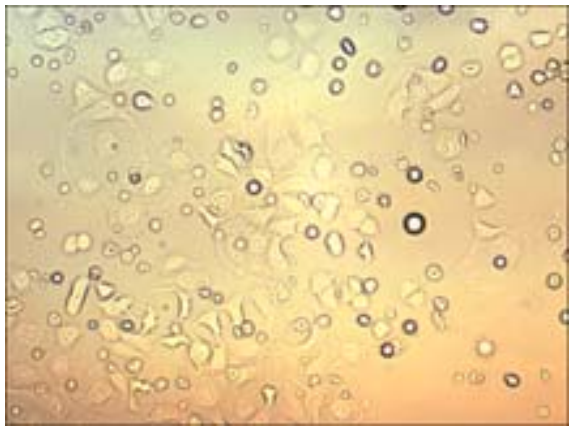

DB75 25 µM

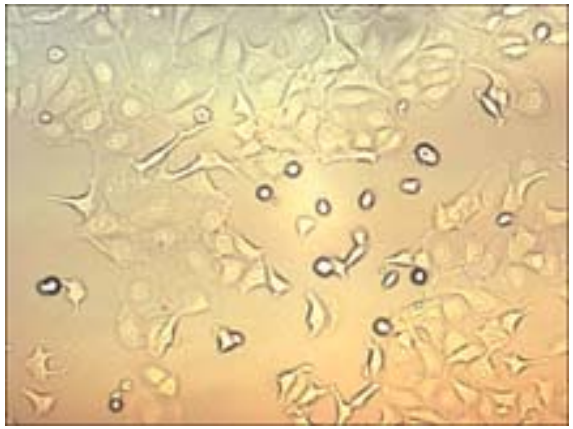

TMS 2 µM

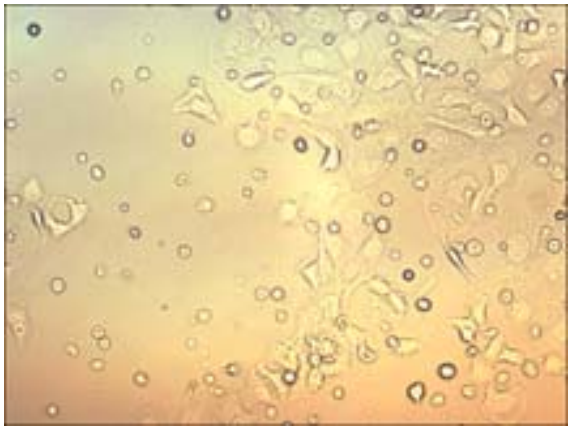

TMS 10 µM

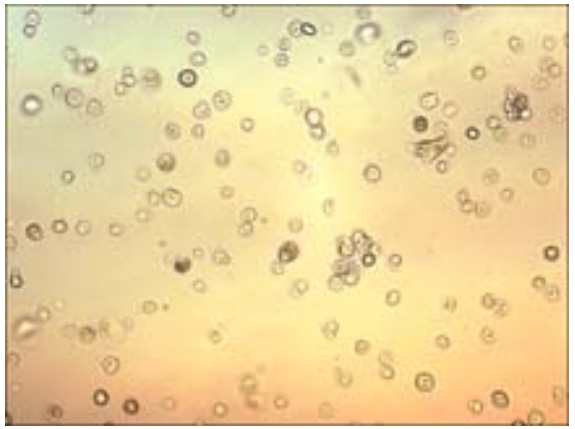

TMS 25 µM

Figure 3.2. Cell morphologic changes and death. 3 x 10^5 MCF-7 cells were treated with DB289 (at 2, 10 µM), M1, M2, M3, DB75 (at 2, 10, 25 µM), DMSO 0.5% v/v (negative control), or TMS (positive control) (at 2, 10, 25 µM) at 37°C for 72 hr, and then observed under microscope (Olympus IX70) with the 10 x objective len. The images were taken using Qcapture 2.56.

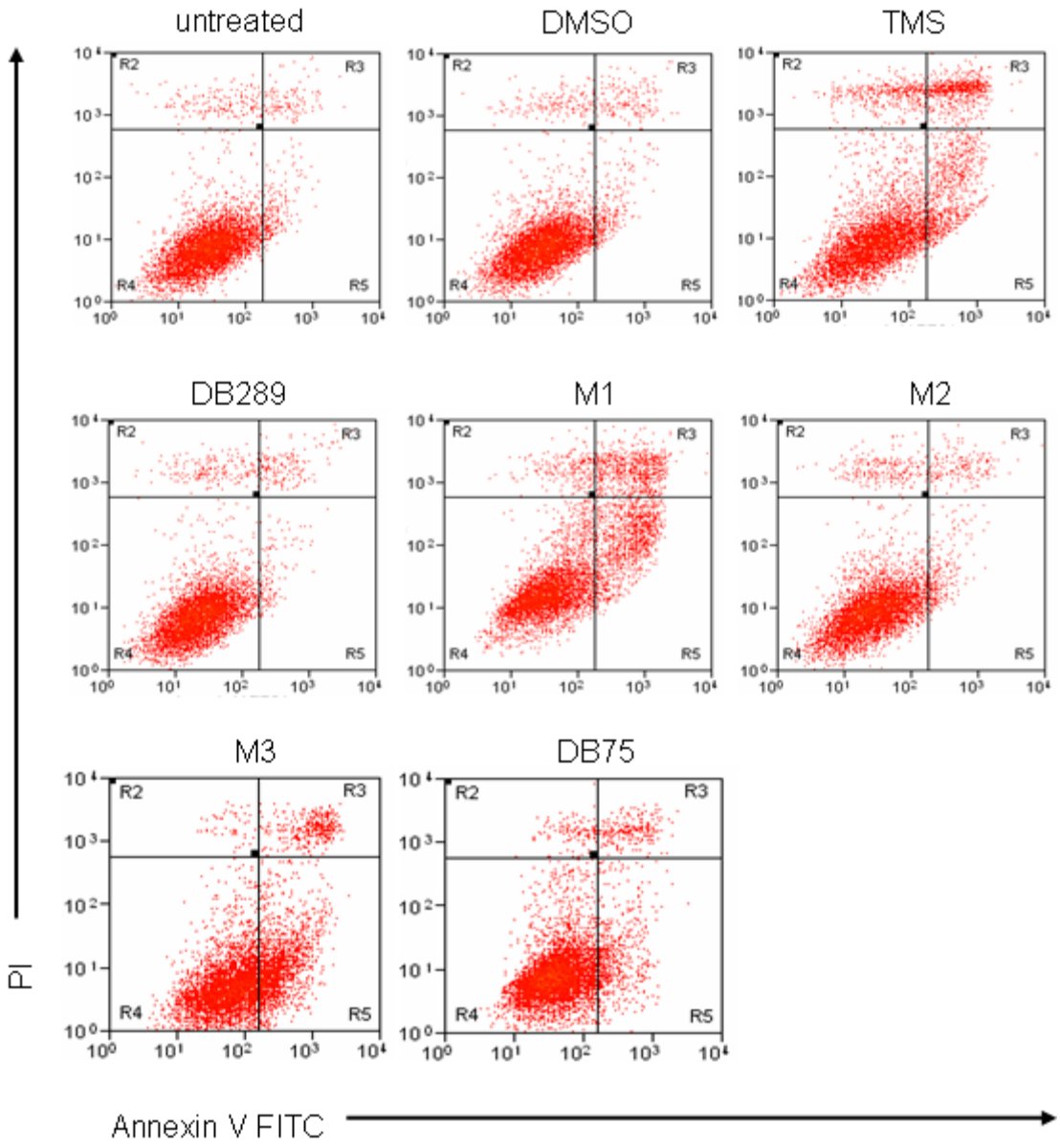

Figure 3.3. Flow cytometry analysis of apoptosis. 3 x 10^5 MCF-7 cells were untreated or treated with solvent (DMSO 0.5% v/v), 10 µM TMS, DB289, M1, M2, M3, DB75 for 72 hr, and stained with Annexin V-FITC and PI. Flow cytometry analysis was performed with a Becton Dickinson FACS Caliber. Data was analyzed using software Cell QuestCell gating on cells with normal size. The horizontal axis represents the fluorescent intensity of Annexin V-FITC, while the vertical axis represents the fluorescent intensity of PI. The region R4 represents viable cells. The region R5 represents early-stage apoptotic cells. The region R3

represents late-stage apoptotic cells. R3 plus R5 represent all the apoptotic cells. The region R2 represents necrotic cells.

A)

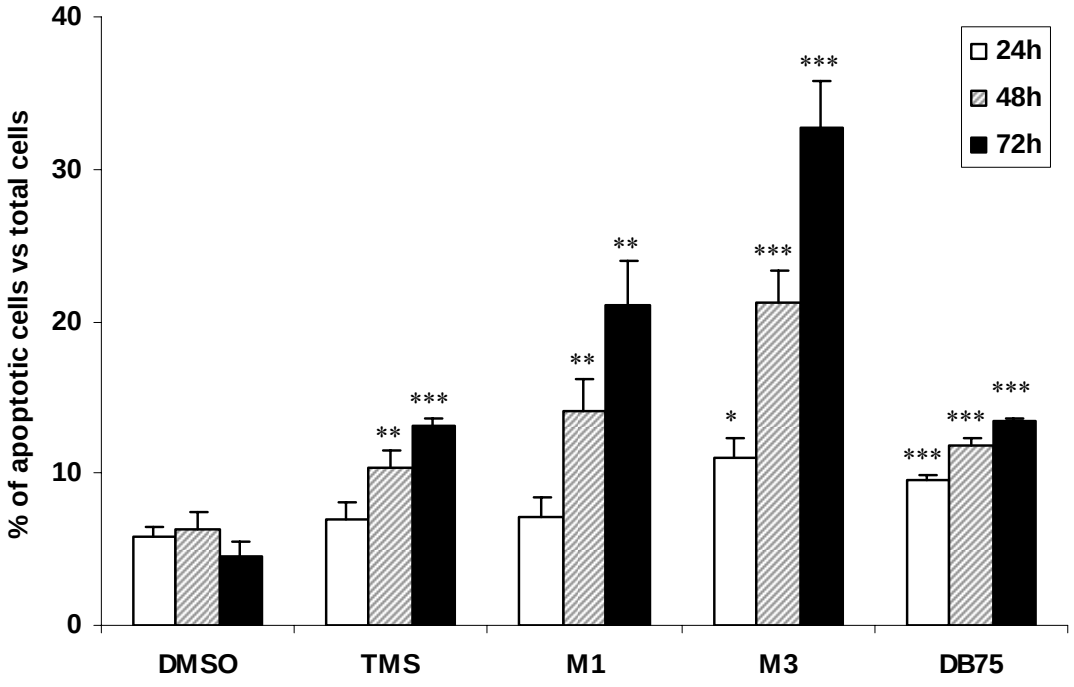
40
30
20
10
0
% of apoptotic cells vs total cells
24h
48h
72h
*
**
***
DMSO
TMS
M1
M3
DB75

B)

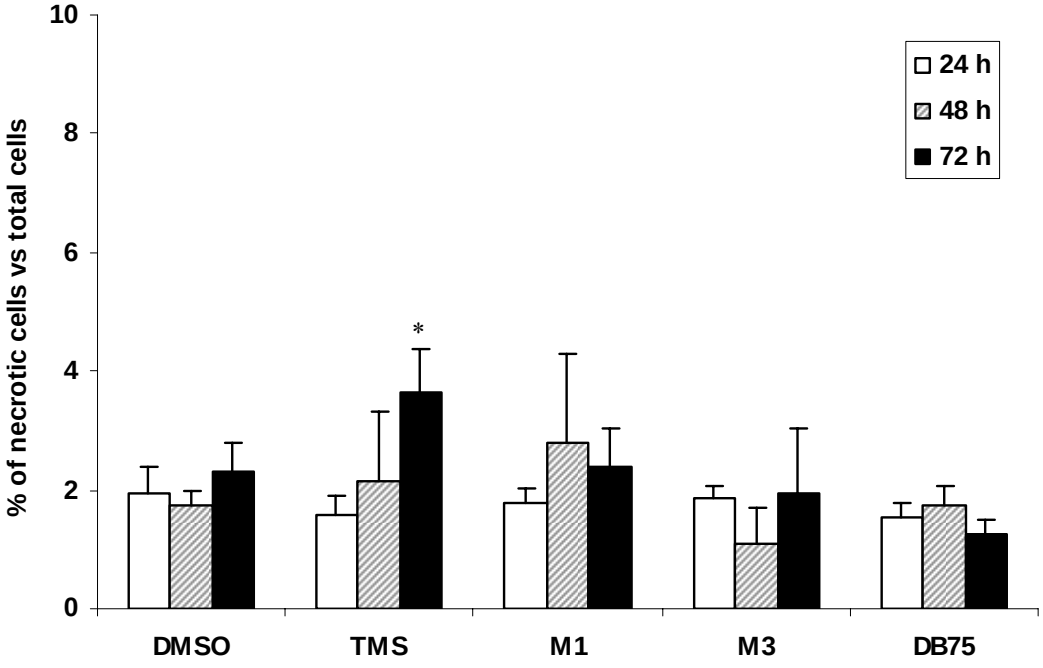
10
8
6
4
2
0
% of necrotic cells vs total cells
24 h
48 h
72 h
*
DMSO
TMS
M1
M3
DB75

Figure 3.4. Time course of the induced apoptosis and necrosis. 3 x 10^5 MCF-7 cells were untreated or treated with solvent (DMSO 0.5% v/v), 10 μM M1, M3, DB75, and TMS for 24, 48, and 72 hrs, and stained with Annexin V-FITC and PI, followed by flow cytometry analysis. a) The percentage of apoptotic cells induced by different compounds. b) The percentage of necrotic cells induced by different compounds. Data are presented as the mean ±S.D. (*n*=3).

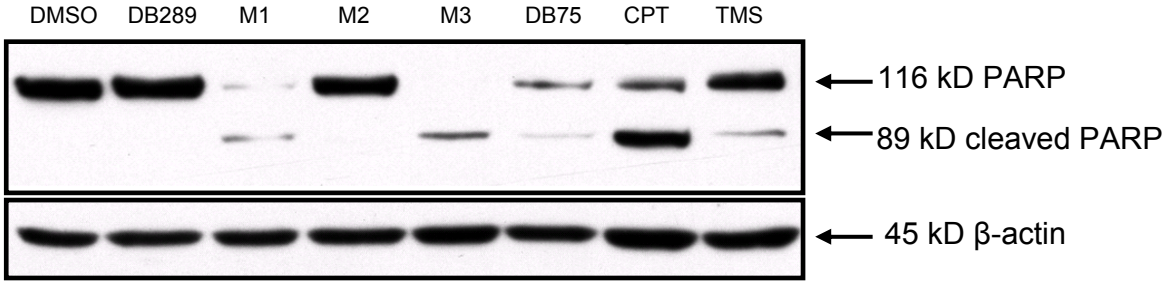

Figure 3.5. Western blotting analysis of the apoptotic marker protein PARP. 1 x 10^6 MCF-7 cells were treated with 10 μM DB289, M1, M2, M3, DB75, TMS, or solvent (DMSO 0.5 % v/v) for 72 hr or treated with 6 μM CPT from 66 hr for 6 hr before harvest. The cell extracts were prepared and whole protein was isolated by 8% SDS-PAGE gel and transferred onto nitrocellulose membranes. PARP cleavage was determined by anti-PARP antibody and propriate secondary antibody, substrate and signal detection method. The molecular weight was determined by comparing with the protein markers.

A)

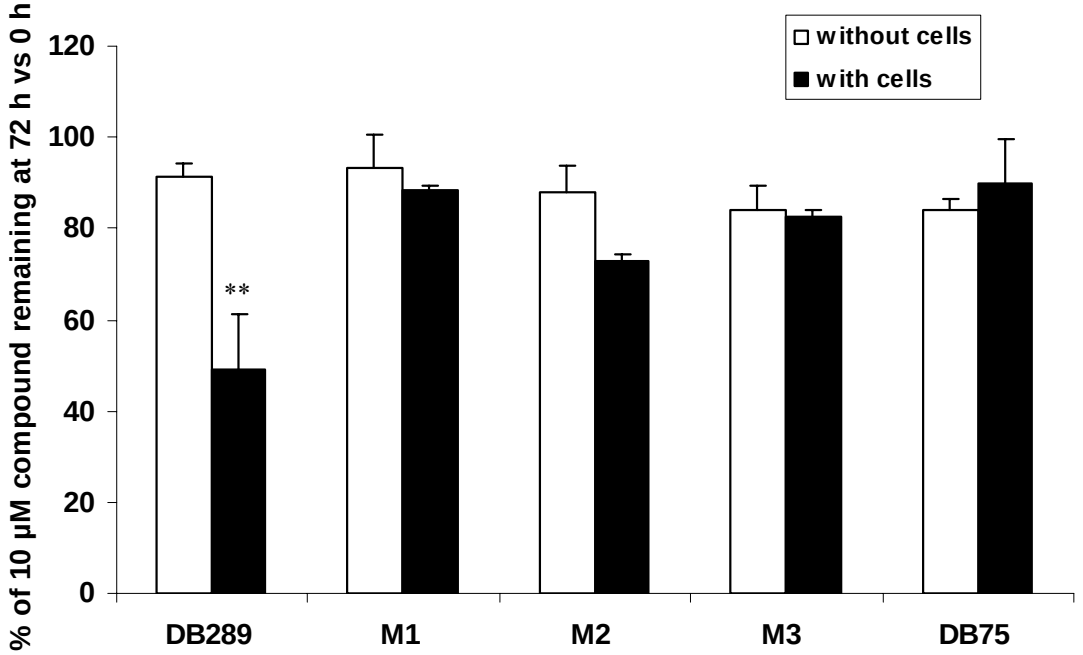

B)

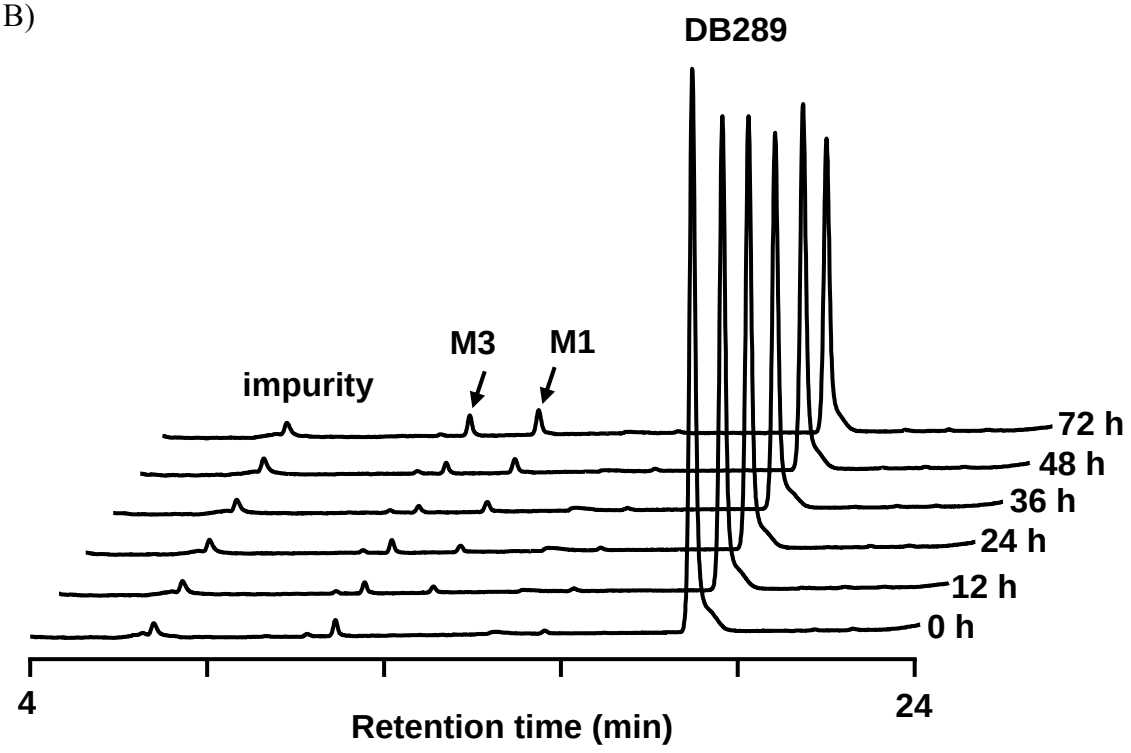

Figure. 3.6. Metabolism of DB289, M1, M2, M3 and DB75 in MCF-7 cells:

100 µl MCF-7 cells were seeded in the 96-well plate at a concentration 3,000 cells/well and incubated them at 37 ^{o}C for 24 hr. Then, the cells or medium without cells (negative control) were treated with a) 1 µM or b) 10 µM DB289 and its metabolites M1, M2, M3 and the active drug DB75 in triplicate.

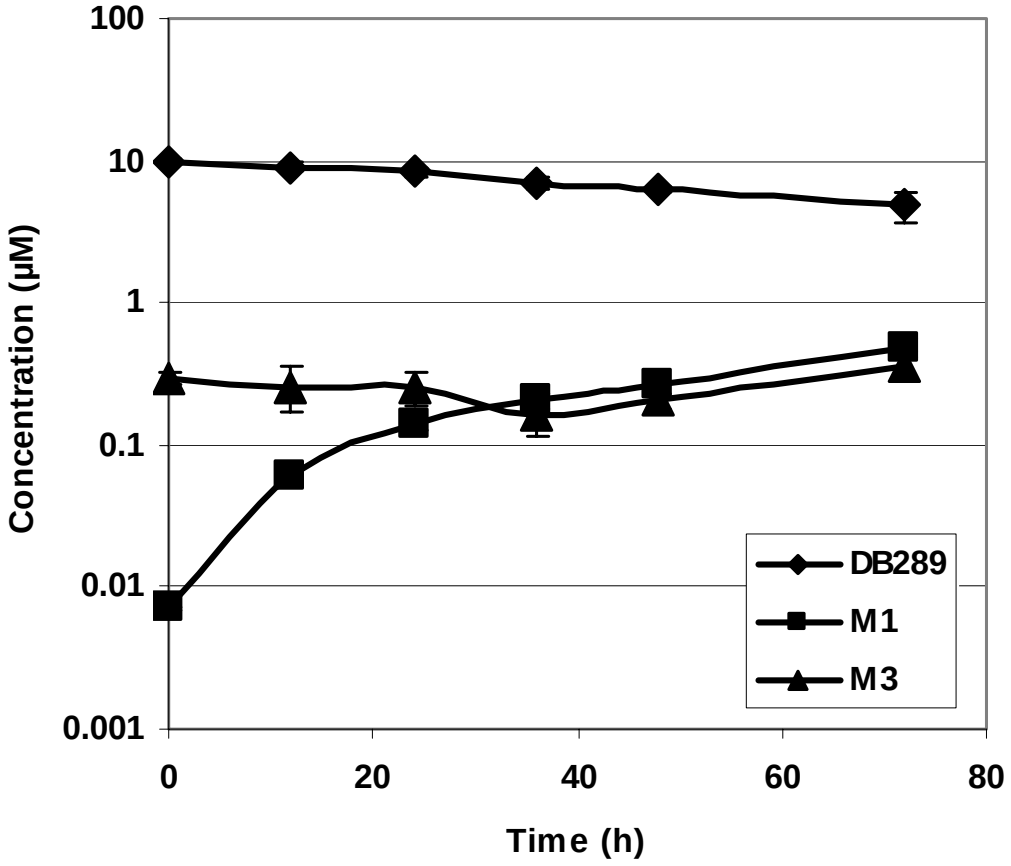

Figure 3.7. Metabolites formatted from DB289 in MCF-7 cells.

100 µl MCF-7 cells were seeded in the 96-well plate at the concentration 3,000 cells/well and incubated at 37 ^{o}C for 24 hr. Then, the cells were treated with 10 µM DB289 for 72 hr. The concentration of DB289 and the metabolites M1 and M2 formed during incubation were determined.

F. ACKNOWLEDGEMENTS

This work was supported by a grant from the Bill and Melinda Gates Foundation.

G. References:

Abboud G, Kaplowitz N. 2007, Drug-induced liver injury. Drug Saf. 30(4):277-94

Amanda M. Mathis,[1] Arlene S. Bridges,[1] Mohamed A. Ismail,[3] Arvind Kumar,[3] Iris Francesconi,[3] Mariappan Anbazhagan,[3] Qiyue Hu,[3] Farial A. Tanious,[3] Tanja Wenzler,[4] Janelle Saulter,[1] W. David Wilson,[3] Reto Brun,[4] David W. Boykin,[3] Richard R. Tidwell,[2] and James Edwin Hall[1,2*]**,2007,** Diphenyl furans and aza analogs: effects of structural modification on in vitro activity, DNA binding, and accumulation and distribution in trypanosomes. Antimicrobial Agents and Chemotherapy, 51 (8), 2801-2810

Anbazhagan M, Saulter J, Hall J and Boykin D (2003) Synthesis of metabolites of the prodrug 2,5-bis(4-O-methoxyamidinophenyl) furan. Heterocycles 60:1133-1145.

Andrea L. Crowell, Chad E. Stephens, arvind Kumar, David W. Boykin, and W. Evan Secor, 2004, Antimicrobial Agent and Chemotherapy, 48 (9), 3602-3605

Back, S.A., Khan, R., Gan, X., Rosenberg, P.A., Volpe, J.J., 1999. A new Alamar Blue viability assay to rapidly quantify oligodendrocyte death. J. Neurosci. Methods 91, 47-54.

Brendle, J.J., A.Outlaw, A. Kumar, D.W.Boykin, D.A.Patrick, R.R.Tidwell, and K.A.Werbovetz. 2002. Antileishmanial activities of several classes of aromatic dications. Antimicrob Agents Chemother 46:797-807

Chun YJ, Lee SK, Kim MY. (2005) Modulation of human cytochrome P450 1B1 expression by 2,4,3',5'-tetramethoxystilbene. Drug Metab Dispos.33:1771–6.

De Souza EM, Menna-Barreto R, Araújo-Jorge TC, Kumar A, Hu Q, Boykin DW, Soeiro MN.2006, Antiparasitic activity of aromatic diamidines is related to apoptosis-like death in Trypanosoma cruzi. Parasitology. 133(1):75-9.

Fitzpatrick, K; Midgley, I; Henderson, SJ; Taylor, LM; Houchen, TL; Wright, SJ; McBurney, A; John, BA; Cybulski, ZR; Hall, JE, et al. Pharmacokinetics and metabolism of the prodrug DB289 in the rat and monkey and its conversion to the active entity, DB75. *Drug Metab Rev.* 2004;36:338–338.

Hatano E.2007,Tumor necrosis factor signaling in hepatocyte apoptosis. J Gastroenterol Hepatol. Jun;22 Suppl 1:S43-4.)

Janelle Y. Saulter, Joseph R. Kurian, Lauren A. Trepanier, Richard R. Tidwell, Arlene S. Bridges, David W. Boykin, Chad E. Stephens, Mariappan Anbazhagan, and James Edwin

Hall. (2005) Unusual dehydroxylation of antimicrobial amidoxime prodrugs by cytochrome b5 and NADH cytochrome b5 reductase. Drug Metabolism and Disposition, 33:1886-1893.

Lian Zhou, Dhiren R. Thakker, Robert D. Voyksner, Mariappan Anbazhagan, David W. Boykin, James E. Hall, Richard R. Tidwell. (2004) Metabolites of an orally active antimicrobial prodrug, 2,5-bis(4-amidinophenyl) furan-bis-O-methylamidoxime, identified by liquid chromatography/tandem mass spectrometry. Journal of Mass Spectrometry, 39(4), 351-360.

Rastogi, S., Joshi, B., Fusaro, G., and Chellappan, S. (2006) Camptothecin Induces Nuclear Export of Prohibitin Preferentially in Transformed Cells through a CRM-1-dependent Mechanism* J. Biol. Chem. 281, 2951-2959

Stephens CE, Patrick DA, Chen H, Tidwell RR and Boykin DW (2001) Synthesis of Deuterium Labelled 2,5-Bis(4-amidinophenyl)furan, 2,5-Bis(4-ethoxyamidinophenyl)furan, and 2,7-Diamidinocarbazole. J. Labelled Cpd. Radiopharm. 44:197-208.

Sturk, L. M., J. L. Brock, C. R. Bagnell, J. E. Hall, and R. R. Tidwell. 2004. Distribution and quantitation of the anti-trypanosomal diamidine 2,5-bis(4-amidinophenyl)furan (DB75) and its N-methoxy prodrug DB289 in murine brain tissue. Acta Trop. 91:131-143.

Tidwell, R.R., S.K.Jones, J.D. Geratz, K.A.Ohemeng, C.A.Bell, B.J.Berger, and J.E.Hall.1990. Development of pentamidine analogues as new agents for the treatment of Pneumocystis carinii pneumonia. Ann N Y Acad Sci 616:421-41

V.McNeil Coffield, Whitney S. Helms, Qi Jiang, and Lishan Su. (2004) Gα mediates a signal that is essential for proliferation and survival of thymocyte progenitors. Journal of Experimental Medicine, 200(10), 1315-1324.

Wang MZ, Saulter JY, Usuki E, Cheung YL, Hall M, Bridges AS et al. (2006). CYP4F enzymes are the major enzymes in human liver microsomes that catalyze the O-demethylation of the antiparasitic prodrug DB289 [2,5-bis(4-amidinophenyl)furan-bis-O-methylamidoxime]. Drug Metab Dispos 34: 1985–1994.

Yeramian P., S. R. Meshnick, S. Krudsood, K. Chalermrut, U. Silachamroon, N. Tangpukdee, J. Allen, R. Brun, J. J. Kwiek, R. Tidwell, and S. Looareesuwan. 2005. Efficacy of DB289 in Thai patients with Plasmodium viax or acute, uncomplicated Plasmodium falciparum infections. J Infect Dis 192: 319-322

Yeramian P, Kruse M, Kecskes A, Allen J, McChesney-Harris L, Trendler K, Hall J E, Tidwell R. (2001) Safety and Clinical Pharmacokinetics of DB289, a New Orally Bioavailable Dication. Interscience Conference on Antimicrobial Agents and Chemotherapy (41st : 2001 : Chicago, Ill.).

Yu LJ, Matias J, Scudiero DA, Hite KM, Monks A, Sausville EA, and Waxman DJ (2001) P450 enzyme expression patterns in the NCI human tumor cell line panel. Drug Metab Dispos 29: 304–312

CHAPTER 4

CYP1B1 INHIBITION BY THE ANTIMICROBIAL PRODRUG DB289 AND ITS METABOLITES M1 AND M2

A. ABSTRACT

2,5-Bis(4-amidinophenyl)furan-bis-*O*-methylamidoxime (DB289) is a potent antimicrobial prodrug that is biotransformed to the active diamidine 2,5-bis(4-amidinophenyl)furan (DB75) by sequential *O*-demethylation and *N*-dehydroxylation reactions. Previous studies have shown that *O*-demethylation reactions are catalyzed by multiple enzymes, including CYP4F2, CYP4F3B, CYP2J2, CYP1A2, CYP1A1, and CYP1B1. Recently, we discovered that recombinant CYP1A1 and CYP1A2 catalyzed the two sequential *O*-demethylations to form M1 and M2, respectively. However, CYP1B1 could only catalyze the first *O*-demethylation from DB289 to form M1, but could not form M2. Studies of M1 metabolism and protein binding studies using ^{14}C-DB289 indicated that M1 may be converted to a reactive intermediate metabolite by CYP1B1. Radiolabeled material was bound tightly to proteins, and could not be released by extensive organic extraction. DB289, M1, and M2 all exhibited inhibitory effects against CYP1B1 using the EROD assay. Different inhibition potencies were seen, with the highest potency IC_{50} value for M1 (0.9 μM), followed by DB289 (2.5 μM) and M2 (9.4 μM). DB289, M1, and M2 also could inhibit carcinogen 1, 3, 5(10)-estratrien-3, 4, 17β-triol (4E2) formation catalyzed by CYP1B1 and non-carcinogen 1, 3, 5(10)-estratrien-2, 3, 17β-triol (2E2) formation catalyzed by CYP1A1 and CYP1A2. Since CYP1B1 has been implicated as a potential anti-cancer target, future investigation of the CYP1B1 inhibition by DB289, M1, and M2 may be helpful for the potential cancer prevention.

INTRODUCTION

DB289 is an antimicrobial prodrug developed for the treatment of a variety of microbial infections (Yeramiam et al. 2005). The phase I metabolic pathway of DB289 to form the active dicationic compound DB75 (figure 4.1) has been determined in vitro using freshly isolated rat hepatocytes (Zhou et al., 2004). These sequential O-demethylation and N-dehydroxylation reactions are catalyzed by multiple enzymes, including CYP4F2, CYP4F3B, CYP2J2, CYP1A2, CYP1A1, and CYP1B1 for the O-demethylations, and cytochrome b5/b5 reductase for the N-dehydroxylations (Wang et al., 2006; Saulter et al., 2005). Interestingly, the conversion of DB289 to M1 catalyzed by the recombinant human CYP1B1 was incomplete and the sequential conversion of M1 to M2 was not observed. Therefore, we hypothesized that DB289, M1 or M2 could inhibit CYP1B1 activity. Since CYP1B1 protein is expressed broadly in tumor cells and very rarely in normal cells, it has been extensively studied for its important role as a universal tumor marker. CYP1B1 has been confirmed to catalyze multiple exogenous and endogenous substrates to form carcinogens and therefore initiate tumorigenesis. A well known example is 1, 3, 5(10)-estratrien-3, 4, 17β-triol (4E2), which is selectively converted by CYP1B1 from endogenous 1, 3, 5(10)-estratrien-3, 17β-diol (E2), and has been reported to be correlated to initiation of various cancers (Spink et al., 1998). So CYP1B1 has been implicated as a potential anti-cancer target (Guengerich et al., 2003) through vaccine, prodrug and inhibitor strategies (Gribben et al., 2005; Potter et al., 2002; Chunet al., 2001). Investigation of CYP1B1 inhibition may be helpful for cancer prevention and anti-cancer drug design.

C. MATERIALS AND METHODS

Chemicals and reagents.

DB289 (2,5-bis-(4-amidinophenyl)furan-bis-*O*-methylamidoxime), M1 (2-(4-hydroxyamidinophenyl)-5-(4-methoxyamidinophenyl)furan), and M2 (2,5-bis(4-amidinophenyl)furan-bis-*O*-amidoxime) were synthesized as previously described (Boykin et al., 1996; Stephens et al., 2001) (figure 4.1). ^{14}C labeled DB289 in methanol solution was obtained from Huntingdon Life Sciences Ltd. (Huntingdon, UK) (Midgley et al., 2007). The radiochemical purity was more than 97% and it was stored in dark at -80^{o}C prior to usage. Human CYP1A1, CYP1A2, and CYP1B1 + P450 reductase Supersomes were purchased from BD Gentest (Bedford, MA, USA). Tetramethoxystilbene (TMS) was obtained from Cayman Chemical (Ann Arbor, MI, USA). 1, 3, 5(10)-estratrien-3, 17β-diol (E2), 1, 3, 5(10)-estratrien-2, 3, 17β-triol (2E2), and 1, 3, 5(10)-estratrien-3, 4, 17β-triol (4E2) were purchased from Steraloids, Inc. (Newport , RI, USA). Flutamide, 7-ethoxyresorufin (7-ERF), resorufin (RF), ammonium formate, formic acid, β-NADPH, and other inorganic chemicals were obtained from Sigma Chemical Co. (St. Louis, MO, USA).

Metabolism studies of DB289, M1, and M2 by human recombinant CYP1s.

Prior to each experiment, DB289, M1, and M2 were prepared as 10 mM stock solutions in DMSO. In the reaction mixtures, compound was added at a final concentration of 1 μM to 100 mM potassium phosphate buffer (pH 7.4) supplemented with 3.3 mM $MgCl_2$. Human recombinant CYPs were added at a final concentration of 10 pmol/ml for CYP1A1, and 50 pmol/ml for CYP1B1 or CYP1A2 to achieve comparable metabolism profiles with suitable amount of metabolites. The mixtures were incubated at 37^{o}C for five min prior to the addition of 1 mM NADPH to initiate the reaction. Aliquots (250 μL) were taken at specific

time points and the reactions were terminated by the addition of 125 µL of acetonitrile and samples were placed on ice. Precipitated protein was removed by centrifugation (21,000 x g for 10 min) and the supernatant was removed and placed in amber HPLC vials and sealed with Teflon lined caps. Samples were analyzed immediately by LC-UV as described below and metabolites were quantitated using authentic standards at different concentrations for calibration.

For the metabolic study of ^{14}C-labeled DB289, the reaction conditions were the same as above. After the sample was quenched and centrifuged, the supernatant solution was transferred and the protein pellet was extracted with acetonitrile and washed by centrifugation three times. The supernatant solution, each extracted solution (extraction 1, 2, 3 respectively), and the final protein pellet were kept and reconstituted in Ultima Gold Universal liquid scintillation cocktail. The luminescent counts were determined and analyzed with QuantaSmart.

HPLC-UV analysis of compounds.

Analysis of DB289 and its metabolites was performed on an Agilent 1100 series HPLC with a UV detector. Ten µl samples were injected and separated on an Agilent ZORBAX bonus-RP column (2.1 x 150 mm, 5 µm). The system was operated at 0.35 mL/min with mobile phase buffer A (0.025% TFA in deionized water) and mobile phase buffer B (0.025% TFA in acetonitrile: deionized water/ 80:20). Mobile phase gradient was 90% buffer A plus 10 % buffer B at time 0 min, to 100% buffer B at time 22 min, followed by post washing with 90% buffer A plus 10 % buffer B for 6 min. The wave length of the UV detector was set to 359 nm. The columns were maintained at room temperature. Authentic standards at different concentrations were used to obtain calibration curves for quantitation.

Ethoxyresorufin *O*-deethylation (EROD) assay.

Reaction mixtures containing 5 pmol/ml CYP1B1, 4 μM 7-ethoxyresorufin as substrate, 3.3 mM magnesium chloride in 100 mM potassium phosphate (pH 7.4) and chemicals (DB289, M1, M2, flutamide) at multiple concentrations (range 1 nM -100 μM) were incubated at 37^{o}C. The control reaction mixtures contained vehicle instead of chemicals. The reactions were initiated by addition of 1 mM β-NADPH. After 5 min, the reactions were quenched by addition of half volume of acetonitrile. The amount of the products was determined by RF-5001 PC Shimadzu fluorimeter with Ex at 510 nm and Em at 586 nm as described previously (Radenac et al., 2004). Resorufin standards at different concentrations were used for calibration. IC_{50} values were determined using GraphPad Prism 4.0 (San Diego, CA) statistical program. The values of drug concentrations were transformed to log scale. The enzyme activity of each sample was expressed as a percentage of signal intensity versus the control (DMSO treated). Sigmoidal dose response curves were created to fit the data and to determine the IC_{50} values.

4E2 and 2E2 formation assay.

Reaction mixtures containing 50 pmol/ml CYP1B1, CYP1A1, or CYP1A2, 1 μM 1, 3, 5(10)-estratrien-3, 17β-diol (E2) as substrate, 3.3 mM magnesium chloride in 100 mM potassium phosphate (pH 7.4) and chemicals (DB289, M1, M2, flutamide, and TMS) at multiple concentrations were incubated at 37^{o}C. The control reaction mixtures contained vehicle instead of chemicals. The reactions were initiated by addition of 1 mM β-NADPH. After 5 min, the reactions were quenched by addition of 0.1 volume of 1 M HCl. The amount of metabolite 1, 3, 5(10)-estratrien-3, 4, 17β-triol (4E2) was determined using the method

described previously (Aoyama et al., 1990). IC_{50} values were determined using GraphPad Prism 4.0 (San Diego, CA) statistical program.

Statistical Analysis

Data are presented as the mean ± SD from independent triplicate experiments unless otherwise noted. $P > 0.05$ was considered as significant. T tests (unpaired, two-tailed) were performed if only two groups were analyzed. ANOVA followed by Tukey's test was used for comparison of more than 2 groups.

D. RESULTS

Metabolism studies of DB289, M1, and M2 by human recombinant CYP1s:

The *O*-demethylation reaction is the first step of the complex metabolic pathway of methoxime prodrug DB289. Multiple P450s were confirmed to be capable of catalyzing this reaction according to previous P450s metabolism screening (Wang et al, 2006; Saulter et al., 2005). In the metabolism study of DB289 catalyzed by CYP1 enzymes, we found very interesting results as shown in figure 4.2. CYP1B1 catalyzed the first *O*-demethylation to form M1 after 30 min reaction at 37^{o}C, but did not form any M2, via the second *O*-demethylation. However, under the similar experimental conditions, both CYP1A1 and CYP1A2 catalyzed the two sequential *O*-demethylations to form M1 and M2, respectively. In order to determine if M1 is a substrate of CYP1B1, we carried out a time course study of M1 metabolism. The substrate M1 could be continuously depleted by CYP1B1 with NADPH present during the time course, with about 42% M1 remaining at the last time point 120 min (figure 4.3B). However, only minor quantities of M2 were formed during this incubation (figure 4.3A). We also examined M2 metabolic stability under the reaction conditions. In a subsequent experiment M2 was not depleted by CYP1B1 during similar incubation (figure 4.3C and 4.3D). Since M2 was metabolically stable in the presence of CYP1B1, it raised a question why M1 was depleted by CYP1B1 but did not form free metabolites that we could detect under the common HPLC-UV conditions for DB289 analogues. One possibility was that M1, or reactive metabolites of M1, may bind protein contents during the metabolic reaction and be removed by coprecipitation with proteins after the reaction mixture was quenched and centrifuged.

Protein binding of ^{14}C-DB289 during CYP1 catalyzed metabolic reactions.

To test this possibility of protein binding during metabolic reactions, we repeated the metabolism study using ^{14}C-labeled DB289 as a substrate in the presence of CYP1 enzymes. After the reaction samples were quenched and centrifuged, the supernatant solution was transferred and the protein pellet was extensively extracted with acetonitrile. Most of the radio activity counts were recovered in the supernatant solution and the first extraction solution. Extraction solutions 2 and 3 had very similar low counts, less than 500 cpm, which confirmed that the extractions had efficiently removed the free ^{14}C -labeled compounds, including prodrug and any metabolites (figure 4.4). The protein pellet from CYP1B1 reaction mixture incubated for 40 min with NADPH had counts (2258 ± 56), which was significantly higher than the counts of its two negative controls, incubated for 0 min with NADPH (541 ± 25) and incubated for 40 min without NADPH (523 ± 28), respectively. In contrast, the protein pellets from CYP1A1 or CYP1A2 had similar low counts (less than 500), whether incubated for 0 or 40 min, with or without NADPH. These results indicated that during metabolism, DB289 and/or its metabolite M1, or a possible reactive metabolite, could bind proteins in the CYP1B1 reaction mixture, but not in CYP1A1 and CYP1A2 reaction mixtures. Since this process was in a NADPH-dependent manner, reactive intermediate metabolite may form in the presence of CYP1B1 and bind protein contents tightly, which could not be released by extensive organic extraction.

Inhibition of CYP1 metabolism.

Based on the above metabolism studies, we knew that CYP1A1 and CYP1A2 catalyzed the two sequential *O*-demethylations from DB289 to M1 and M2, respectively (figure 4.5A). However, CYP1B1 could only catalyze the first *O*-demethylation from DB289 to form M1, but not further to form M2. The second *O*-demethylation may be inhibited (figure 4.5B).

Consistently, CYP1B1 could only catalyze the first *O*-demethylation from M1 to form M2 (figure 4.5C). M1 may be catalyzed to form reactive intermediate metabolites, which bind to protein tightly.

Inhibition of DB289, M1, and M2 against CYP1B1.

In order determine the direct inhibitory effects of DB289 and each *O*-demethylated metabolite M1 and M2, we used 7-ethoxyresorufin as the marker substrate to measure CYP1B1 activity in the presence of these compounds at different concentrations (range 1 nM -100 μM). The results are shown in figure 4.6. With progressively increasing concentrations, all the tested compounds exhibited higher inhibition against CYP1B1 activity. Flutamide, a known CYP1B1 inhibitor (Rochat et al., 2001), served as a positive control. IC50 values were 11.3 μM for flutamide, 0.9 μM for M1, 2.5 μM for DB289 and 9.4 μM for M2. Control activity in the absence of inhibitors was 2.2 pmol min^{-1} pmol $CYP1B1^{-1}$. These results indicated that DB289 and each *O*-demethylated metabolite M1 and M2 were all inhibitors of CYP1B1, with M1 the most potent one among them.

Inhibition of carcinogen 4E2 and 2E2 formation by DB289, M1, and M2.

The carcinogen 4E2 is mainly formed by CYP1B1 instead of CYP1A1 and CYP1A2 from endogenous substrate E2. In contrast, non-carcinogen 2E2 is the product catalyzed by CYP1A1 and CYP1A2 from E2. Since DB289, M1, and M2 showed inhibitory effects against CYP1B1 in the EROD assay, we also were interested to test if carcinogen 4E2 formation by CYP1B1 could also be inhibited by these compounds. The results are shown in the table 4.1. DB289, M1, and M2 and the positive control chemicals flutamide and TMS all exhibited inhibitory effects against carcinogen 4E2 formation catalyzed by CYP1B1 with different potency. TMS showed the highest potency (IC_{50}= 0.09 ± 0.02 μM) and flutamide

showed the lowest potency (IC_{50}= 5.3 ± 0.46 μM). M1 has a potency (IC_{50}= 0.12 ± 0.02 μM) close to TMS. DB289 and M2 both had potency with IC_{50} values less than 1 μM. These compounds also inhibited non-carcinogen 2E2 formation by CYP1A1 and CYP1A2. DB289, M1, M2, and TMS showed preferential inhibition against CYP1A1 verse CYP1A2.

E. DISCUSSION

The anti-trypanosomal dimethoxime prodrug DB289 has a complex metabolic pathway. The *O*-demethylation step could be catalyzed by multiple P450s. CYP1A1 and CYP1A2 catalyzed the two sequential *O*-demethylations to form M1 and M2, respectively. However, CYP1B1 could only catalyze the first *O*-demethylation from DB289 to form M1, but not further to form M2. Metabolism studies of M1 and protein binding studies of ^{14}C-DB289 indicated that M1 may be converted to a reactive intermediate metabolite by CYP1B1 and bind tightly to proteins, which could not be released by extensive organic extraction.

The EROD assay is a standard assay to measure CYP1 enzyme activity. DB289, M1, and M2 all exhibited inhibitory effects against CYP1B1 using this assay. In the future, more precise experiments need to be done to determine their inhibition types, especially using preincubation experiments to determine if M1 is an irreversible inhibitor.

The positive control chemical TMS is the most potent and selective inhibitor against CYP1B1 reported to date. Its inhibition type was determined as reversible competitive inhibition. There has been no selective irreversible CYP1B1 inhibitor reported, yet. DB289, M1, and M2 all exhibited selective inhibition against CYP1B1 versus CYP1A1 and CYP1A2 by 4E2 and 2E2 formation assay. Since M1 was depleted by CYP1B1 and there was no free metabolite formed during the reaction, it will be very interesting to know if it is a selective irreversible inhibitor against CYP1B1 in future investigations.

TMS also showed inhibitory effects against mutagenesis and therefore was considered for the potential cancer prevention application. New selective CYP1B1 inhibitors, especially irreversible inhibitors may also be interesting candidate for such purpose.

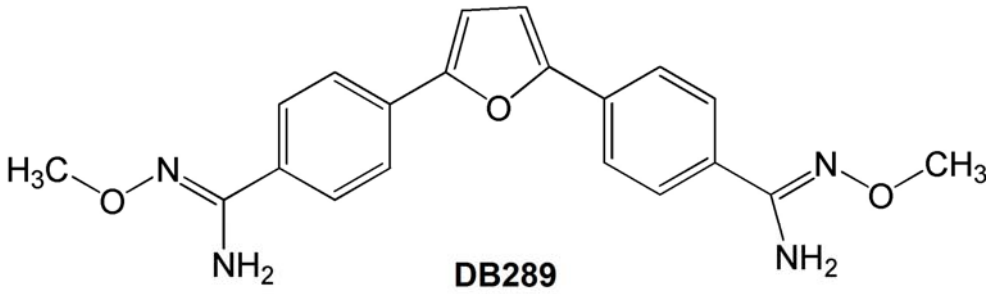

DB289

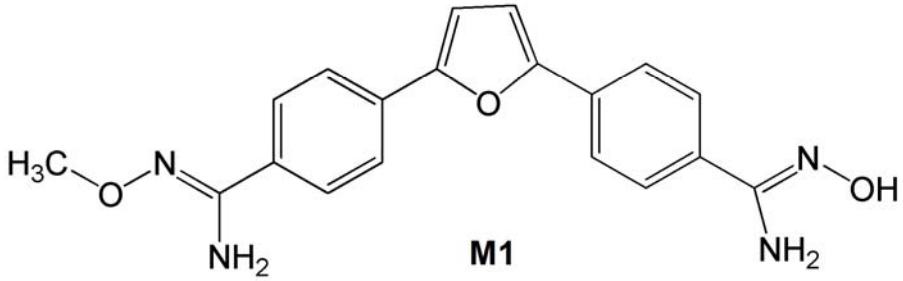

M1

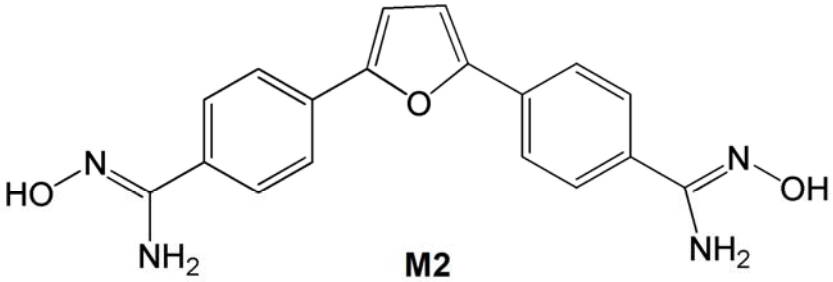

M2

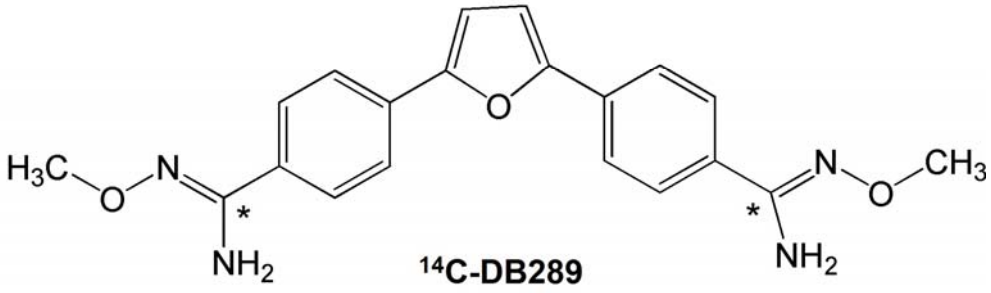

^{14}C-DB289

Figure 4.1. Chemical structures of synthetic compounds DB289, M1, M2, and ^{14}C-labeled DB289. * indicates the positions of ^{14}C-radiolabels.

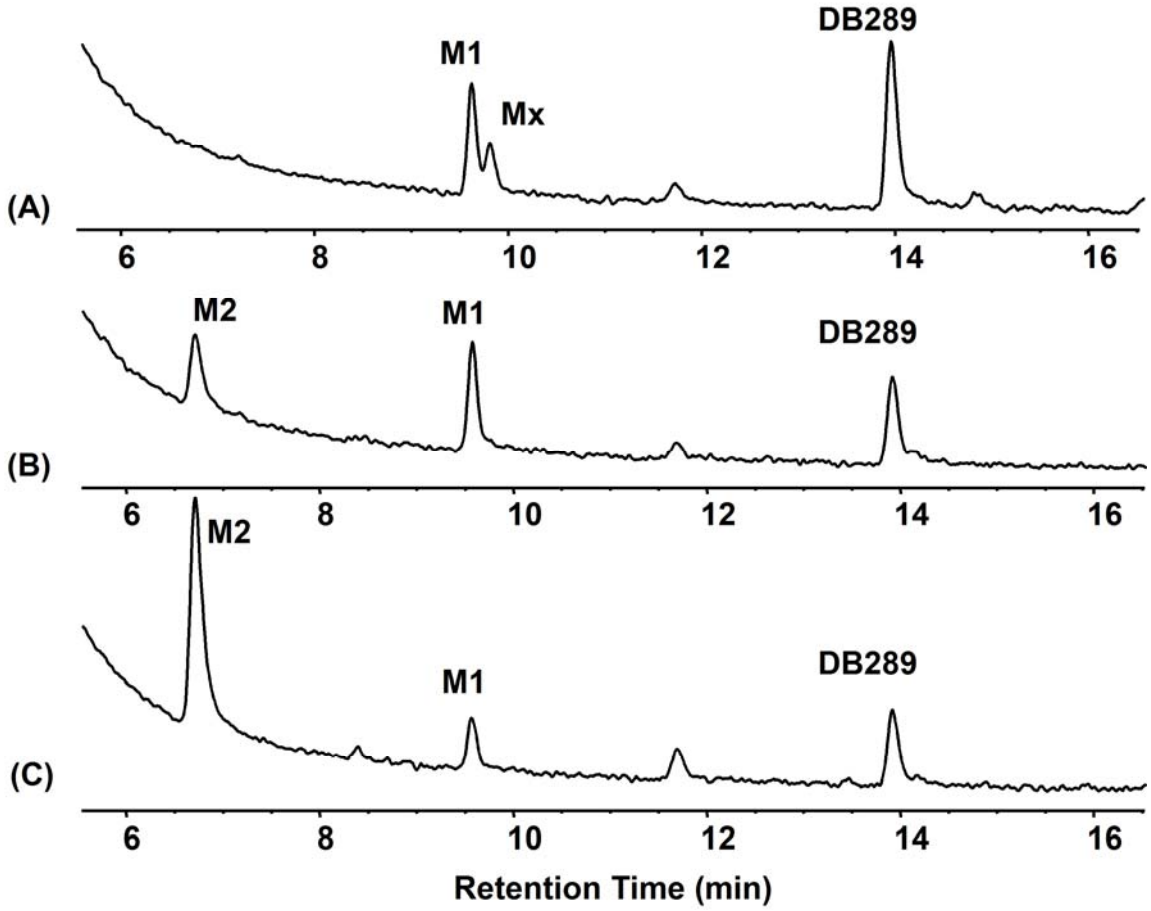

Figure 4.2. *In vitro* metabolism of DB289. Substrate was incubated with (A) 50 pmol /ml CYP1B1; (B) 10 pmol /ml CYP1A1; (c) 50 pmol /ml CYP1A2. Reactions were performed at 37^{o}C for 30 min.

A)

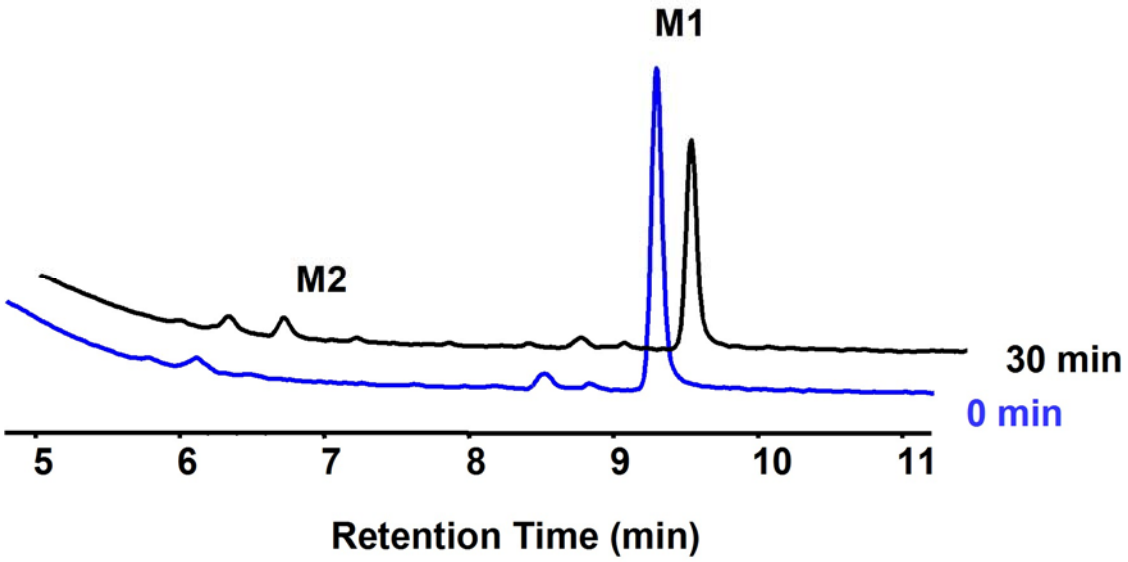
M1
M2
30 min
0 min
5
6
7
8
9
10
11
Retention Time (min)

B)

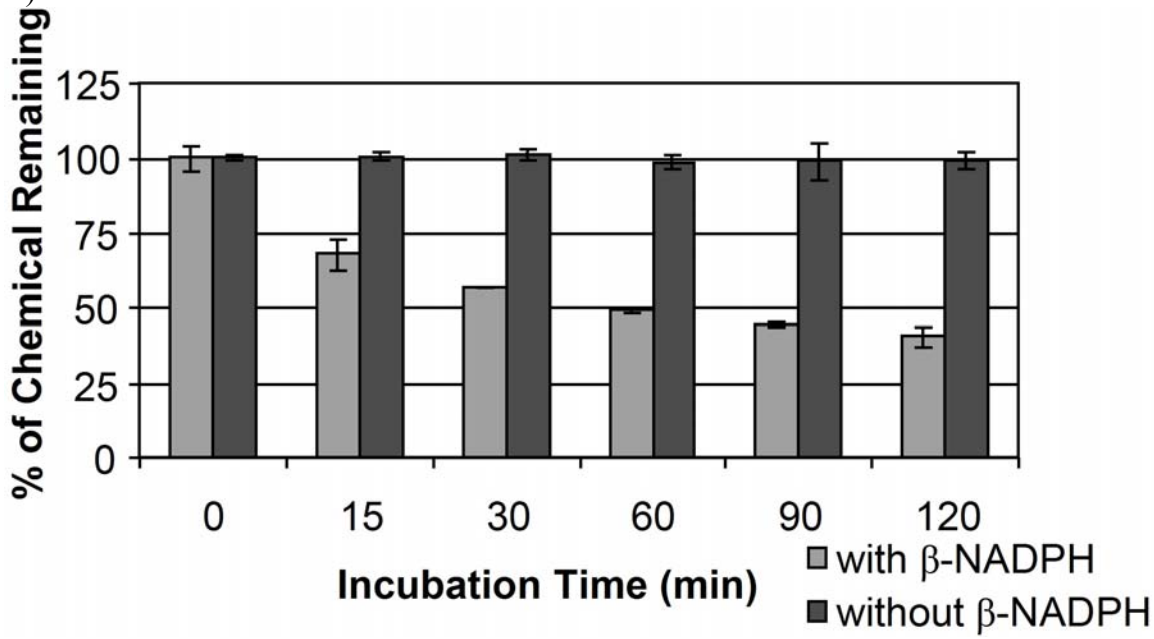
% of Chemical Remaining
125
100
75
50
25
0
0
15
30
60
90
120
Incubation Time (min)
with β-NADPH
without β-NADPH

C)

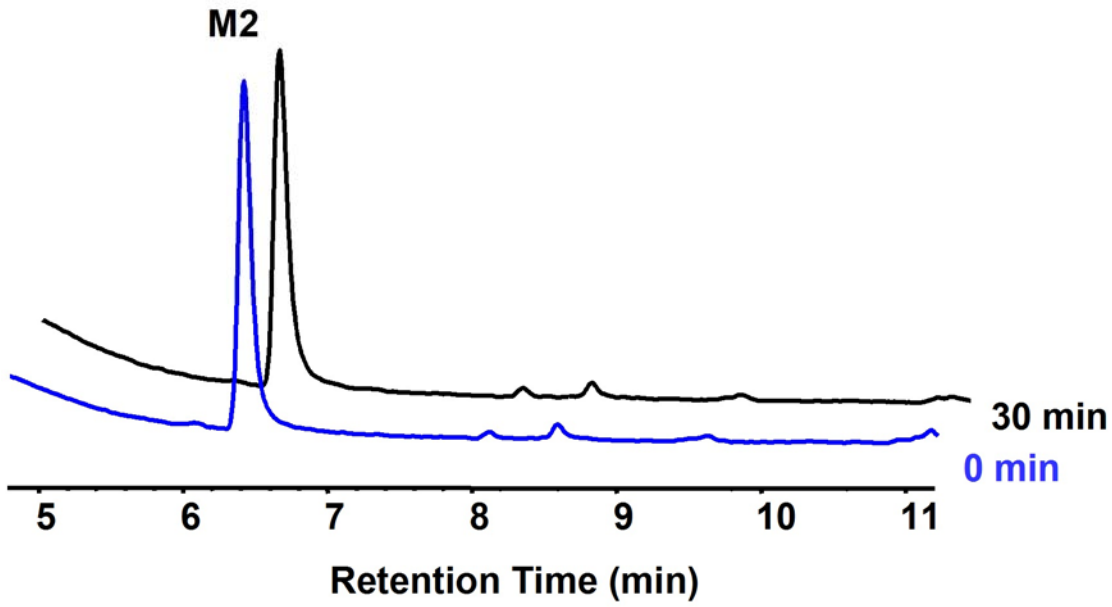

D)

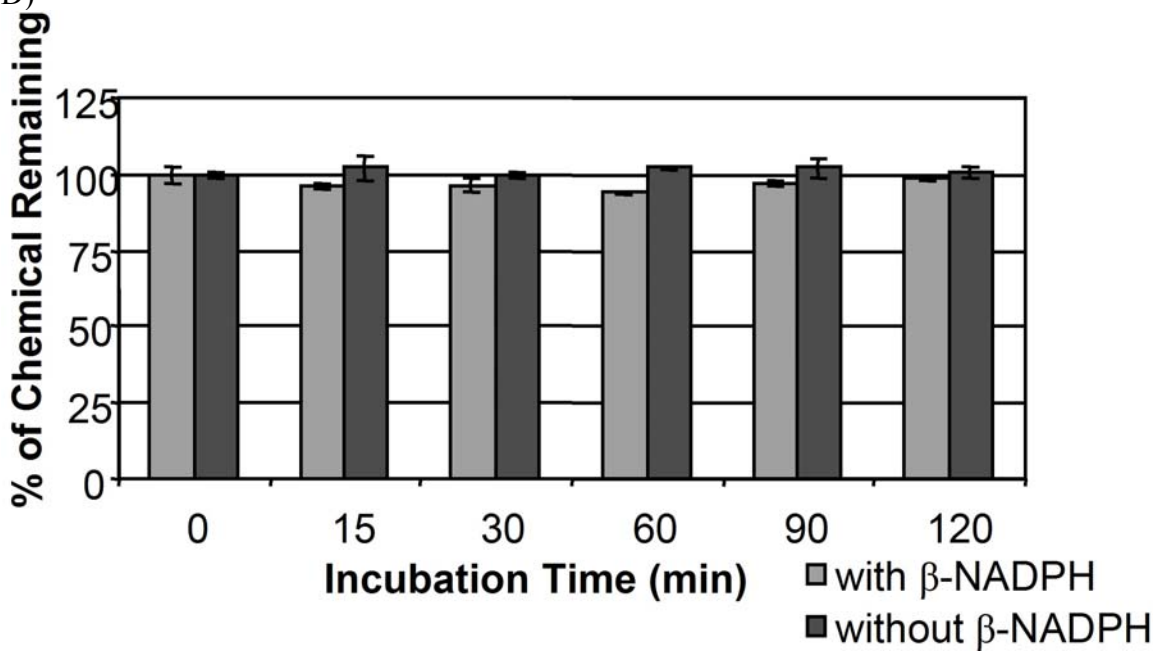

Figure 4.3. Substrate depletion by CYP1B1. (A) M1 was incubated with CYP1B1. Samples at time 0 min and 30 min were analyzed by HPLC; (B) M1 depletion by CYP1B1 at multiple time points during the incubation were quantitated by HPLC; (C) M2 was incubated with CYP1B1. Samples at time 0 min and 30 min were analyzed by HPLC; (D) M2 depletion by

CYP1B1 at multiple time points during the incubation were quantitated by HPLC-UV. Control reactions were initiated with water instead of β-NADPH.

A)

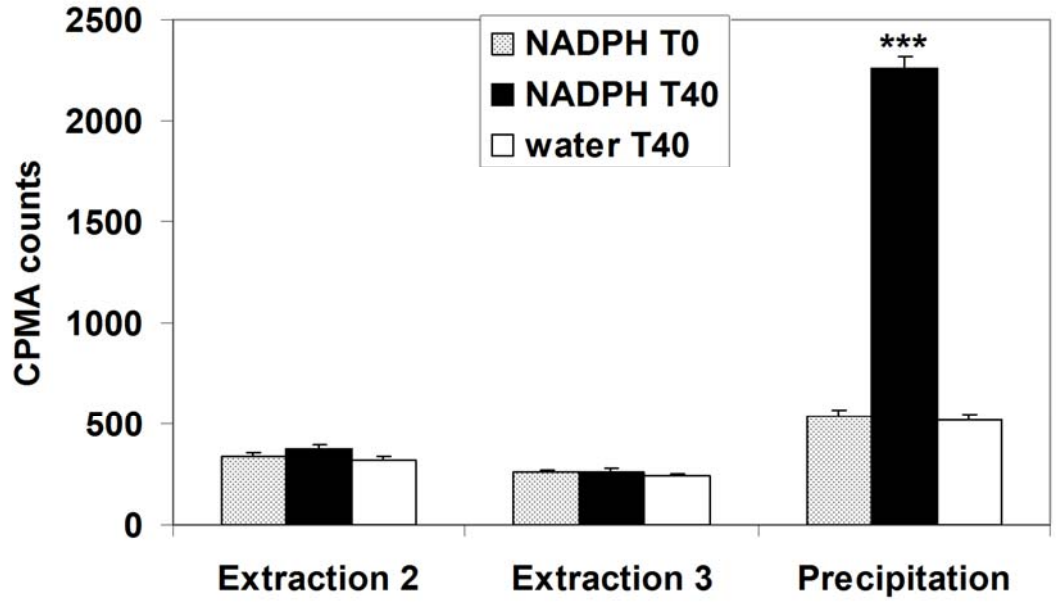
2500
2000
1500
1000
500
0
CPMA counts
NADPH T0
NADPH T40
water T40
***
Extraction 2
Extraction 3
Precipitation

B)

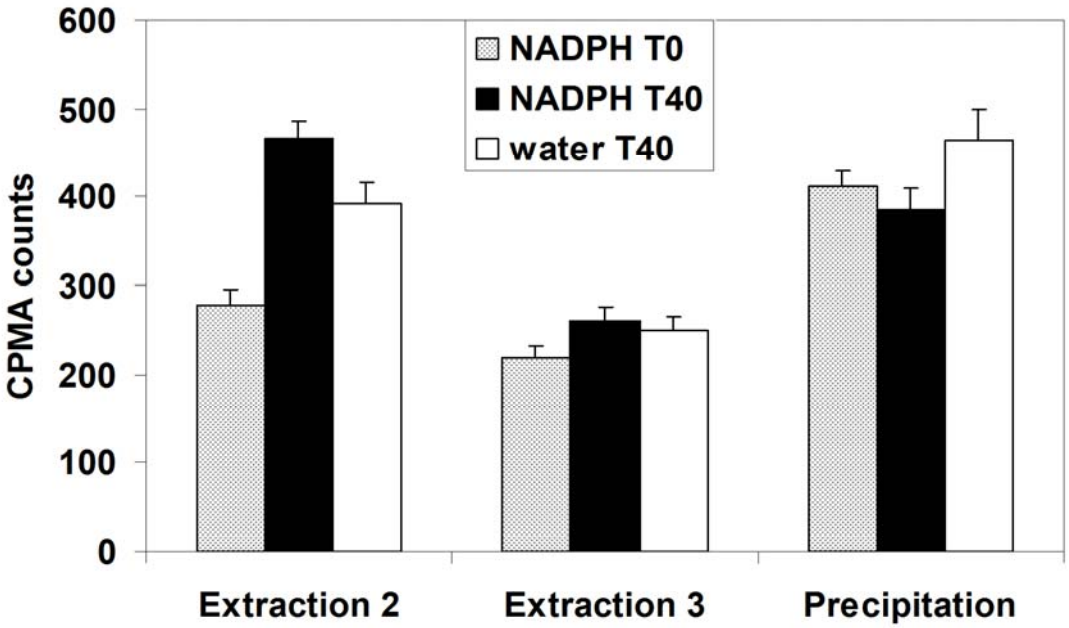
600
500
400
300
200
100
0
CPMA counts
NADPH T0
NADPH T40
water T40
Extraction 2
Extraction 3
Precipitation

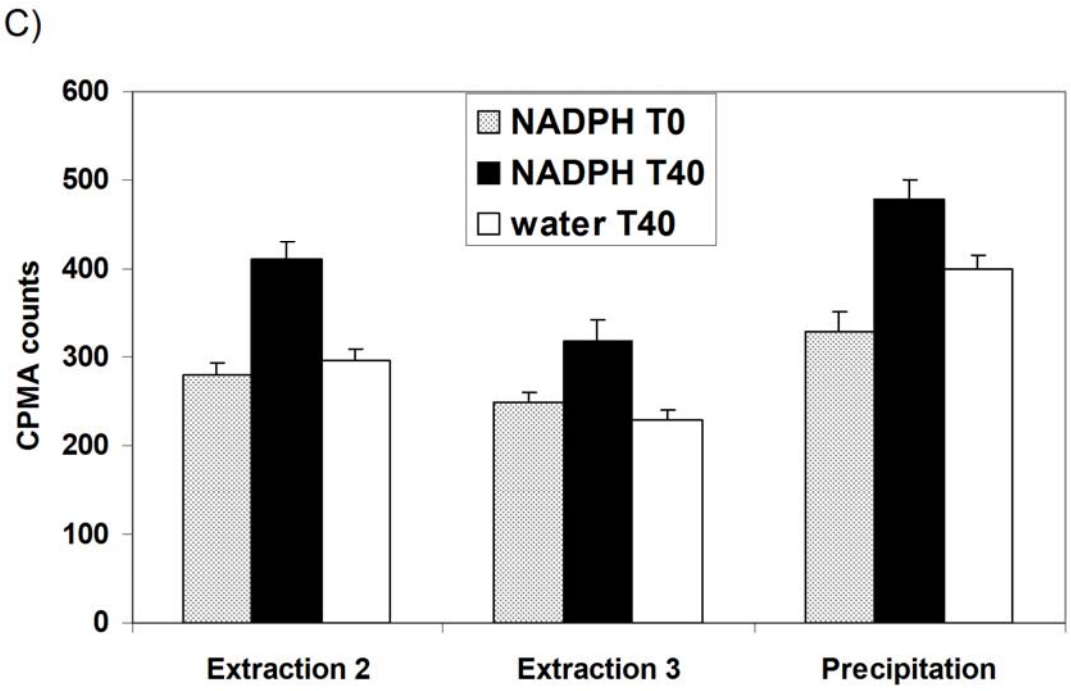

Figure 4.4. Radio activity counts remaining in extraction solutions and protein precipitaion. ^{14}C-DB289 was metabolized by A) CYP1B1, B) CYP1A1, and C) CYP1A2 in the presence of NADPH or water at reaction time 0 and 40 min.

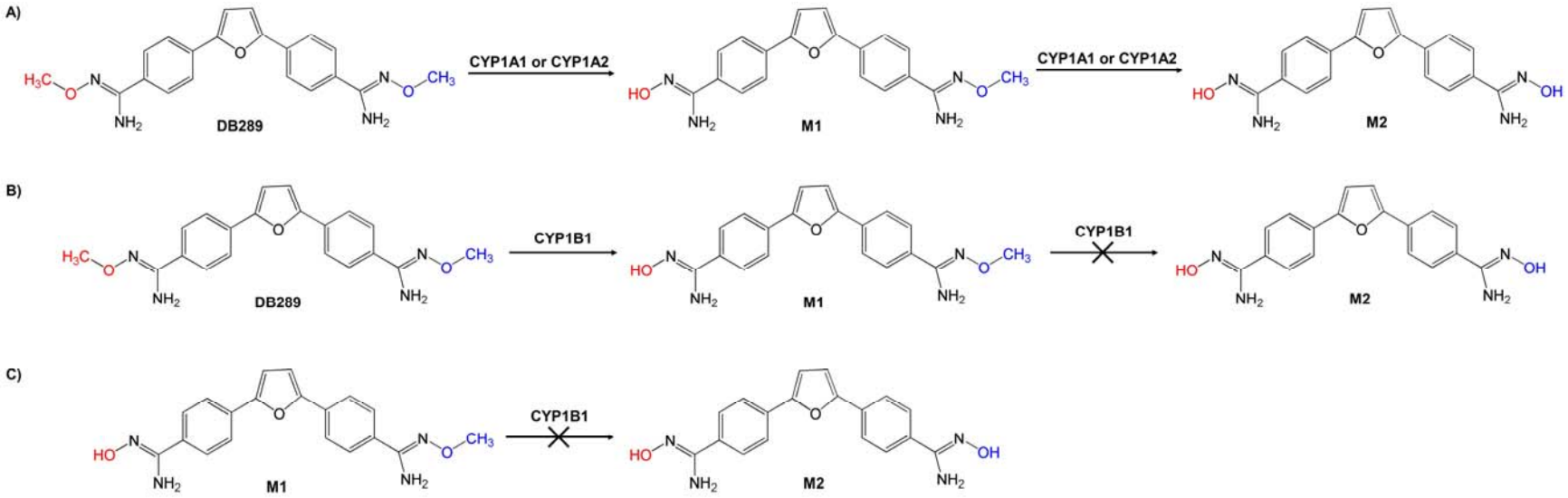

Figure 4.5. Metabolic pathways. A) DB289 was metabolized by CYP1A1 or CYP1A2 to form M1 and M2 sequentially. B) DB289 was metabolized by CYP1B1 to form M1, but not to further form M2. C) M1 was not metabolized by CYP1B1 to form M2.

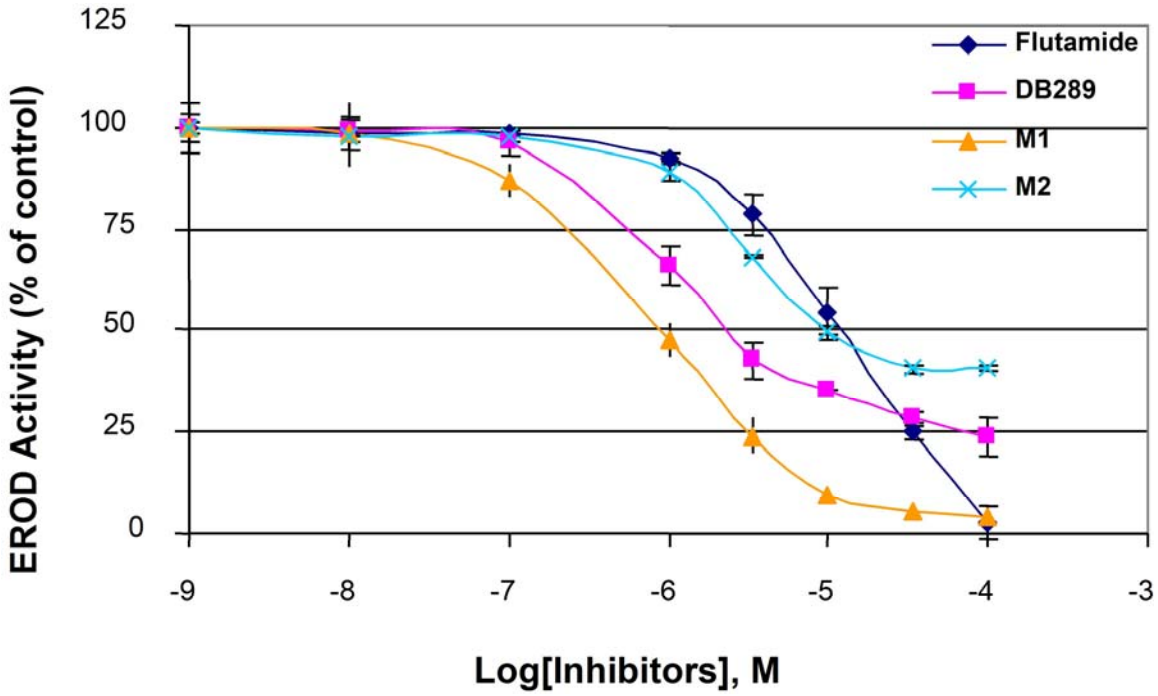

Figure 4.6. Concentration-dependent inhibition of EROD activities catalyzed by CYP1B1. The activities were determined in the presence of inhibitors: flutamide, DB289, M1 or M2 at concentrations (range 1 nM -100 μM). The control activities were determined in the absence of inhibitors.

Table 4.1.

Inhibitory effects by DB289 and its metabolites M1 and M2 on carcinogen 4E2 formation catalyzed by CYP1B1 and non-carcinogen 2E2 formation catalyzed by CYP1A1 and CYP1A2.

Assay conditions were as described in Materials and Methods. The data represent the mean from three separate experiments.

	IC50 (μM)				
	DB289	M1	M2	Flutamide	TMS
4E2 by CYP1B1	0.32 ± 0.03	0.12 ± 0.02	0.58 ± 0.04	5.3 ± 0.46	0.09 ± 0.02
2E2 by CYP1A1	0.3 ± 0.04	0.63 ± 0.04	2.1 ± 0.3	>10	0.74± 0.03
2E2 by CYP1A2	3.2 ± 0.28	2 ± 0.13	>10	0.95 ± 0.11	6.3 ± 0.5

F. ACKNOWLEDGEMENTS

This work was supported by a grant from the Bill and Melinda Gates Foundation.

G. References:

Aoyama T, Korzekwa K, Nagata K, Gillette J, Gelboin HV, Gonzalez FJ. Estradiol metabolism by complementary deoxyribonucleic acid-expressed human cytochrome P450s. Endocrinology 1990;126:

Bertrand Rochat, Janine M. Morsman, Graeme I. Murray, William D. Figg, and Howard L.Mcleod. Human CYP1B1 and Anticancer Agent Metabolism: Mechanism for Tumor-Specific Drug Inactivation? The Journal of Pharmacology and Experimental Therapeutics 2001, 296 (2), 537-541.

F. Peter Guengerich, Young-Jin Chun, Donghak Kim, Elizabeth M. J. Gillam, Tsutomu Shimada. Cytochrome P450 1B1: a target for inhibition in anticarcinogenesis strategies. Mutation Research 2003, 523-524: 173-182.

Lian Zhou, Dhiren R. Thakker, Robert D. Voyksner, Mariappan Anbazhagan, David W. Boykin, James E. Hall, Richard R. Tidwell. (2004) Metabolites of an orally active antimicrobial prodrug, 2,5-bis(4-amidinophenyl) furan-bis-O-methylamidoxime, identified by liquid chromatography/tandem mass spectrometry. Journal of Mass Spectrometry, 39(4), 351-360.

Radenac, G.; Coteur, G.; Danis, B.; Dubois, Ph.; Warnau, M. Measurement of EROD Activity: Caution on Spectral Properties of Standards Used. 2004 Mar. Biotechnol. 6, 307-311.

Stephens CE, Patrick DA, Chen H, Tidwell RR and Boykin DW (2001) Synthesis of Deuterium Labelled 2,5-Bis(4-amidinophenyl)furan, 2,5-Bis(4-ethoxyamidinophenyl) furan, and 2,7-Diamidinocarbazole. J. Labelled Cpd. Radiopharm. 44:197-208.

Yeramian, P., S. R. Meshnick, S. Krudsood, K. Chalermrut, U. Silachamroon, N. Tangpukdee, J. Allen, R. Brun, J. J. Kwiek, R. Tidwell, and S. Looareesuwan. 2005. Efficacy of DB289 in Thai patients with Plasmodium viax or acute, uncomplicated Plasmodium falciparum infections. J Infect Dis 192: 319-322

Spink DC, Spink BC, Cao JQ, De Pasquale JA, Pentecost BT, Fasco MJ, Li Y, Sutter TR. Differential expression of CYP1A1 and CYP1B1 in human breast epithelial cells and breast tumor cells. Carcinogenesis 1998; 19: 291–8.

CHAPTER 5

CONCLUSIONS AND FUTURE STUDIES

Conclusions and Future Studies

The agents that are currently available as anti-trypanosomals are generally unsatisfactory due to a combination of their low efficacy, dangerous side effects and difficulty in administration. Aromatic diamidines have long been used for the treatment of parasitic diseases such as human African trypanosomiasis.

The investigations described here have focused primarily on *O*-methyl amidoxime prodrug DB289 and aza analogues DB844, and their metabolites (Chapters 2-4). The novel metabolites MX and MY were formed from these prodrugs catalyzed by CYP1 enzymes. The analysis of the purified MX and MY using LC-MS generated essential structural information of MX to MY. The structure of MY was assianged as methyl 4-(5-(5-(N'-methoxycarbamimidoyl)pyridin-2-yl)furan-2-yl)benzoate. Further study is needed to synthesize and confirm the MX structure. In the future, we need investigate if MX and MY can form in other tissues and organs especially brain, lung, ovaries, testes, and prostate, where CYP1A1 and CYP1B1 are expressed. Since MX was an unstable metabolite, it may have chance to react with biomolecules when it forms in cells, although the amounts of MX and MY were very low in our *in vitro* studies using human recombinant CYP1A1 and CYP1B1. So, the efficacy and toxicity of MX and MY may need be investigated in the future.

DB289 failed in the extended phase I clinical trial for African trypanosomiasis due to its severe toxicity to liver and kidney. DB75 has been confirmed to be capable of inducing apoptotic-like death in *Trypanosome cruzi*. Before these studies began, little was known with if DB75 or the prodrug DB289 and its intermediate metabolites could induce apoptosis or necrosis in human cells. In the cell-based toxicity assays and apoptotic analysis using flow

cytometry and western blotting, these apoptotic effects by M1, M3 and DB75 were confirmed in MCF-7 cells. The metabolic study also demonstrated that M1, M3 and DB75 mainly contribute to the apoptotic effects.

In previous pharmacokinetics study of single orally dosed DB289, metabolism formed M1 had a relative short half life, M3 had relatively long half life and high levels in blood and urine, DB75 had much longer half life and accumulated in liver. They all can induce apoptosis in our results. In future studies, we need examine their cytotoxic effects to hepatic cells, especially DB75. Another important consideration is that the clinical toxicity is after repeated dosage for a long time, so the intermediated metabolites M1 and M3 may also have chance to accumulate and generate the toxicity if the P450 are inhibited after long time dosing. M1 and M3 are more potent to induce apoptosis than DB75 but less abundant in liver and blood. So further study is needed to determine how much they may contribute the toxicity. The interesting thing is that M2 shows a short half life and low level in the pharmacokinetics study and it doesn't induce apoptosis or necrosis in our results. So in the future we will be eager to know if M2 is a safe scaffold to design other less toxic prodrugs. There are also some questions in our experiments that are not clear yet. First, although DB75 has been confirmed as a DNA binder and can distribute in nucleus in human cell lines (Lansiaux et al., 2002), it is not known how it crosses cell membrane. M1 and M3 may pass the cell membrane by passive diffusion. But the targets of M1 and M3 to induce apoptosis are not known, which could be different from the targets of DB75. Elucidaiton of the whole process of the apoptosis by these compounds may be also important.

Metabolism study of DB289 and M1 showed that CYP1B1 could only catalyze the first *O*-demethylation from DB289 to form M1, but not further to form M2. Metabolism study of M1

and protein binding study of ^{14}C-DB289 indicated that M1 may convert to reactive intermediate metabolite by CYP1B1 and bind tightly to proteins, which could not be released by extensive organic extraction. DB289, M1, and M2 all exhibited inhibitory effects against CYP1B1 using EROD assay. In the future, more precise experiments need to do to determine their inhibition types, especially using preincubation experiments to determine if M1 is an irreversible inhibitor. The positive control chemical TMS is the most potent and selective inhibitor against CYP1B1 being reported to now days. Its inhibition type was determined as reversible competitive inhibition. There was no selective irreversible CYP1B1 inhibitor being reported, yet. DB289, M1, and M2 all exhibited selective inhibition against CYP1B1 verse CYP1A1 and CYP1A2 by 4E2 and 2E2 formation assay. Since M1 was depleted by CYP1B1 and there was no free metabolite formed during reaction, it will be very interesting to know if it a selective irreversible inhibitor against CYP1B1 in the future investigations. TMS also showed inhibitory effects against mutagenesis and therefore was considered for the potential cancer prevention application. New selective CYP1B1 inhibitors, especially irreversible inhibitors may also be interesting candidate for such purpose.